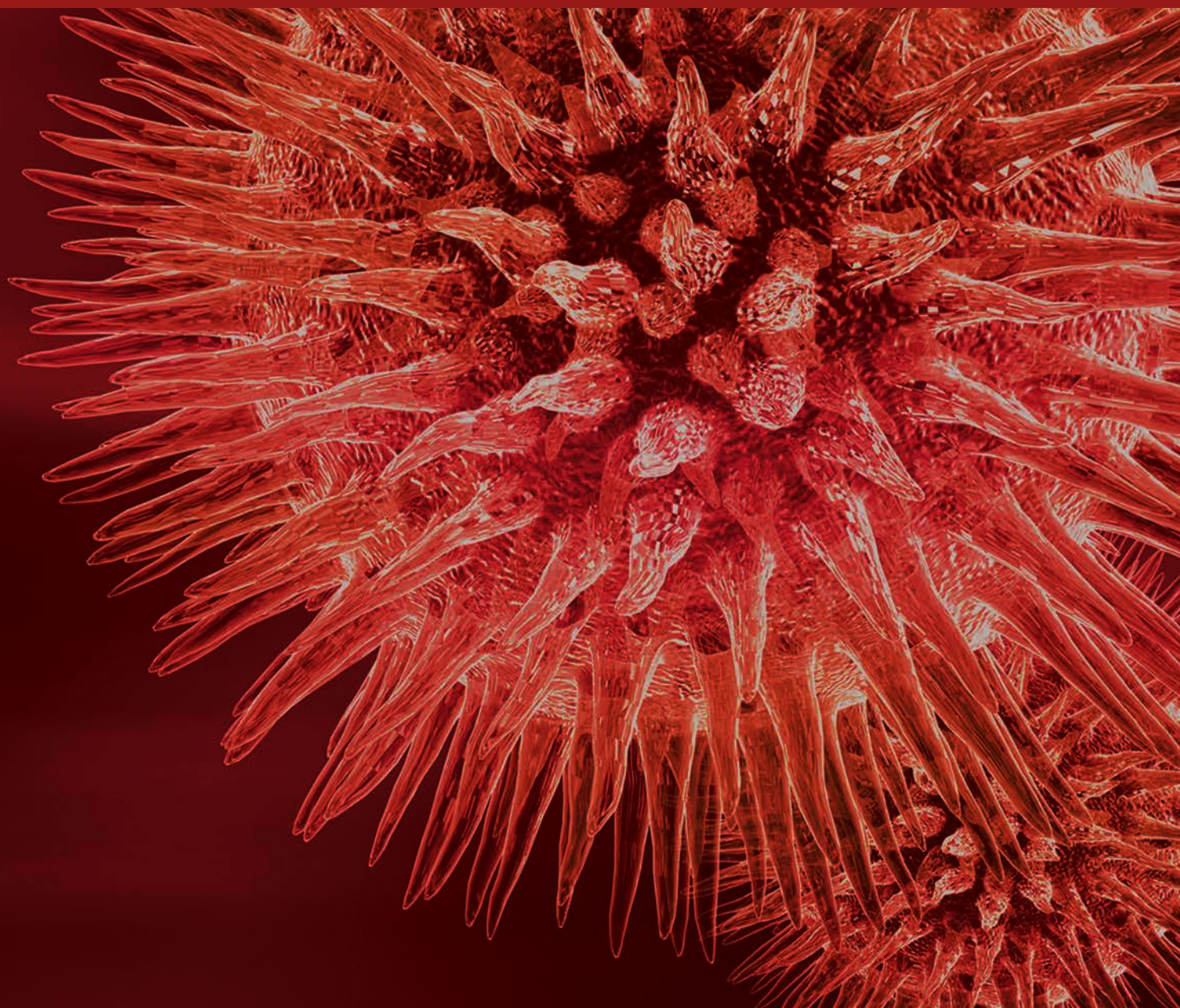


# Tissue Engineering and Oral Rehabilitation in the Stomatognathic System

Guest Editors: Tomasz Gedrange, Christiane Kunert-Keil, Friedhelm Heinemann, and Marzena Dominiak





---

# **Tissue Engineering and Oral Rehabilitation in the Stomatognathic System**

BioMed Research International

---

## **Tissue Engineering and Oral Rehabilitation in the Stomatognathic System**

Guest Editors: Tomasz Gedrange, Christiane Kunert-Keil,  
Friedhelm Heinemann, and Marzena Dominiak



---

Copyright © 2017 Hindawi Publishing Corporation. All rights reserved.

This is a special issue published in “BioMed Research International.” All articles are open access articles distributed under the Creative Commons Attribution License, which permits unrestricted use, distribution, and reproduction in any medium, provided the original work is properly cited.

## Contents

---

**Tissue Engineering and Oral Rehabilitation in the Stomatognathic System**

Tomasz Gedrange, Christiane Kunert-Keil, Friedhelm Heinemann, and Marzena Dominiak  
Volume 2017, Article ID 4519568, 2 pages

**Assessment of Temperature Rise and Time of Alveolar Ridge Splitting by Means of Er:YAG Laser, Piezosurgery, and Surgical Saw: An Ex Vivo Study**

Jacek Matys, Rafał Flieger, and Marzena Dominiak  
Volume 2016, Article ID 9654975, 8 pages

**Hypothyroidism Affects Olfactory Evoked Potentials**

Teodor Świdziński, Kamila Linkowska-Świdzińska, Hanna Czerniejewska-Wolska, Bożena Wiskirska-Woźnica, Maciej Owecki, Maria Danuta Głowacka, Anna Frankowska, Katarzyna Łącka, Mariusz Glapiński, Zofia Maciejewska-Szaniec, and Piotr Świdziński  
Volume 2016, Article ID 9583495, 7 pages

**Bone Regeneration after Treatment with Covering Materials Composed of Flax Fibers and Biodegradable Plastics: A Histological Study in Rats**

Tomasz Gredes, Franziska Kunath, Tomasz Gedrange, and Christiane Kunert-Keil  
Volume 2016, Article ID 5146285, 8 pages

**Influence of Botulinumtoxin A on the Expression of Adult MyHC Isoforms in the Masticatory Muscles in Dystrophin-Deficient Mice (Mdx-Mice)**

Ute Ulrike Botzenhart, Constantin Wegenstein, Teodor Todorov, and Christiane Kunert-Keil  
Volume 2016, Article ID 7063093, 10 pages

**Long-Term Fatigue and Its Probability of Failure Applied to Dental Implants**

María Prados-Privado, Juan Carlos Prados-Frutos, Sérgio Alexandre Gehrke, Mariano Sánchez Siles, José Luis Calvo Guirado, and José Antonio Bea  
Volume 2016, Article ID 8927156, 8 pages

## Editorial

# Tissue Engineering and Oral Rehabilitation in the Stomatognathic System

**Tomasz Gedrange,<sup>1</sup> Christiane Kunert-Keil,<sup>1</sup>  
Friedhelm Heinemann,<sup>2</sup> and Marzena Dominiak<sup>3</sup>**

<sup>1</sup>*Department of Orthodontics, University Hospital TU Dresden, Fetscherstr. 74, 01307 Dresden, Germany*

<sup>2</sup>*Department of Prosthodontics, Gerodontology and Biomaterials, Medical University of Greifswald, Rotgerberstr. 8, 17487 Greifswald, Germany*

<sup>3</sup>*Department of Dental Surgery, Silesian Piast Medical University, 26 Krakowska St., 50-424 Wrocław, Poland*

Correspondence should be addressed to Christiane Kunert-Keil; [christiane.kunert-keil@uniklinikum-dresden.de](mailto:christiane.kunert-keil@uniklinikum-dresden.de)

Received 29 November 2016; Accepted 4 December 2016; Published 10 January 2017

Copyright © 2017 Tomasz Gedrange et al. This is an open access article distributed under the Creative Commons Attribution License, which permits unrestricted use, distribution, and reproduction in any medium, provided the original work is properly cited.

The stomatognathic system is a functional unit characterized by several structures: skeletal components, dental arches, soft tissues, and the temporomandibular joint and masticatory muscles. These structures act in harmony to perform different functional tasks (to speak, to break food down into small pieces, and to swallow). On the other hand, the various components of the stomatognathic system influence each other. The restoration of function of the various components of the stomatognathic system is a major focus of research from different disciplines. For that reason stomatognathic diseases are treated by dentists and maxillofacial surgeons as well as otorhinolaryngologists. Furthermore, the preservation of the masticatory muscles is nowadays also at the forefront of scientists.

The current special issue summarizes five articles of different research aspects on the highly topical field of tissue engineering and oral rehabilitation in head and neck area. The issue presents a wide range of findings from basic and clinical research with interdisciplinary contributors from clinics, specialist doctors, and biologists.

The preservation of the bone with bone substitute materials as well as autologous bone plays an important role. Although these topics are explored for some time, there are always new aspects and improvements. T. Gredes et al., in Germany, in “Bone Regeneration after Treatment with Covering Materials Composed of Flax Fibers and

Biodegradable Plastics: A Histological Study in Rats” have focused on bone regeneration using green biocomposites. These authors could demonstrate that composites from unmodified and transgenic modified flax fibers can be used as bone covering materials. The biocomposites prevent the growth of connective tissue into the bone defect.

Among other qualities of the bone, augmentation and surgical procedures play also an important role in the insertion of implants. Oral implantology is one of the fastest growing fields in oral rehabilitation. In implantology, minimally invasive surgical techniques are increasingly used, including piezosurgery. This is an ultrasound-assisted technique. During the operative preparation of the implantation bed, there is very often a strong heat development which can lead to thermal damage of the surrounding tissue. J. Matys et al. in Poland dealt with this topic “Assessment of Temperature Rise and Time of Alveolar Ridge Splitting by means of Er:YAG Laser, Piezosurgery, and Surgical Saw: An Ex Vivo Study.” They found no temperature rise on the bone over 10°C when using piezosurgery and Er:YAG laser as well as surgical saw and postulated that these surgical techniques are useful and safe for ridge splitting.

It is well known that a lot of factors can influence the osseointegration of dental implants and can cause dental implants failure. The manuscript by M. Prados-Privado et al. in Spain “Long-Term Fatigue and Its Probability of Failure

Applied to Dental Implants” highlighted different fatigue analysis based on a cumulative damage model and probabilistic finite elements. With these analyses the authors found worst behavior of cylindrical implants compared to conical implants.

Furthermore, the function and composition of orofacial muscles are important for the maintenance of oral function. Patients with muscle diseases may suffer severe malocclusions, feeding difficulties, and weight loss, because of progressively impairing orofacial function. Furthermore it is known that the loss of teeth is followed by functional loss of orofacial muscles. It is becoming evident that more data about the muscle regeneration process are needed to develop strategies for improving life quality of the patients. The article by U. U. Botzenhart et al. from Germany “Influence of Botulinumtoxin A on the Expression of Adult MyHC Isoforms in the Masticatory Muscles in Dystrophin-Deficient Mice” fits very well with this topic. The authors describe that the neurotoxin botulinum toxin A causes muscular atrophy with signs of dystrophic phenotype in healthy mice, while mice with inherited muscle weakness do not show any changes in the MyHC isoform expression.

Many metabolic or hormonal diseases can influence both bone metabolism and muscle function. This is known, among other things, for hypothyroidism, which can lead to diminished length growth of the bones and myopathy. The work is complemented by a work by T. Świdziński et al. in Poland “Hypothyroidism Affects Olfactory Evoked Potentials.” These authors were able to demonstrate that the sense of smell is also strongly impaired in patients with clinical hypothyroidism, whereas patients with subclinical hypothyroidism do not show any swelling difficulties compared to healthy patients.

In conclusion, this special issue summarized various aspects of regeneration from different parts of the stomatognathic system. Both the implantology and the large area of bone substitute materials are still propagated in the focus of science.

*Tomasz Gedrange  
Christiane Kunert-Keil  
Friedhelm Heinemann  
Marzena Dominiak*

## Research Article

# Assessment of Temperature Rise and Time of Alveolar Ridge Splitting by Means of Er:YAG Laser, Piezosurgery, and Surgical Saw: An Ex Vivo Study

Jacek Matys,<sup>1</sup> Rafał Flieger,<sup>2</sup> and Marzena Dominiak<sup>3</sup>

<sup>1</sup>Private Dental Healthcare, Ul. Lipowa 18, 67-400 Wschowa, Poland

<sup>2</sup>Private Dental Healthcare, Ul. Naclawska 11, 64-000 Kościan, Poland

<sup>3</sup>Department of Dental Surgery, Medical University of Wrocław, Ul. Krakowska 26, 50-425 Wrocław, Poland

Correspondence should be addressed to Jacek Matys; [jacek.matys@wp.pl](mailto:jacek.matys@wp.pl)

Received 18 April 2016; Revised 6 June 2016; Accepted 13 October 2016

Academic Editor: Gasparini Giulio

Copyright © 2016 Jacek Matys et al. This is an open access article distributed under the Creative Commons Attribution License, which permits unrestricted use, distribution, and reproduction in any medium, provided the original work is properly cited.

The most common adverse effect after bone cutting is a thermal damage. The aim of our study was to evaluate the bone temperature rise during an alveolar ridge splitting, rating the time needed to perform this procedure and the time to raise the temperature of a bone by 10°C, as well as to evaluate the bone carbonization occurrence. The research included 60 mandibles ( $n = 60$ ) of adult pigs, divided into 4 groups ( $n = 15$ ). Two vertical and one horizontal cut have been done in an alveolar ridge using Er:YAG laser with set power of 200 mJ (G1), 400 mJ (G2), piezosurgery unit (G3), and a saw (G4). The temperature was measured by K-type thermocouple. The highest temperature gradient was noted for piezosurgery on the buccal and lingual side of mandible. The temperature rises on the bone surface along with the increase of laser power. The lower time needed to perform ridge splitting was measured for a saw, piezosurgery, and Er:YAG laser with power of 400 mJ and 200 mJ, respectively. The temperature rise measured on the bone over 10°C and bone carbonization occurrence was not reported in all study groups. Piezosurgery, Er:YAG laser (200 mJ and 400 mJ), and surgical saw are useful and safe tools in ridge splitting surgery.

## 1. Introduction

The important condition for predictable and aesthetic implantation is the availability of sufficient surrounding and supporting hard and soft tissues [1]. Due to the significant loss of alveolar bone additionally surgical procedures are necessary [2]. Augmentation of the resorbed alveolar crest can be achieved, for example, with onlay bone grafts, membrane techniques, bone distraction, and ridge splitting [3].

Dr. Hilt Tatum 1970s introduced a method of ridge splitting or bone spreading using specific instruments like D-shaped graduated osteotomes/wedges and tapered channel formers [4]. Later, Summers [5], Scipioni et al. [6] in 1994, and Sethi and Kaus [7] in 2000 revived and published articles on edentulous ridge expansion with 97–98.8% implant survival rate for over 5 years. With the emergence of implant dentistry and introduction of micro saws, piezo saws, and specific ridge split osteotomy, this technique has become an integral

part of implant dentistry, wherein primarily bone expansion techniques were indicated in regions of division bone volume and density of D3 or D4. Bone due to its dynamic viscoelastic nature, thinner ridges (<3.5 mm) can be expanded with better controlled instrumentation with less risk for fracture, trauma, and bone perforations. The softer the trabecular bone quality, the lower the elastic modulus and the greater the viscoelastic nature of the ridge. Therefore, the lower the density of the bone, the easier and more predictable the bone expansion [8].

Lateral ridge split technique is a way to solve the problem of the width in narrow ridges with adequate height. Simultaneous insertion of dental implants will considerably reduce the edentulism time. Dental implant placement in atrophic ridges with deficiency in the bone volume with onlay bone-grafting techniques (autografts/allografts) needs some time between bone grafting and dental implant insertion (3–6 months) and there is always the possibility of bone graft failure. Crest split augmentation technique with simultaneous

implant insertion will reduce the time of edentulism treatment. Bone compression and increase in trabecular density are other advantages of this technique [9]. For creating split between the cortical plates, different osseous surgical tools such as hand instruments (chisels), rotary instruments (surgical burs, saws), and piezosurgery instruments have been used successfully [10].

The piezosurgery device produces specific ultrasound frequency modulation (22 000–35 000 Hz). The unit provides extreme precision and safety as well as micrometric cutting. Moreover, the device causes less bleeding during and after the operation and the healing process is shorter [11].

Thermodynamic effects in bone produced by bur were widely described in the literature [12–14]. But modern medical technology is still developing and in the last two decades the following gained more and more popularity: erbium-chromium: yttrium-scandium-gallium-garnet (Er,Cr:YSGG) and erbium: yttrium-aluminum-garnet (Er:YAG) lasers. These lasers operate in the infrared spectrum at a wavelength of 2.78 (Er,Cr:YSGG) and 2.94 (Er:YAG)  $\mu\text{m}$  and show good absorption in water; hence, these lasers afford good results in bone surgery [15, 16].

Extremely important during bone surgery is temperature rise, which is key factor for osseointegration process. When preparing and placing implants into a bone tissue, a non-traumatic surgical technique is critical. The heat generated during the preparation of the implant site is a major factor influencing surgery failure [17].

Eriksson and Albrektsson [18, 19] showed that increasing the temperature of the bone tissue by  $10^{\circ}\text{C}$  for 60 seconds induces permanent changes in the bone structure; therefore, the tissue temperature gradient ( $\Delta T_a$ ) below  $10^{\circ}\text{C}$  should be considered optimal and safe.

*Objective.* To the authors best knowledge, thermodynamics effects during alveolar ridge splitting were not described in the literature. The aim of the study was to evaluate temperature gradient on pig model during ridge splitting by means of Er:YAG laser, piezosurgery unit, and surgical saw. Additionally, time of ridge splitting procedure and carbonization occurrence were assessed.

## 2. Materials and Methods

*2.1. Samples Preparation.* The research included 60 mandibles ( $n = 60$ ) of recently slaughtered pigs (breed: *Złotnicka Biała*) intended for consumption and which had been obtained from a butcher. The skin of each mandible in the area between incisor (I1) and first molar (M1) tooth was cut off. The specimens were randomly divided in 4 groups ( $n = 15$ ) according to the ridge splitting method and then were washed under the tap water and left for 4 hours before the research was commenced. In every specimen, preparation of the soft tissues in region of canine (C) and first molar (P1) tooth gave access to the buccal and lingual part of the mandibular alveolar ridge. The specimens after preparation were placed motionless in a clamp. The ethical approval was not required for this animal ex vivo study.

*2.2. Surgical Procedure.* In the study area of the mandible a ridge splitting procedure has been done by two vertical cuts, 1 cm in length on the buccal side and 1 horizontal cut on the alveolar ridge 1 cm in length and 1 cm in depth by means of Er:YAG laser (LiteTouch®, Syneron Dental, Yokneam, Israel), piezosurgery unit (Piezotome Solo, Acteon, New Jersey, USA), and a saw disc (Hager & Meisinger GmbH, Hansemannstr., Germany) for a high-speed contra-angle hand piece (Intra C09-C3 27:1 Kavo, Biberach, Germany). In the buccal and lingual area of mandible  $2.5 \times 2.5$  mm holes were made in the bone with a ball-shaped diamond bur for a high-speed contra-angle hand piece (Intra C09-C3 27:1 Kavo, Biberach, Germany) operated with a physiodispenser (Intrasurg300®, Kavo, Biberach, Germany) for temperature measure (Figure 1).

*2.3. Measurement Procedure.* The specimens were placed in a container with water at a temperature of  $22^{\circ}\text{C}$  for 20 minutes; the temperature was monitored with a Medicare Clinical Products (MCP) Gold mercury thermometer (Medicare Products Inc., New Delhi, India). The temperature of the bone was measured by means of a calibrated digital Thermocouple Meter, TM-902C thermometer (Zhangzhou Weihua Electronic Co., Fujian, China) with the temperature probe of the K, Thermocouple Probe, TP-02 type (Zhangzhou Weihua Electronic Co., Fujian, China). The measurement error was 0.75%. The temperature was measured in a continuous manner by means of probes attached in the central point of the prepared bone holes on the buccal and lingual side of the mandible. The highest difference of the bone temperature was recorded. The time of the bone preparation was measured with a sports stopwatch SPI7 XL-009A (Fuzhou Swell Electronic Co., Ltd, Fujian, China).

*2.4. Study Groups.* The study specimens ( $n = 60$ ) were divided into 4 groups: G1 ( $n = 15$ ), G2 ( $n = 15$ ), G3 ( $n = 15$ ), and G4 ( $n = 15$ ).

G1 group: Er:YAG laser (LiteTouch, Syneron Dental, Yokneam, Israel), operation mode for hard tissues (HT), was used, power: 200 mJ, frequency: 30 Hz, energy density per pulse:  $15.07 \text{ J}/\text{cm}^2$ , water spray cooling (100%): 14 mL/min., tip angle set at  $70^{\circ}$ , size of the tip:  $1.3 \times 6$  mm, and distance: 10 mm.

G2 group: Er:YAG laser (LiteTouch, Syneron Dental, Yokneam, Israel), operation mode for hard tissues (HT), was used, power: 400 mJ, frequency: 19 Hz, energy density per pulse:  $30.14 \text{ J}/\text{cm}^2$ , water spray cooling (100%): 14 mL/min., tip angle set at  $70^{\circ}$ , size of the tip:  $1.3 \times 6$  mm, and distance: 10 mm.

G3 group: piezosurgery unit (Piezotome Solo, Acteon, New Jersey, USA) was used: the parameters of the piezosurgery: tip: BSIS (cortical bone), CS1 (cutting depth), power: D1, and water spray cooling: 20 mL/min.

G4 group (control): tip: saw disc (Hager & Meisinger GmbH, Hansemannstr, Germany), saw diameter:

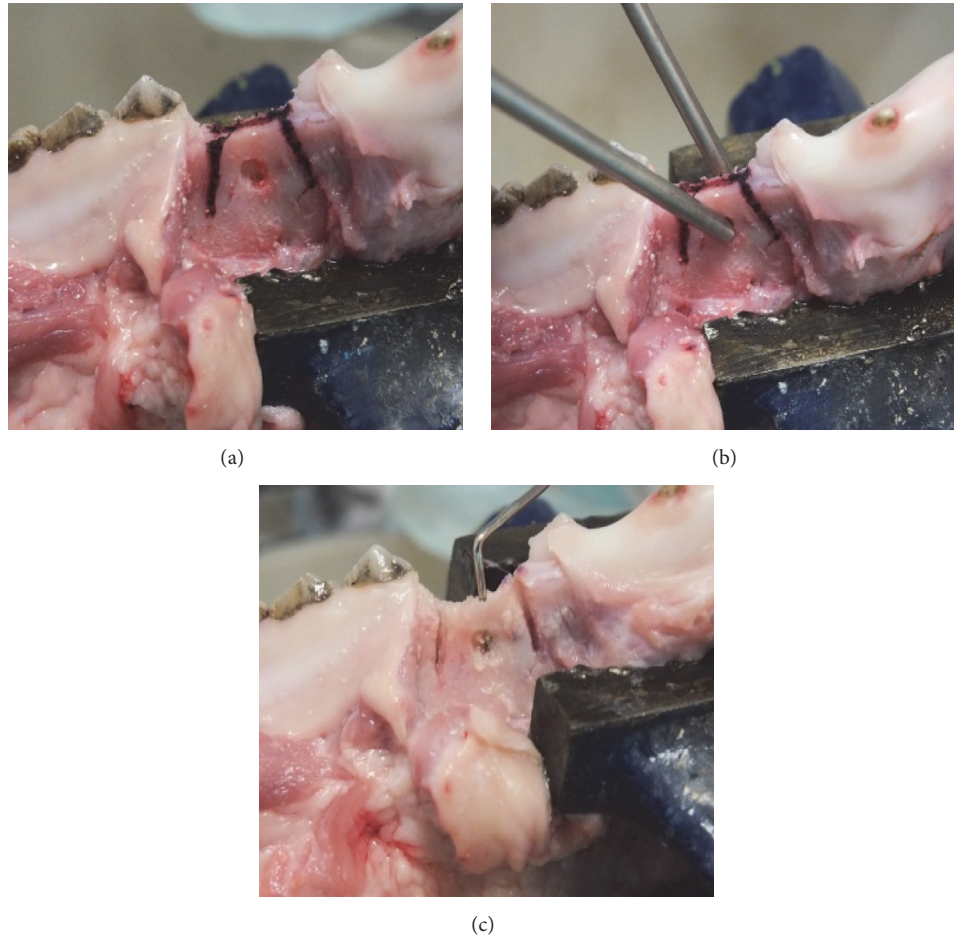


FIGURE 1: Monitoring and measurement of reaction to changes in temperature of the bone. (a) An alveolar ridge with cutting marks. (b) The thermocouples attached to the bone. (c) The control of osteotomies depth with a periodontal probe.

10 mm, speed: 1000 rpm, and water spray cooling: 20 mL/min.

2.4.1. *Statistical Analysis.* The statistical analysis was performed by means of ANOVA variance analysis and *t*-test with the use of the programme Statistica 12 (StatSoft, Krakow, Poland) with free 30-day trial license. Values below  $P = 0.05$  were considered to be statistically significant.

### 3. Results

An analysis of temperature gradient on bone surfaces revealed significant higher rise for piezosurgery (G3) on both lingual and buccal sides of an alveolar ridge as compared to Er:YAG laser (200 mJ, 400 mJ) and a saw (G4) (Table 1). The mean bone temperature increases during osteotomies using surgical saw were lower than in cases when the Er:YAG laser and piezosurgery were used. Furthermore, the temperature gradient measured in the lingual region of the mandible was significant lower as compared to the buccal part for each group. The bone cutting by means of piezosurgery caused much more temperature increases in the lingual region of a

TABLE 1: Mean temperature gradient and standard deviation data measured in buccal and lingual sides of an alveolar ridge.

Variable	$\Delta T_a$ ( $^{\circ}\text{C}$ ) $\pm$ SD buccal	$\Delta T_a$ ( $^{\circ}\text{C}$ ) $\pm$ SD lingual	<i>P</i> value (buccal versus lingual area)
Group 1 ( $n = 15$ )	$2.23 \pm 0.47$	$1.19 \pm 0.49$	0,0000021
Group 2 ( $n = 15$ )	$3.49 \pm 0.54$	$2.09 \pm 0.27$	0,0000927
Group 3 ( $n = 15$ )	$6.19 \pm 0.70$	$3.17 \pm 0.35$	0,0000775
Group 4 ( $n = 15$ )	$0.93 \pm 0.27$	$0.53 \pm 0.21$	0,0000966

mandible even when comparing with an Er:YAG laser with energy set of 200 mJ and a saw on the buccal side.

A significant bone temperature increase was observed following Er:YAG laser irradiation and a piezosurgery operation as compared to the saw in the buccal area of the mandible (Figure 2). Depending on the cutting device used, significant differences in bone temperature rise on the lingual side of an alveolar ridge between each group were also observed. Our findings show that following bone cutting with the Er:YAG laser, piezosurgery, and saw, the bone temperature on buccal

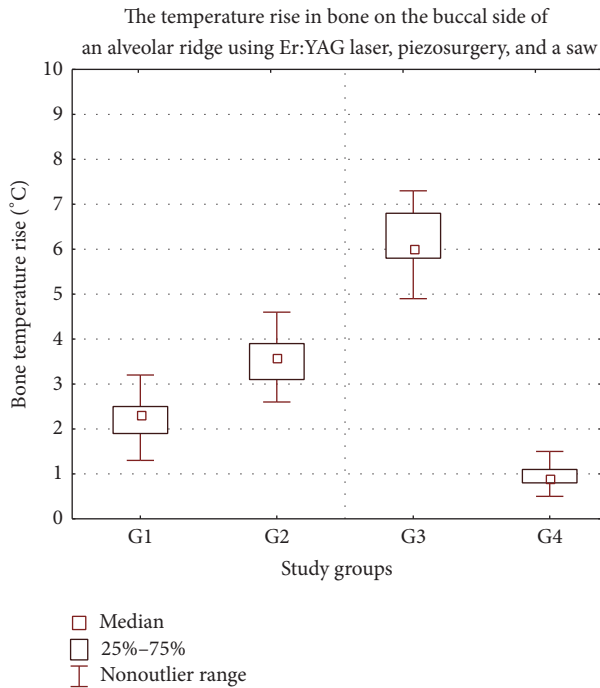


FIGURE 2: Increase in the temperature of the bone prepared with laser and saw in the buccal side of an alveolar ridge of a mandible. G1 (Er:YAG 200 mJ), G2 (Er:YAG 400 mJ), G3 (piezosurgery), and G4 (saw). °C: Celsius grade.

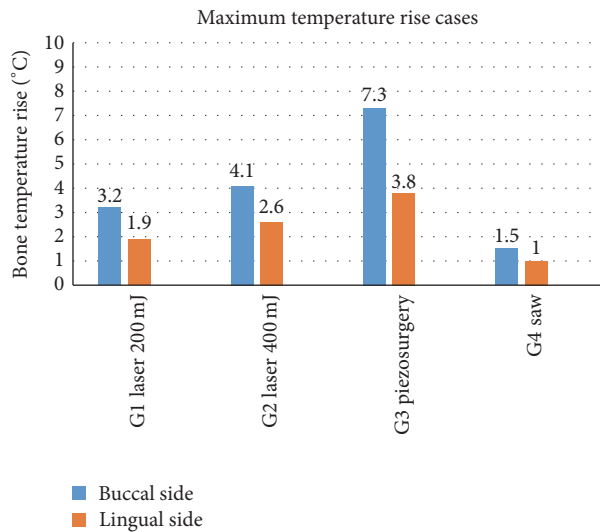


FIGURE 3: The highest results in temperature increase measured on the buccal and lingual side of an alveolar ridge of a mandible. °C: Celsius grade.

side increased much more rapidly than it measured on the lingual side.

The maximum bone temperature of 7.3°C was noted for a specimen prepared using piezosurgery device (Figure 3). Additionally, the maximum temperature of none of the mandible rose by more than 10°C when applying different

TABLE 2: Mean time required to perform mandibular ridge splitting. The results showed significant differences in comparison with ridge splitting time in comparison between each group, respectively ( $P < 0.05$ ).

Study groups	Time $t$ (sec) $\pm$ SD
Group 1 ( $n = 15$ )	538.47 $\pm$ 70
Group 2 ( $n = 15$ )	360.73 $\pm$ 58.03
Group 3 ( $n = 15$ )	305.13 $\pm$ 54.84
Group 4 ( $n = 15$ )	172.07 $\pm$ 41.56
$P$	<0.05

devices used in this study. Furthermore, the bone temperature after irradiation with an Er:YAG laser for energy of 400 mJ raised more quickly in comparison with the cases of energy equal 200 mJ.

The analysis of the ridge splitting time revealed significant differences in time needed for the bone osteotomies using Er:YAG laser and a piezosurgery as compared to the saw. Furthermore, significant differences in ridge splitting time depending on the cutting device used were also observed (Table 2). The time needed to perform a ridge splitting following an Er:YAG laser with power of 200 mJ and 400 mJ was 3- and 2-times longer as compared to the saw, respectively.

We also observed no signs of carbonization occurrence during bone cutting by means of Er:YAG laser, piezosurgery, and surgical saw.

#### 4. Discussion

To the best of our knowledge, the comparison of Er:YAG laser, piezosurgery device, and saw on contra-angle for ridge bone splitting has not been discussed in the literature.

Heat is defined as a process in which energy flows from hot to cold objects. Despite the simple definition, heat transfer is an extremely complex physical phenomenon to analyze. A great deal of research has been expended to measure heat production during bone cutting with different techniques. Several important issues arise when dealing with temperature recording in bone tissue concerning the measuring device, the distance of the thermometer probe from the heat source, the cooling system, and the thermal properties of bone (e.g., type and shape of bone samples, thermal conductivity, and heat capacity). To overcome the limits related to the large number of factors at stake, a proper methodological approach and dedicated technical environment are essential [20].

In 2011, Rashad et al. [21] and Esteves et al. [22] prepared implant bed using two different ultrasonic devices (Piezosurgery, Mectron Medical Technology and VarioSurg, NSK) and one conventional drill. Result of their research showed that the heat production and time required for implant site preparation using both ultrasonic devices were significantly higher than those for conventional drilling ( $P < 0.01$ ). Our study showed similar results for piezosurgery compared to the surgery saw during bone osteotomies.

Moreover, Agrawal et al. [23] suggested piezoelectric devices advantage over traditional methods of alveolar bone splitting due to the factors such as micrometric bone cut,

clear surgical field, and selective cut. The authors emphasized that the piezosurgery device which operates with modulated ultrasound micro movements with oscillating frequency from 29 to 32 kHz, making it specifically suitable for osteotomies but not for a soft tissue cutting. According to researchers maximum surgical visibility is allowed during osteotomy, thanks to cavitation effect of the sterile saline. Stübinger et al. [24] also underlined advantage of piezoelectric unit over conventional rotary instruments in ridge splitting osteotomy. The authors drew attention to the biological aspects associated with the use of this type of devices. In their opinion one of the main benefits of using piezosurgery is reduced blood loss which improves healing conditions. Furthermore the constant irrigation helps to reduce thermal damage and thus reduces the risk of bone necrosis.

However, histopathological examination carried out by the Esteves et al. [22] on the rat bone exposed to create defects of 2 mm in diameter by using piezosurgery (piezo group) and conventional drilling (drill group) revealed that bone healing was similar in both groups with the exception of a slightly higher amount of newly formed bone observed at 30 days after surgery ( $P < 0.05$ ). Ma et al. [25] in their studies reached similar conclusions. The purpose of their study was to compare bone healing of experimental osteotomies applying either piezosurgery or two different oscillating saw blades in a rabbit model. Authors claimed that all three osteotomy techniques revealed an advanced gap healing starting after one week. The most pronounced new bone formation took place between two and three weeks, whereby piezoelectric surgery revealed a tendency to faster bone formation and remodeling.

Our study which has taken into account an increase in temperature of the bone also has demonstrated the advantage of using piezosurgery as compared to conventional methods based on the rotary instruments in bone surgery.

In 2015 Rashad et al. [26] showed different result in comparison with temperature rise among sonic, ultrasonic, and conventional drills. Results of their newer findings were associated with lower heat generation compared to the conventional saw osteotomy. Copious irrigation seems to play a critical role in preventing heat generation in the osteotomy site. Lamazza et al. [27] described temperature gradient rise during piezoelectric implant bed preparation. Their study showed temperature gradient increase lower by  $10^{\circ}\text{C}$  after one minute of piezosurgery working. Our findings showed similar results.

Pandurić et al. [28] compared an Er:YAG laser (pulse energy, 1,000 mJ; pulse duration, 300  $\mu\text{s}$ ; frequency, 20 Hz) and surgical drill for osteotomy in oral surgery. The temperature rise and time were assessed in their study. The Er:YAG laser removed significantly more bone tissue than the drill ( $P < 0.01$ ) in a significantly shorter time ( $P < 0.01$ ). Also the temperature was statistically lower during the laser preparation. Results are different than our findings. In another in vitro study on mandibular bones irradiated by an Er,Cr:YSGG laser Kimura et al. [29] stated that a temperature rise over  $10^{\circ}\text{C}$  ( $\Delta\text{Ta}$ ) could be recorded 30 s after laser

application. In our study a temperature rise over  $10^{\circ}\text{C}$  has not been recorded.

Romeo et al. [30] compared the peripheral bone damage induced by different cutting systems. The Er:YAG laser, piezosurgery, and high-speed and low speed drill have been utilized in their research. Four different parameters were analyzed: cut precision, depth of incision, peripheral carbonization, and presence of bone fragments. All sections obtained with the Er:YAG laser showed poor peripheral carbonization. The sections obtained by traditional drilling also showed poor peripheral carbonization. Piezosurgery incisions showed superficial incisions without thermal signs but with irregular margins. The level of carboxylation was evaluated with an optical microscope. The results of our study were similar. Making the optical evaluation by sight, we have not found carbonization in tested samples.

Results of our findings are also in coinciding with studies conducted by Lewandrowski et al. [31]. They compared the interaction of Er:YAG laser and traditional saw on the bone tissue. Based on the assessment of collected histological samples, they concluded that extent of thermal damage at the osteotomy sites was comparable for laser and mechanically saws.

Yoshino et al. [32] also in their study showed no severe thermal damage for Er:YAG laser compared to electro-surgery. Er:YAG laser irradiation without water coolant easily ablated bone tissue, and thermal alteration in the treated surface was minimal. In our studies for all specimens the thermal damage and carbonization of the bone have been not reported. Also results of lack of or minimal thermal damage in their research were similar to those of Martins et al. [33], Papadaki et al. [34], and Li et al. [35].

Stübinger [36], exchanging basic clinical benefits of using Er:YAG laser, stressed that in contrast to conventional osteotomy an Er:YAG laser enables noncontact interventions, no mechanical vibration, free and elaborate cut geometries, and aseptic effects. Passi et al. [37] also appreciated clinical benefits of Er:YAG laser in bone surgery compared to traditional drill method. Their study comprised 40 subjects requiring removal of impacted mandibular third molar, randomly categorized into two equal groups of 20 each, who had their impacted third molar removed either using Er:YAG laser or surgical bur as per their group, using standard methodology of extraction of impacted teeth. In next step they evaluated clinical parameters such as bleeding, pain, time taken for bone cutting, trismus, postoperative swelling, wound healing, and complications. Their study found that clinical parameters like bleeding, pain, and swelling were significantly lower in laser group than in the bur group. Wound healing and complications were assessed clinically and there was no significant difference in both the groups. Additionally, the laser group required almost double the time taken for bone cutting than bur. Stübinger et al. [38] demonstrated similar mind about the runtime of bone surgery using the Er:YAG laser. They emphasized that laser osteotomy was time-intensive and offered no depth control, and therefore it demonstrated only slight advantages for intraoral bone-grafting technics.

In our study, the time needed to carry out the alveolar ridge splitting on an animal model was also the highest for the laser group.

Many surgical techniques were adopted for a bone extension procedure. The bone ridge splitting is a surgical technique included an implant placement and guided bone regeneration in 1 stage. The ridge expansion technique in 1 stage was suggested as an alternative to horizontal and vertical augmentation techniques. The ridge splitting technique and osteodistractor are considered efficient to increase bone width with lower failure rate [39, 40]. The use of the osteotomes in a less dense bone (D3, D4) allows fracturing of bone trabeculae [41, 42]. However, this technique does not ameliorate peri-implant bone density. It was shown by Büchter et al. [43] that fractured trabeculae in a peri-implant bone, caused using the osteotome technique, induce a delayed secondary stability in comparison with conventional drilling protocol.

After alveolar ridge extension using saws and screw type osteotomes some proportion of bone undergoes necrosis due to interruption of the Havers' and Volkmann's canals. Vascular interruption, caused by drilling and cutting the bone, leads to necrosis of the osteocytes and thus to bone devitalization [44]. Also a temperature increase in bone over 10°C leads to death of osteocytes and to bone necrosis; thus, precise knowledge concerning the heat generation induced by laser, piezosurgery device, and a saw seems to be key factor of therapeutic success after ridge splitting procedure. All these facts together make variable ridge extension protocols using modern bone cutting devices necessary.

The recent study's showed superiority of Er:YAG during bone surgery, as compared to diode, Nd:YAG, KTP lasers. Fornaini et al. [45] pointed out the lower increase for Er:YAG and higher for diode laser. Their ex vivo study showed that laser utilization gives no risks of dangerous thermal elevation to the tissues. The key factors for preparing the bone and soft tissue by use of Er:YAG lasers are type of laser (Gaussian distribution of energy), short laser pulses duration, low power of laser beam, fluid pumping technology (fluid pressure), time of emission of a laser beam, and type of laser tip. Er:YAG laser without optic fiber and with rectangular energy distribution profile generate high uniform power with regard to the beam and with low energy losses during transport. In most of the presently used lasers, the energy beam is transported to the tip by means of an optic fiber, which distorts the energy distribution. In such lasers, the highest energy is located only in the middle of the beam and it is much lower at the edges. Concentration of the beam power in the very centre (older technology) with relatively low power and high frequency settings may cause thermal damage in the bone. A new laser technology results in reductions of Er:YAG laser defects, for example, overheating and carbonization [46, 47].

Furthermore in our study the Magnum tip 1.3 mm in diameter and 6 mm in length was used. This is the only one tip which allows transferring laser light without its defocusing. Therefore this tip does not change laser beam distribution of energy from flat-top to Gaussian profile as compared to glass optic fiber. Hence, higher energy density irradiated

target tissue in shorter time causes less thermal damage. Thus, quantity of energy irradiated on the target area is the most productive and ablation of the tissue is fast and cuts are clean without carbonation effects. Further studies should be conducted to establish predictable and safe clinical protocol of different procedures in laser surgery. Additionally, an influence of tip size on temperature change in the bone should be evaluated.

## 5. Conclusions

The Er:YAG laser has great potential in advancing surgical techniques where precision in osseous preparation is required. Piezosurgery, Er:YAG laser, and surgical saw are useful and safe tools in ridge splitting surgery. For all devices the temperature rise was below 10°C, which confirmed safeness and predictability of these methods.

## Competing Interests

The authors declare that they have no competing interests.

## References

- [1] W. Bednarz, "The thickness of periodontal soft tissue ultrasonic examination—current possibilities and perspectives," *Dental and Medical Problems*, vol. 48, no. 3, pp. 303–310, 2011.
- [2] B. Ella, M. Laurentjoye, C. Sedarat, J.-C. Coutant, E. Masson, and A. Rouas, "Mandibular ridge expansion using a horizontal bone-splitting technique and synthetic bone substitute: an alternative to bone block grafting?" *The International Journal of Oral & Maxillofacial Implants*, vol. 29, no. 1, pp. 135–140, 2014.
- [3] N. S. Rajput, J. Bhaskar, M. Valiathan, S. C. Chandrasekaran, and M. N. Alam, "Placement of dental implant in a knife edge ridge in anterior aesthetic zone," *Journal of Clinical and Diagnostic Research*, vol. 7, no. 10, pp. 2376–2377, 2013.
- [4] H. Tatum Jr., "Maxillary and sinus implant reconstructions," *Dental clinics of North America*, vol. 30, no. 2, pp. 207–229, 1986.
- [5] R. B. Summers, "A new concept in maxillary implant surgery: the osteotome technique," *Compendium*, vol. 15, no. 2, pp. 152–162, 1994.
- [6] A. Scipioni, G. B. Bruschi, and G. Calesini, "The edentulous ridge expansion technique: a five-year study," *The International Journal of Periodontics & Restorative Dentistry*, vol. 14, no. 5, pp. 451–459, 1994.
- [7] A. Sethi and T. Kaus, "Maxillary ridge expansion with simultaneous implant placement: 5-year results of an ongoing clinical study," *The International Journal of Oral & Maxillofacial Implants*, vol. 15, no. 4, pp. 491–499, 2000.
- [8] R. Mechery, N. Thiruvalluvan, and A. Sreehari, "Ridge split and implant placement in deficient alveolar ridge: case report and an update," *Contemporary Clinical Dentistry*, vol. 6, no. 1, pp. 94–97, 2015.
- [9] A. Rahpeyma, S. Khajehahmadi, and V. R. Hosseini, "Lateral ridge split and immediate implant placement in moderately resorbed alveolar ridges: how much is the added width?" *Journal of Dental Research*, vol. 10, no. 5, pp. 602–608, 2013.

- [10] O. Moses, Y. Blasbalg, and R. Herzberg, "Split crest to enlarge horizontal dimension of alveolar ridge. An overview of techniques and case demonstration," *Refuat Hapeh Vehashinayim*, vol. 28, no. 1, pp. 53–78, 2011.
- [11] M. Rahnama, Ł. Czupkałło, L. Czajkowski, J. Graszka, and J. Wallner, "The use of piezosurgery as an alternative method of minimally invasive surgery in the authors' experience," *Wideochirurgia i Inne Techniki Maloinwazyjne*, vol. 8, no. 4, pp. 321–326, 2013.
- [12] C. J. Kerawala, I. C. Martin, W. Allan, and E. D. Williams, "The effects of operator technique and bur design on temperature during osseous preparation for osteosynthesis self-tapping screws," *Oral Surgery, Oral Medicine, Oral Pathology, Oral Radiology, and Endodontics*, vol. 88, no. 2, pp. 145–150, 1999.
- [13] S. Kondo, Y. Okada, H. Iseki et al., "Thermological study of drilling bone tissue with a high-speed drill," *Neurosurgery*, vol. 46, no. 5, pp. 1162–1168, 2000.
- [14] W. Allan, E. D. Williams, and C. J. Kerawala, "Effects of repeated drill use on temperature of bone during preparation for osteosynthesis self-tapping screws," *British Journal of Oral and Maxillofacial Surgery*, vol. 43, no. 4, pp. 314–319, 2005.
- [15] E. C. Sung, T. Chenard, A. A. Caputo, M. Amodeo, E. M. Chung, and I. M. Rizoiu, "Composite resin bond strength to primary dentin prepared with ER,CR:YSSG laser," *Journal of Clinical Pediatric Dentistry*, vol. 30, no. 1, pp. 45–50, 2005.
- [16] I. M. Rizoiu, L. R. Eversole, and A. I. Kimmel, "Effects of an erbium, chromium: yttrium, scandium, gallium, garnet laser on mucocutaneous soft tissues," *Oral Surgery, Oral Medicine, Oral Pathology, Oral Radiology, and Endodontics*, vol. 82, no. 4, pp. 386–395, 1996.
- [17] S. K. Mishra and R. Chowdhary, "Heat generated by dental implant drills during osteotomy—a review: heat generated by dental implant drills," *The Journal of Indian Prosthodontist Society*, vol. 14, no. 2, pp. 131–143, 2014.
- [18] A. R. Eriksson and T. Albrektsson, "Temperature threshold levels for heat-induced bone tissue injury: a vital-microscopic study in the rabbit," *The Journal of Prosthetic Dentistry*, vol. 50, no. 1, pp. 101–107, 1983.
- [19] T. Albrektsson and A. Eriksson, "Thermally induced bone necrosis in rabbits: relation to implant failure in humans," *Clinical Orthopaedics and Related Research*, vol. 195, pp. 311–312, 1985.
- [20] G. E. Chacon, D. L. Bower, P. E. Larsen, E. A. McGlumphy, and F. M. Beck, "Heat production by 3 implant drill systems after repeated drilling and sterilization," *Journal of Oral and Maxillofacial Surgery*, vol. 64, no. 2, pp. 265–269, 2006.
- [21] A. Rashad, A. Kaiser, N. Prochnow, I. Schmitz, E. Hoffmann, and P. Maurer, "Heat production during different ultrasonic and conventional osteotomy preparations for dental implants," *Clinical Oral Implants Research*, vol. 22, no. 12, pp. 1361–1365, 2011.
- [22] J. C. Esteves, E. Marcantonio Jr., A. P. de Souza Faloni et al., "Dynamics of bone healing after osteotomy with piezosurgery or conventional drilling—histomorphometrical, immunohistochemical, and molecular analysis," *Journal of Translational Medicine*, vol. 11, article 221, 2013.
- [23] D. Agrawal, A. S. Gupta, V. Newaskar, A. Gupta, S. Garg, and D. Jain, "Narrow ridge management with ridge splitting with piezotome for implant placement: report of 2 cases," *The Journal of Indian Prosthodontist Society*, vol. 14, no. 3, pp. 305–309, 2014.
- [24] S. Stübinger, A. Stricker, and B.-I. Berg, "Piezosurgery in implant dentistry," *Clinical, Cosmetic and Investigational Dentistry*, vol. 7, pp. 115–124, 2015.
- [25] L. Ma, S. Stübinger, X. L. Liu, U. A. Schneider, and N. P. Lang, "Healing of osteotomy sites applying either piezosurgery or two conventional saw blades: a pilot study in rabbits," *International Orthopaedics*, vol. 37, no. 8, pp. 1597–1603, 2013.
- [26] A. Rashad, P. Sadr-Eshkevari, M. Heiland et al., "Intraosseous heat generation during sonic, ultrasonic and conventional osteotomy," *Journal of Cranio-Maxillo-Facial Surgery*, vol. 43, no. 7, pp. 1072–1077, 2015.
- [27] L. Lamazza, D. Laurito, M. Lollobrigida, O. Brugnoletti, G. Garreffa, and A. De Biase, "Identification of possible factors influencing temperatures elevation during implant site preparation with piezoelectric technique," *Annali di Stomatologia*, vol. 5, no. 4, pp. 115–122, 2014.
- [28] D. G. Pandurić, I. Bago, D. Katanec, J. Žabkar, I. Miletić, and I. Anić, "Comparison of Er:YAG Laser and surgical drill for osteotomy in oral surgery: An Experimental Study," *Journal of Oral and Maxillofacial Surgery*, vol. 70, no. 11, pp. 2515–2521, 2012.
- [29] Y. Kimura, D. G. Yu, A. Fujita et al., "Effects of erbium, chromium YSSG laser," *Journal of the California Dental Association*, vol. 72, article 1178, 2001.
- [30] U. Romeo, A. Del Vecchio, G. Palata, G. Tenore, P. Visca, and C. Maggiore, "Bone damage induced by different cutting instruments—an in vitro study," *Brazilian Dental Journal*, vol. 20, no. 2, pp. 162–168, 2009.
- [31] K.-U. Lewandrowski, C. Lorente, K. T. Schomacker, T. J. Flotte, J. W. Wilkes, and T. F. Deutsch, "Use of the Er:YAG laser for improved plating in maxillofacial surgery: comparison of bone healing in laser and drill osteotomies," *Lasers in Surgery and Medicine*, vol. 19, no. 1, pp. 40–45, 1996.
- [32] T. Yoshino, A. Aoki, S. Oda et al., "Long-term histologic analysis of bone tissue alteration and healing following Er:YAG laser irradiation compared to electrosurgery," *Journal of Periodontology*, vol. 80, no. 1, pp. 82–92, 2009.
- [33] G. L. Martins, E. Puricelli, C. E. Baraldi, and D. Ponzoni, "Bone healing after bur and Er:YAG laser osteotomies," *Journal of Oral and Maxillofacial Surgery*, vol. 69, no. 4, pp. 1214–1220, 2011.
- [34] M. Papadaki, A. Doukas, W. A. Farinelli, L. Kaban, and M. Troulis, "Vertical ramus osteotomy with Er:YAG laser: a feasibility study," *International Journal of Oral and Maxillofacial Surgery*, vol. 36, no. 12, pp. 1193–1197, 2007.
- [35] Z.-Z. Li, L. Reinisch, and W. P. Van de Merwe, "Bone ablation with Er:YAG and CO<sub>2</sub> laser: study of thermal and acoustic effects," *Lasers in Surgery and Medicine*, vol. 12, no. 1, pp. 79–85, 1992.
- [36] S. Stübinger, "Advances in bone surgery: the Er:YAG laser in oral surgery and implant dentistry," *Clinical, Cosmetic and Investigational Dentistry*, vol. 2, pp. 47–62, 2010.
- [37] D. Passi, U. S. Pal, S. Mohammad et al., "Laser vs bur for bone cutting in impacted mandibular third molar surgery: a randomized controlled trial," *Journal of Oral Biology and Craniofacial Research*, vol. 3, no. 2, pp. 57–62, 2013.
- [38] S. Stübinger, C. Landes, O. Seitz, and R. Sader, "Er:YAG laser osteotomy for intraoral bone grafting procedures: a case series with a fiber-optic delivery system," *Journal of Periodontology*, vol. 78, no. 12, pp. 2389–2394, 2007.
- [39] A. Stricker, J. Fleiner, S. Stübinger, R. Schmelzeisen, M. Dard, and D. D. Bosshardt, "Bone loss after ridge expansion with or

- without reflection of the periosteum,” *Clinical Oral Implants Research*, vol. 26, no. 5, pp. 529–536, 2015.
- [40] Y.-L. Tang, J. Yuan, Y.-L. Song, W. Ma, X. Chao, and D.-H. Li, “Ridge expansion alone or in combination with guided bone regeneration to facilitate implant placement in narrow alveolar ridges: a retrospective study,” *Clinical Oral Implants Research*, vol. 26, no. 2, pp. 204–211, 2015.
- [41] M. M. Shalabi, J. G. C. Wolke, A. J. E. de Ruijter, and J. A. Jansen, “A mechanical evaluation of implants placed with different surgical techniques into the trabecular bone of goats,” *Journal of Oral Implantology*, vol. 33, no. 2, pp. 51–58, 2007.
- [42] M. M. Shalabi, J. G. C. Wolke, A. J. E. De Ruijter, and J. A. Jansen, “Histological evaluation of oral implants inserted with different surgical techniques into the trabecular bone of goats,” *Clinical Oral Implants Research*, vol. 18, no. 4, pp. 489–495, 2007.
- [43] A. Büchter, J. Kleinheinz, H. P. Wiesmann et al., “Biological and biomechanical evaluation of bone remodelling and implant stability after using an osteotome technique,” *Clinical Oral Implants Research*, vol. 16, no. 1, pp. 1–8, 2005.
- [44] P. Trisi, M. Berardini, A. Falco, and M. P. Vulpiani, “Effect of implant thread geometry on secondary stability, bone density, and bone-to-implant contact: a biomechanical and histological analysis,” *Implant Dentistry*, vol. 24, no. 4, pp. 384–391, 2015.
- [45] C. Fornaini, E. Merigo, P. Vescovi et al., “Different laser wavelengths comparison in the second-stage implant surgery: an ex vivo study,” *Lasers in Medical Science*, vol. 30, no. 6, pp. 1631–1639, 2015.
- [46] J. Matys, M. Dominiak, and R. Flieger, “Energy and power density: a key factor in lasers studies,” *Journal of Clinical and Diagnostic Research*, vol. 9, no. 12, pp. ZL01–ZL02, 2015.
- [47] J. Matys, U. Botzenhart, T. Gedrange, and M. Dominiak, “Thermodynamic effects after Diode and Er:YAG laser irradiation of grade IV and V titanium implants placed in bone—an ex vivo study. Preliminary report,” *Biomedical Engineering/ Biomedizinische Technik*, vol. 61, no. 5, 2016.

## Research Article

# Hypothyroidism Affects Olfactory Evoked Potentials

**Teodor Świdziński,<sup>1</sup> Kamila Linkowska-Świdzińska,<sup>2</sup>  
Hanna Czerniejewska-Wolska,<sup>3</sup> Bożena Wiskirska-Woźnica,<sup>3</sup> Maciej Owecki,<sup>4</sup>  
Maria Danuta Głowacka,<sup>5</sup> Anna Frankowska,<sup>5</sup> Katarzyna Łącka,<sup>4</sup>  
Mariusz Glapiński,<sup>6</sup> Zofia Maciejewska-Szaniec,<sup>6</sup> and Piotr Świdziński<sup>3</sup>**

<sup>1</sup>Department of Biophysics, ul. Fredry 10, 61-701 Poznań, Poland

<sup>2</sup>Department of Conservative Dentistry and Periodontology, University of Medical Sciences, ul. Bukowska 70, 60-567 Poznań, Poland

<sup>3</sup>Department of Phoniatics and Audiology, University of Medical Sciences, ul. Przybyszewskiego 49, 60-355 Poznań, Poland

<sup>4</sup>Department of Endocrinology, Metabolism and Internal Medicine, University of Medical Sciences, ul. Przybyszewskiego 49, 60-355 Poznań, Poland

<sup>5</sup>Department of Organization and Management in Health Care, University of Medical Sciences, ul. Smoluchowskiego 11, 60-179 Poznań, Poland

<sup>6</sup>Department of Oral Rehabilitation, Division of Prosthodontics, University of Medical Sciences, ul. Bukowska 70, 60-567 Poznań, Poland

Correspondence should be addressed to Kamila Linkowska-Świdzińska; [kamila.swidzinska@gmail.com](mailto:kamila.swidzinska@gmail.com)

Received 18 April 2016; Revised 23 June 2016; Accepted 11 July 2016

Academic Editor: Christiane Kunert-Keil

Copyright © 2016 Teodor Świdziński et al. This is an open access article distributed under the Creative Commons Attribution License, which permits unrestricted use, distribution, and reproduction in any medium, provided the original work is properly cited.

**Background.** Objective electrophysiological methods for investigations of the organ of smell consist in recordings of olfactory cortex responses to specific, time restricted odor stimuli. In hypothyroidism have impaired sense of smell. **Material and Methods.** Two groups: control of 31 healthy subjects and study group of 21 with hypothyroidism. The inclusion criterion for the study group was the TSH range from 3.54 to 110  $\mu$ IU/mL. **Aim.** Assessment of the latency time of evoked responses from the olfactory nerve N1 and the trigeminal nerve N5 using two smells of mint and anise in hypothyroidism. **Results.** The smell perception in subjective olfactory tests was normal in 85% of the hypothyroid group. Differences were noticed in the objective tests. The detailed intergroup analysis of latency times of recorded cortical responses  $P_{N5}$  and  $P_{N1}$  performed by means between the groups of patients with overt clinical hypothyroidism versus subclinical hypothyroidism demonstrated a significant difference ( $p < 0.05$ ) whereas no such differences were found between the control group versus subclinical hypothyroidism group ( $p > 0.05$ ). **Conclusion.** We can conclude that registration of cortex potentials at irritation of olfactory and trigeminal nerves offers possibilities for using this method as an objective indicator of hypothyroidism severity and prognostic process factor.

## 1. Introduction

Hypothyroidism, condition in which the thyroid fails to produce a sufficient amount of hormones, manifests itself mainly in the form of general constitutional symptoms such as fatigue, constipation, increased sensitivity to cold, weight gain, thinning hair, skin dryness, and hoarseness of voice. The symptoms of a nervous system disorder, most frequently in the form of peripheral neuropathy, do not manifest themselves in a way that significantly impairs the patient's ability.

Peripheral neuropathy may occur particularly in the course of severe and persistent untreated hypothyroidism. Although the relationship between hypothyroidism and peripheral neuropathy is not entirely understood, it is known that hypothyroidism may cause fluid retention in the tissues and thus exert pressure on peripheral nerves [1–3].

Peripheral neuropathy may, in turn, be one of the causes of olfactory disorders. The studies by Mackay-Sim and Beard conducted on mice indicate that thyroxine is necessary for normal development of the nervous system,

including the genesis of new olfactory receptor neurons [4, 5]. Although hypothyroidism disrupts development of the olfactory epithelium, it does not cause however complete atrophy of neurons [6]. Olfactory disorders are most frequently caused by conduction disorders of the sensory stimulus mainly due to upper respiratory tract infections, infections of the nose and sinuses, and injuries or as an idiopathic disorder [7–9]. In our study we excluded this group of patients.

In primary hypothyroidism, disorders of smell and taste turn out to be frequent pathologies [10], which is confirmed also by other researchers who indicate that hypothyroidism significantly influences smell perception attenuating or even suppressing it completely. There is, however, little information considering the relationship between severity of hypothyroidism and intensity of smell disorders [11–13]. It seems evident therefore that a distinction should be drawn between the stages of smell disorders depending on the form of hypothyroidism: mild subclinical versus overt clinical forms. Olfactory reactions that can be disturbed in thyroid diseases are difficult to assess subjectively, without the use of specialist equipment. In view of the above, the diagnostic tests used in olfactory disorders are divided into subjective and objective methods, wherein objective methods (in contrast to subjective tests assessing the thresholds of smell perception) are based on changes in registration of smell cortex evoked potentials, characterized by greater accuracy and repeatability [7, 14–16].

Since the impact of subclinical hypothyroidism on the sense of smell seems to be unclear, and due to the fact that there have been no distinct differences drawn in this respect between overt and subclinical forms of hypothyroidism, the aim of this work was to evaluate the relationship between intensity of hypothyroidism and the state of olfactory reactions measured by objective method.

## 2. Material and Methods

The material comprised 2 groups: the first group consisted of 31 healthy subjects aged 24 to 66 years (mean 51 years) without symptoms of smell disorders displaying a free access to the olfactory region in the nasal cavity in the rhinological test, and the other study group included 21 patients aged 24 to 71 years (mean 54 years) with hypothyroidism. Prior to commencement of the olfactory tests, an informed consent was obtained from each participant to undergo the procedures, and subsequently the subjects received complete ear nose and throat examination to exclude cases of smell disturbances such as nasal and sinus disease, upper respiratory tract infection, head trauma, atrophy of nasal mucosa, and cases with taste disorders.

All the subjects underwent subjective threshold tests of smell perception determined by Ellsberg's olfactory test modified by Pruszevicz and olfactory objective tests recording latency times of responses from cranial nerves I and V using two smells of mint and anise.

The inclusion criterion for the study hypothyroid group was the TSH level from 3.54 to 110  $\mu$ IU/mL. The subclinical

form was determined for  $3.51 \leq \text{TSH} \leq 10 \mu\text{IU/mL}$ ; values above the limit were regarded as representing the overt clinical form. All patients underwent examination by two endocrinologists to confirm the diagnosis and all of them were enrolled into the study at the time of diagnosis. In each patient, signs and symptoms of various degrees of hypothyroidism were found, with a broad range of intensity that increased in line with TSH levels. We observed the following clinical symptoms and signs: weight gain, hair loss, dry skin, decreased libido, easy fatigability, menstrual abnormalities (both oligo- and polymenorrhea and metrorrhagia), peripheral edema, hoarse voice, memory, and concentration problems. Importantly, all the smell examinations shown in this paper were performed prior to the administration of levothyroxine treatment. The reference group consisted of 31 subjects matched for age with the study group for whom the TSH value was normal and ranged from 0.1 to 3.50  $\mu$ IU/mL. In none of them any signs or symptoms of thyroid disease were found.

Disturbances in perception thresholds of the olfactory test within the subjective scale were evaluated using Ellsberg's olfactory method modified by Pruszevicz [13, 17]. The method is however subjective, depending on individual perception of the patient. Measurements based on recordings of smell cortex potentials are more accurate.

The subjective Ellsberg method modified by Pruszevicz was used primarily for selection of the control group and to obtain preliminary information on the state of the organ of smell in the other participants of the experiment. Thresholds of perception for those with a normal sense of smell determined by Pruszevicz for both oils of mint and anise are 12 mL. It is the volume of the saturated vapors of these oils at room temperature about  $(22 \pm 1)^\circ\text{C}$  administered with a syringe in about 0.5 sec into each nostril separately. Identical quality and the production of these oils according to the manufacturer—The National Chemical Reagents POCh—are guaranteed for 50 years [9, 15]. In the control group the scope of the thresholds of perception for both anise and mint oils ranged in 3–8 mL. The method of registering olfactory cortical response by T. Świdziński was used with similar stimulus lasting for 0.5 s with speed of 10–30 mL/s. This range of applied speed of stimulus provides optimal recording cortical olfactory response. For speeds less than 5 mL/s single questionable entries for the control group were obtained, whereas at speeds greater than 50 mL/sec single false responses from the trigeminal nerve endings during the anise oil examination were registered. It can be suggested that they were caused by nonspecific mechanical or thermal stimulants.

The apparatus for recordings of ERP (evoked reaction potentials) as well as the authors' self-designed device that enables appropriate dispensing of olfactory stimuli were used [15]. The modified self-designed device for objective measurement of cortex reaction potentials evoked by olfactory stimuli, which proves to be a unique investigation, is at present routinely used in our center in diagnostics and clinical evaluation of the organ of smell.

TABLE 1: Mean values, ranges, and standard deviations of recorded latency times of olfactory potentials  $P_{N1}$  and  $P_{N5}$  for all the groups of the subjects in stimulation with concentrated vapors of mint and anise oils.

Latency in ms	Hypothyroidism						Reference group (norm)		
	Subclinical			Overt clinical			$P_{N1}$ mint	$P_{N1}$ anise	$P_{N5}$ mint
	$P_{N1}$ mint	$P_{N1}$ anise	$P_{N5}$ mint	$P_{N1}^*$ mint	$P_{N1}^{**}$ anise	$P_{N5}^*$ mint			
Mean	597	588	291	658	667	337	603	571	301
Minimum	500	500	200	570	550	270	450	450	200
Maximum	730	720	380	750	780	460	710	670	410
Standard deviation	88.1	72.6	55.0	58.8	71.8	51.9	77.1	78.9	55.3

\*  $p < 0.05$ , \*\*  $p < 0.005$  (Kruskal-Wallis test).

Application of the olfactory stimulus is synchronized with the inspiration phase of the subject in our study. Automatically, using the vacuum sensor that reacts to the onset of each inspiration, the olfactory applicator starts the device for recording the averaged evoked responses.

The ERA 2250 apparatus by Madsen Electronics is used to record evoked responses by means of Beckman electrodes placed to the forehead and bilaterally to the nape (or the neck). The technique of summing and averaging responses to a quantitatively identical stimulus was used. The number of repetitions was 10 stimuli, and the response recording time ranged from 0 to 1000 ms. Olfactory stimuli (anise, mint) were used for the tests in the volumes of 5 and 10 cm<sup>3</sup> ranging within the norms determined by Pruszewicz for the modified Ellsberg's method [13] and additionally 15 cm<sup>3</sup>. Anise oil stimulated endings of the olfactory nerve and mint oil endings of the olfactory and trigeminal nerves. It was possible to differentiate responses to stimuli irritating nerve V endings (potential  $P_{N5}$  within latency range 200–410 ms) as well as nerve I endings (potential  $P_{N1}$  within latency range 460–700 ms). The Kruskal-Wallis, Mann-Whitney's significant differences tests, descriptive statistical tests, and Spearman's rank correlation tests were used.

Results of the objective olfactory tests in hypothyroid patients (both forms of hypothyroidism) were compared to the results obtained from healthy subjects from the reference group. Moreover, the effect of increased TSH on the latency of smell cortex potentials  $P_{N1}$  and  $P_{N5}$  in the subjects with 2 forms of hypothyroidism was evaluated.

### 3. Results

The groups markedly differed in TSH levels; the patients were divided into groups with different TSH in  $\mu\text{IU/mL}$  levels: first, control group interval between minimum 0.01 and maximum 3.01, median 1.23; second group, subclinical form, interval between minimum 3.54 and maximum 10.00, median 5.80; and the third group, clinical overt form, interval between minimum 12.90 and maximum 110.00, median 20.51. The significance of differences test (Kruskal-Wallis) in these groups was  $p \ll 0.001$ .

In the subjective olfactory tests performed using Ellsberg's olfactory test method modified by Pruszewicz in the hypothyroid patients, the smell perception thresholds (mint and anise) were normal in 85% cases.

In the remaining 15% of our patients we found abnormal results of subjective tests of smell perception (mint, anise) thresholds, as well as a lack of cortical potentials in electro-physiological registration after olfactory stimulation (5% of cases) or slight cortical responses with very late latencies, over 400 ms (10% of cases).

However, differences were noticed in the objective tests in which evaluation concerned recordings of electric responses to olfactory stimulation of nerves N1 and N5 by means of aromatic smells, mint and anise in groups of healthy subjects and hypothyroidism.

Table 1 shows mean values, medians, ranges, and standard deviations of recorded latency times of olfactory potentials for both study groups and the reference group. As seen there, the mean latencies of cortical responses ( $P_{N1}$  potential) in the study groups differ significantly in the Kruskal-Wallis test for stimulation with mint oil ( $p < 0.05$ ) and with anise oil ( $p < 0.005$ ).

A similar dependence was found ( $p < 0.05$ ) at cortical recording for nerve V stimulation with mint oil ( $P_{N5}$  potential). Simultaneously, however, differences between the mean latency values of the studied potentials in the subclinical hypothyroid group are not statistically significant in comparison to the healthy controls (Mann-Whitney's test  $p > 0.05$ ).

Graphs in Figures 1 and 2 present a comparison of mean values, ranges, and standard deviations of  $P_{N1}$  and  $P_{N5}$  potentials in the subclinical and overt clinical hypothyroid groups as well as in controls.

Analysis of the correlation between TSH values and latencies of smell cortex evoked responses to olfactory and trigeminal nerves stimulation indicated that the greater the TSH value, the longer the latency of the recorded potential.

Figures 3–5 show correlations between the parameters (TSH versus latency) under analysis for all the three study groups of subjects. We also presented here the value of the correlation coefficient  $r_s$ -Spearman's rank for significance of  $p$ .

The growing trend (visible in Figures 3–5) between TSH and latencies for the analyzed potentials proves to be a statistically significant relationship for  $P_{N1}$  at mint and anise stimulation (Figures 3 and 4) as well as for  $P_{N5}$  at mint stimulation (Figure 5).

Spearman's rank correlation coefficient that served to describe the correlation strength of two measurable features, namely, TSH values and latencies of cortical responses,

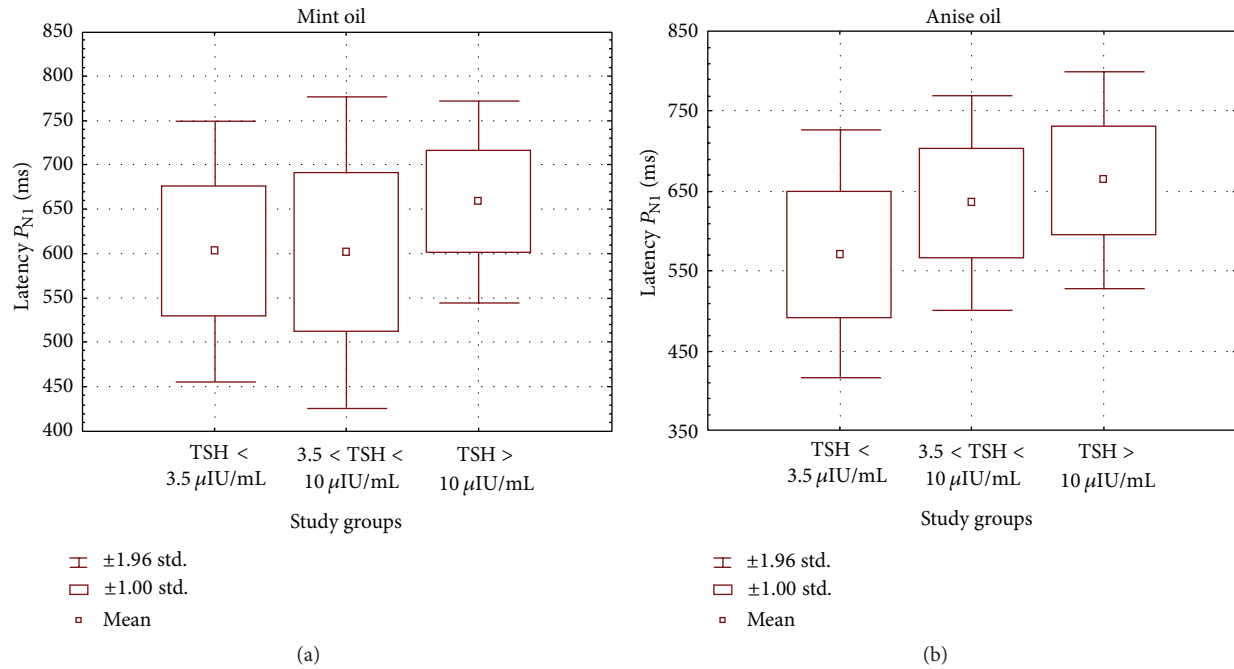


FIGURE 1: Mean values, ranges, and standard deviations of cortical response latencies in the study groups of hypothyroid patients (subclinical group  $3.51 \leq \text{TSH} \leq 10 \mu\text{IU/mL}$  and clinical group  $\text{TSH} > 10 \mu\text{IU/mL}$ ) and healthy subjects ( $\text{TSH} < 3.5 \mu\text{IU/mL}$ ) for  $P_{N1}$  potential at olfactory stimulation with (a) mint and (b) anise.

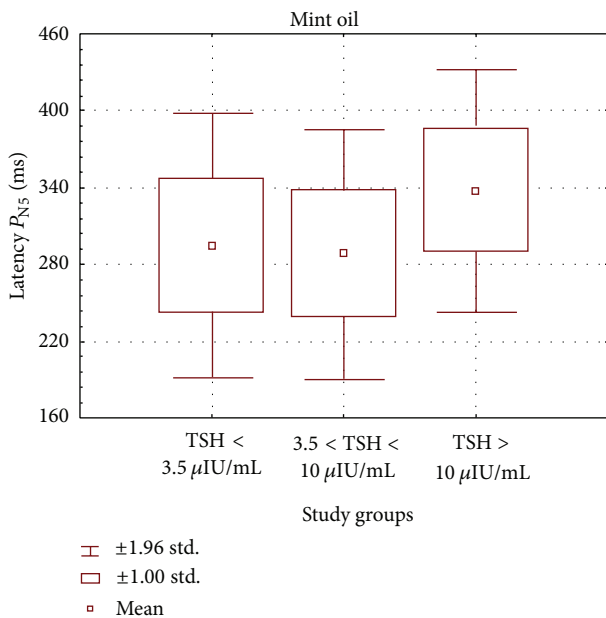


FIGURE 2: Mean values, ranges, and standard deviations of cortical response latencies in the study groups of hypothyroid patients (subclinical group  $3.51 \leq \text{TSH} \leq 10 \mu\text{IU/mL}$  and clinical group  $\text{TSH} > 10 \mu\text{IU/mL}$ ) and healthy subjects ( $\text{TSH} < 3.5 \mu\text{IU/mL}$ ) for  $P_{N5}$  potential at olfactory stimulation with mint.

demonstrated a strong *positive* correlation between increased TSH and prolonged latencies for potential  $P_{N1}$  at olfactory stimulation with mint and anise ( $r_s = 0.42$  and  $0.34$ ) as

well as for potential  $P_{N5}$  at olfactory stimulation with mint ( $r_s = 0.39$ ).

Furthermore, the analysis of latency times of recorded cortical responses  $P_{N1}$  and  $P_{N5}$  performed with the Mann-Whitney  $U$  test between the groups of patients with overt clinical hypothyroidism versus subclinical hypothyroidism demonstrated a significant difference ( $p < 0.05$ ) whereas no such differences were found between the control group versus subclinical hypothyroidism group ( $p > 0.05$ ).

Detailed results are presented in Table 2.

Moreover, it was also observed that above the TSH limit =  $30 \mu\text{IU/mL}$  there were no recorded cortical responses in as many as 70% cases, particularly as regards potential  $P_{N5}$ , despite the fact that, in the subjective tests, normal threshold values of olfactory perception were obtained.

In addition, detailed results of the studies demonstrated also that there were no differences in latency times for  $P_{N1}$  as well as  $P_{N5}$  in the hypothyroid group and in the reference group for different values of olfactory stimulations in  $\text{cm}^3$  (5, 10, 15  $\text{cm}^3$ ) both at stimulations with anise oil as well as mint oil (Kruskal-Wallis test  $p > 0.05$ ).

It was noted, however, that irrespective of the volume of inhaled stimulus fragrance, rapid olfactory fatigue was observed. Therefore, the number of olfactory stimuli for an averaged response was limited to 10 repetitions in our tests.

#### 4. Discussion

Apart from an effect on subjective perception of fragrances, a symptom of olfactory disorders proves to be a change

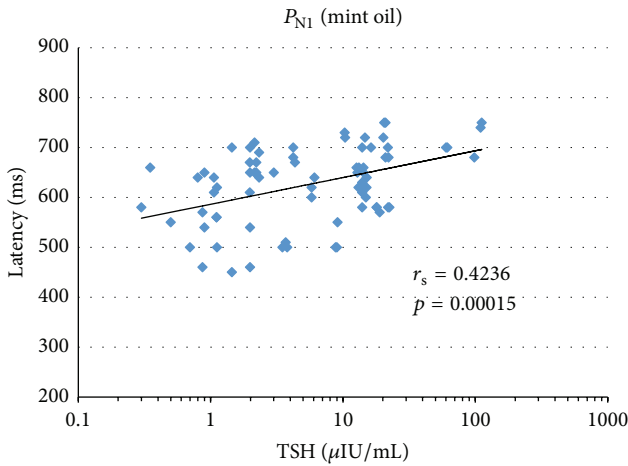


FIGURE 3: Results of the correlation between TSH and latency of smell cortex evoked potentials  $P_{N1}$  at mint oil stimulation.

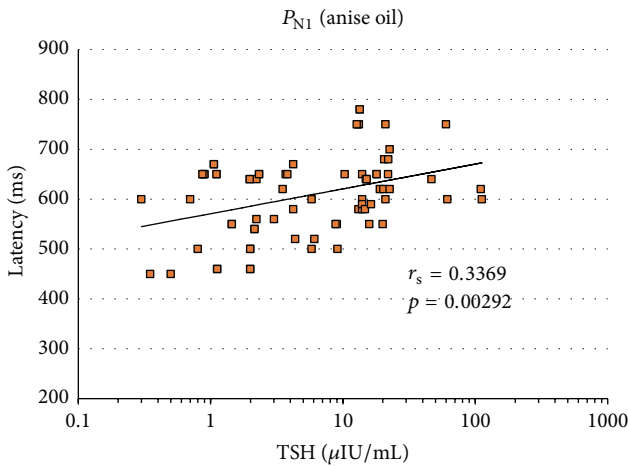


FIGURE 4: Results of the correlation between TSH and latency of smell cortex evoked potentials  $P_{N1}$  at anise oil stimulation.

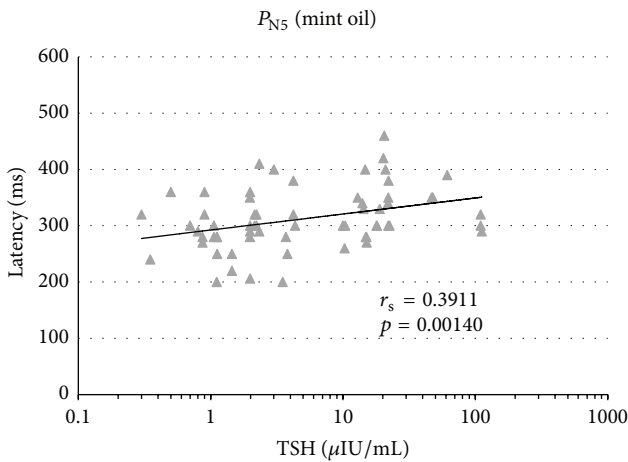


FIGURE 5: Results of the correlation between TSH and latency of smell cortex evoked potentials  $P_{N5}$  at mint oil stimulation.

TABLE 2: Difference significance test in latencies of recorded cortical responses  $P_{N1}$  and  $P_{N5}$  between the groups of patients with overt clinical versus subclinical hypothyroidism as well as between the control group versus subclinical hypothyroidism group.

Potential	Mann-Whitney's $U$ test in study groups		
	Control TSH < 3.5	Subclinical $3.5 \leq \text{TSH} \leq 10$	Overt clinical TSH > 10
$P_{N1}$ mint	$p = 0.9903$	$p = 0.0246$	
$P_{N1}$ anise	$p = 0.6844$	$p = 0.0114$	
$P_{N5}$ mint	$p = 0.8238$	$p = 0.0181$	

in parameters of objective ERP recording of smell cortex potentials such as latency time or response amplitude. A subjective olfactory perception does not always correlate with objective tests of the central nervous system (CNS) responses [18].

The methods used in clinical practice for objective examination of the olfactory function are based on recording reflex reactions. Such methods are, for example, so-called reflex olfactometry (olfactorhinometry according to Gundziol and Mlynski [7]), changes in cerebral bioelectrical function (EEG olfactometry acc. to Roux and Synek [14]) and recording of smell cortex potentials (as averaged responses to strictly normalized olfactory stimuli in Hummel's method [16]), and the method by Świdziński [15]. The latter was used to test hypothyroidism. The main problem in computer-based olfactometry that consists in averaging cortex potentials is the manner of stimulation [14, 19, 20].

A considerable difficulty seems to be how to ensure repeatable application of olfactory impulses. There have been introduced, however, the so-called impulse olfactometers in which it is possible to control parameters of the stimulus [19, 21, 22], yet another difficulty seems to be elimination of simultaneous irritation of other afferent endings [23].

The following authors were able to overcome this difficulty. Fikentscher, who had used the olfactory method according to Ellsberg, obtained clear cortex responses with latency time 500–1000 ms [24]. Making use of the impulse olfactometer with the electronically amplified olfactory stimulus (designed by Giesen and Mrowiński), Alber et al. (1972) made computerized averaging of 1.5-second electroencephalogram sections in responses to an olfactory stimulus [25]. Then, Herberhold obtained cortex evoked olfactory potentials using 10–20 mL stimuli with 100–200 ms stimulation time. He obtained two separate potentials of 250 ms latency time for responses from the trigeminal nerve and 500 ms for those from the olfactory nerve [8].

Methods of recording the potentials of smell used by us turned out to be accurate, and problems with stimulation of the olfactory organ were overcome. This objective olfactometry method is author's method [15].

The objective test method for mint and anise fragrance stimulation that has been used in our center for several years providing us with wide clinical experience appears to comply with the requirements of an objective investigation. Implementing this method in diseases of the upper respiratory tract as a complementary method, for instance, in injuries of the craniofacial skeleton and surgical operations of the nasopharyngeal tumors, has already become quite common [5–7, 26, 27].

Hence, there have been further attempts to spread the use of this method to disease entities that may be accompanied by peripheral neuropathies even without clear clinical symptoms of olfactory disorders, for example, in neurological diseases such as Alzheimer's, Parkinson's, and Creutzfeldt-Jakob's diseases [28].

As obtained in our study, disturbances of latency response to cortical stimulation on the olfactory nerve and trigeminal probably are related to disturbances of the cortex not receptor. Studies of other authors using more sophisticated methods to stimulate the olfactory structures (such as pyridine and nitrobenzene) affirm opportunity for differentiation of sensory or cortical disorders [10, 29]. This is all more understandable that in the majority of respondents olfactory functions on discrete scents of mint and anise were not disturbed, though we found also in all this cases delayed latencies of cortical potentials  $P_{N1}$  and  $P_{N5}$ .

To date, no studies have been undertaken to analyze latencies of olfactory responses recorded from nerves I and V in hypothyroidism in both subclinical and overt forms.

The method designed for receptor stimulation in the olfactory region of the nasal cavity as well as the analysis of latencies of smell cortex evoked potentials allow us to differentiate responses to stimulation of N5 endings (shorter latency) and N1 endings (longer latency) and can become useful in monitoring changes in olfactory disorders caused by hypothyroidism.

There seems to be no immediate link between subjective perception of fragrance and the delay of recorded smell cortex potentials in different forms of hypothyroidism.

In this paper we show for the first time that the greater the TSH values, the longer the latency of smell cortex potentials recorded from both the trigeminal nerve N5 and the olfactory nerve N1.

## 5. Conclusions

The results from analyses of the obtained recordings allow us to conclude that registration of cortex potentials at irritation of olfactory and trigeminal nerves offers possibilities for use in clinical practice as one of the basic methods in objective olfactometry, and its use in hypothyroidism as an objective indicator of hypothyroidism severity may prove helpful in the diagnostic and prognostic processes.

## Competing Interests

The authors declare that they have no competing interests.

## References

- [1] A. Misiunas, H. Niepomniszcze, B. Ravera, G. Faraj, and E. Faure, "Peripheral neuropathy in subclinical hypothyroidism," *Thyroid*, vol. 5, no. 4, pp. 283–286, 1995.
- [2] P. Penza, R. Lombardi, F. Camozzi, C. Ciano, and G. Lauria, "Painful neuropathy in subclinical hypothyroidism: clinical and neuropathological recovery after hormone replacement therapy," *Neurological Sciences*, vol. 30, no. 2, pp. 149–151, 2009.
- [3] K. El-Salem and F. Ammari, "Neurophysiological changes in neurologically asymptomatic hypothyroid patients: a prospective cohort study," *Journal of Clinical Neurophysiology*, vol. 23, no. 6, pp. 568–572, 2006.
- [4] J. Weingaertner, P. Proff, V. Bienengraeber, T. Gedrange, J. Fanghaenel, and K. Lotz, "In vivo study of apoptosis as a creative agent of embryonic development of the primary nasal duct in rats," *Journal of Cranio-Maxillofacial Surgery*, vol. 34, no. 2, pp. 3–7, 2006.
- [5] K. Lotz, P. Proff, V. Bienengraeber, J. Fanghaenel, T. Gedrange, and J. Weingaertner, "Apoptosis as a creative agent of embryonic development of bucca, mentum and nasolacrimal duct. An in vivo study in rats," *Journal of Cranio-Maxillofacial Surgery*, vol. 34, supplement 2, pp. 8–13, 2006.
- [6] A. Mackay-Sim and M. D. Beard, "Hypothyroidism disrupts neural development in the olfactory epithelium of adult mice," *Brain Research*, vol. 433, no. 2, pp. 190–198, 1987.
- [7] H. Gudziol and G. Mlynski, "Die Olfakto-Rhinorheometrie-eine objektiverende Methode zur Überprüfung des Riechsinnes," *Laryngologie, Rhinologie, Otologie*, vol. 61, no. 09, pp. 513–515, 1982.
- [8] C. Herberhold, "Computer-olfaktometrie mit getrenntem nachweis von trigeminus und olfactorius-reaktionen," *Archiv für Klinische und Experimentelle Ohren-, Nasen- und Kehlkopfheilkunde*, vol. 202, p. 394, 1972.
- [9] A. Obrębowski, T. Świdziński, and P. Świdziński, "Elektrophysiological olfactometry in clinical practice," *Postępy w Chirurgii Głowy i Szyi*, vol. 2, pp. 15–21, 2014.
- [10] R. J. McConnell, C. E. Menendez, F. R. Smith, R. I. Henkin, and R. S. Rivlin, "Defects of taste and smell in patients with hypothyroidism," *The American Journal of Medicine*, vol. 59, no. 3, pp. 354–364, 1975.
- [11] A. Pruszewicz, A. Obrębowski, M. Walczak, P. Stajgis, B. Stawny, and K. Łącka, "Przydatność badań węchu i smaku w schorzeniach endokrynologicznych," *Otolaryngologia Polska*, vol. 22, no. 1, pp. 804–806, 2004.
- [12] M. Walczak, A. Pruszewicz, K. Łącka, and M. Karlik, "Stan narządu powonienia we wrodzonej niedoczynności tarczycy," *Otolaryngologia Polska*, vol. 56, no. 5, pp. 577–581, 2002.
- [13] M. Walczak, A. Pruszewicz, K. Łącka, and M. Karlik, "Disorders of smell in congenital hypothyroidism," *Polish Journal of Endocrinology*, vol. 53, supplement 1-2, p. 396, 2002.
- [14] J. Rous and V. Synek, "Objektivni stanoveni intensity cichoveho ujemu pomoci galvanickeho kozniho reflex," *Česka Otolaryngologia*, vol. 15, p. 271, 1966.
- [15] T. Świdziński, A. Obrębowski, A. Pruszewicz, and P. Świdziński, "The use of an automated apparatus for testing olfactory efficiency," *Medical & Biological Engineering & Computing*, vol. 37, supplement 2, part 2, pp. 1300–1301, 1999.
- [16] T. Hummel and A. Welge-Lüssen, "Taste and smell. An update. Assessment of olfactory function," *Advances in Oto-Rhino-Laryngology Home*, vol. 63, pp. 84–98, 2006.

- [17] A. Obrębowski, A. Pruszeicz, Z. Szejma, B. Rydzewski, and J. Tyczyńska, "Olfaktometria obiektywna," *Otolaryngologia Polska*, vol. 1, supplement 131, pp. 48–53, 1977.
- [18] C. M. Philpott, C. R. Wolstenholme, P. C. Goodenough, A. Clark, and G. E. Murty, "Comparison of subjective perception with objective measurement of olfaction," *Otolaryngology—Head and Neck Surgery*, vol. 134, no. 3, pp. 488–490, 2006.
- [19] H. Gudziol and K. H. Gramowski, "Olfacto-EEG-investigations with normal persons," *HNO-Praxis*, vol. 7, no. 2, pp. 102–105, 1982.
- [20] A. Svitavska and B. Uchytíl, "Objektivni olfaktometricky dismutacni test pro overeni anosmickych poruch," *Ceska Otolaryngologia*, vol. 18, p. 151, 1969.
- [21] M. Giesen and D. Mrowinski, "Klinische Untersuchungen mit einem Impuls-Olfactometer," *Sitzungsbericht Freie Vorträge*, vol. 196, no. 2, pp. 377–380, 1970.
- [22] C. Semeria, "Studio delle reazioni psico-galvanometriche alla stimolazione olfattiva," *Minerva Otorinolaringologica*, vol. 6, p. 97, 1956.
- [23] H. J. Gerhardt and Ch. Rauch, "Objektive Olfaktometrie-Erfahrungen mit Atmungsregistrierung unter Geruchreiz," *Zeitschrift für Laryngologie, Rhinologie, Otologie und ihre Grenzgebiete*, vol. 42, p. 658, 1963.
- [24] B. Roseburg and R. Fikentscher, *Klinische Olfaktologie und Gustologie*, Johann Ambrosius Barth, Leipzig, Germany, 1977.
- [25] K. Alber, D. Mrowiński, M. Giesen, and W. Schwab, "Objektive Olfaktometrie in der klinischen Diagnostik," *Archiv für Klinische und Experimentelle Ohren-, Nasen- und Kehlkopfheilkunde*, vol. 199, no. 2, pp. 687–692, 1972.
- [26] J. Fanghänel, T. Gedrange, and P. Proff, "The face-physiognomic expressiveness and human identity," *Annals of Anatomy*, vol. 188, no. 3, pp. 261–266, 2006.
- [27] J. Fanghänel and T. Gedrange, "On the development, morphology and function of the temporomandibular joint in the light of the orofacial system," *Annals of Anatomy*, vol. 189, no. 4, pp. 314–319, 2007.
- [28] T. Kovács, "Mechanisms of olfactory dysfunction in aging and neurodegenerative disorders," *Ageing Research Reviews*, vol. 3, no. 2, pp. 215–232, 2004.
- [29] R. I. Henkin, L. M. Levy, and A. Fordyce, "Taste and smell function in chronic disease: a review of clinical and biochemical evaluations of taste and smell dysfunction in over 5000 patients at the Taste and Smell Clinic in Washington, DC," *American Journal of Otolaryngology—Head and Neck Medicine and Surgery*, vol. 34, no. 5, pp. 477–489, 2013.

## Research Article

# Bone Regeneration after Treatment with Covering Materials Composed of Flax Fibers and Biodegradable Plastics: A Histological Study in Rats

**Tomasz Gredes, Franziska Kunath, Tomasz Gedrange, and Christiane Kunert-Keil**

*Department of Orthodontics, Carl Gustav Carus Campus, TU Dresden, Fetscherstrasse 74, 01307 Dresden, Germany*

Correspondence should be addressed to Tomasz Gredes; [tomasz.gredes@uniklinikum-dresden.de](mailto:tomasz.gredes@uniklinikum-dresden.de)

Received 26 April 2016; Revised 14 July 2016; Accepted 17 July 2016

Academic Editor: Radovan Zdero

Copyright © 2016 Tomasz Gredes et al. This is an open access article distributed under the Creative Commons Attribution License, which permits unrestricted use, distribution, and reproduction in any medium, provided the original work is properly cited.

The aim of this study was to examine the osteogenic potential of new flax covering materials. Bone defects were created on the skull of forty rats. Materials of pure PLA and PCL and their composites with flax fibers, genetically modified producing PHB (PLA-transgen, PCL-transgen) and unmodified (PLA-wt, PCL-wt), were inserted. The skulls were harvested after four weeks and subjected to histological examination. The percentage of bone regeneration by using PLA was less pronounced than after usage of pure PCL in comparison with controls. After treatment with PCL-transgen, a large amount of new formed bone could be found. In contrast, PCL-wt decreased significantly the bone regeneration, compared to the other tested groups. The bone covers made of pure PLA had substantially less influence on bone regeneration and the bone healing proceeded with a lot of connective tissue, whereas PLA-transgen and PLA-wt showed nearly comparable amount of new formed bone. Regarding the histological data, the hypothesis could be proposed that PCL and its composites have contributed to a higher quantity of the regenerated bone, compared to PLA. The histological studies showed comparable bone regeneration processes after treatment with tested covering materials, as well as in the untreated bone lesions.

## 1. Introduction

Autografts are still the gold standard in bone grafting because of immediate availability and high success rate, though their amount and applications are limited due to donor site morbidity and graft resorption [1]. The use of autografts is currently becoming narrower and they are often substituted for likewise efficient bone allografts [2]. Host integration and limited long-term functional capacity still require improvement of bone substitutes [3, 4]. Most allografts can provide vastly superior mechanical stability, which is indispensable for therapy of extensive bone damage, caused by traumatic injury, degenerative disease, or tumor resection [5]. In case of severe bone fractures or bone damage, the use of pins, nails, screws, or plates is a reliable method of producing rigid internal fixation and a functionally stable fracture site to keep bone fragments together [6–8]. The most commercially used bone plates and screws are made of metallic materials which are not particularly compatible

with such noninvasive diagnostic imaging procedure like magnetic resonance imaging (MRI) and computed tomography (CT) because of metal-related artifacts [9]. Although metal plate fixation will be mostly use after complicated bone fracture, they do not remain without disadvantages. Beside possible corrosion and fatigue strength, the rigid metal plates can cause by the stress shielding effect considerable bone atrophy in plated segment, especially a decreased cortical density and mineral content [10]. Many polymers or polymer-based composites are contemplated as an alternative for bone fixation due to their biocompatibility, high strength-to-weight ratio, radiolucency, biofunctionality, and nontoxicity of degradation by-products [11–13]. Though unreinforced polymers are more ductile than metals and ceramics, they are often not stiff enough to be used to replace or retain hard tissues. A better mechanical property, due to strength and stiffness requirements for hard tissue substitution, exhibits polymer-based composites [14]. They have already been multifunctionally applied, for instance, as biosensors, coatings,

and load-bearing implants [15]. Biodegradable composites gain more and more importance for creation of surgical devices which avoid an additional surgery for their removal. The continuous degradation and a gradual load transfer of these materials could stimulate the healing and remodeling of bone tissue [14, 16]. Among the many synthetic biocompatible and biodegradable polymers, polylactide (PLA) and their copolymers have been approved for human clinical uses [17]. PLA has already been used for craniofacial fracture and ankle fixation [17, 18]. PLA and polylactide-co-glycolide (PLGA) are often used for drug delivery, tissue engineering, and manufacturing of medical implants and surgical sutures [19]. PLA occurs in metabolism of all microorganisms and animals incorporated into the tricarboxylic acid cycle; hence, its degradation and excreted products are assumed to be completely nontoxic [20]. Zygomatic fracture fixation with PLA or metal showed similar results; however, 60% of the patients treated with PLA showed intermittent swelling at the implantation site [17, 18].

A very good biocompatibility with bone cells exhibits also polycaprolactone (PCL), used in several biomedical applications, inter alia in scaffolds for bone and cartilage tissue engineering [21]. Owing to the relatively low melting point of PCL, its mechanical properties can be improved in melting techniques by bonding with other polymers or stiffer materials, in the form of particles or fibers [14, 22, 23]. Another group of polymers, polyhydroxyalkanoates, represented by 3-hydroxybutyric acid (PHB) and its copolymers, gained a fixed place in the biomedical field, due to their biocompatibility, biodegradability, and physical and mechanical properties [24, 25]. PHB scaffolds are highly compatible with osteoblast and can induce ectopic bone formation [26]. Recently, it could be shown that PHB membranes can act as matrix for cell migration, proliferation, differentiation, and vascularization in process of bone healing [27]. It was speculated that PHB patches or PHB in form of composites could be an interesting examination object in the treatment of bony defects.

Polymer-based and fiber-reinforced composite materials have been already investigated in animal studies for biocompatible bone defect fillings, adhesion, and anchoring into bone [12, 28, 29]. These materials were reinforced with natural as well as glass or carbon fibers. Flax fibers exhibit better mechanical properties than other natural fibers, comparable to those of glass fibers [30]. Modification of flax fibers to create therapeutic dressing could be of medical interest. One of the first studies on the transgenic flax fibers overproducing various antioxidative compounds has demonstrated promising therapeutic results for a wound dressing [31]. Other genetic modifications of flax plants allowed the synthesis of PHB in the plant fibers which improved their mechanical features and offered thereby an attractive material for industry and medicine [32–34]. This material did not show any inflammation response after subcutaneous insertion and a good *in vitro* and *in vivo* biocompatibility was shown in previous studies [35–37].

Due to preliminary molecular-biological analyses and earlier studies to bone regeneration after usage of PHB, it was hypothesized that composites from transgenic flax plants producing PHB showed faster bone regeneration in

comparison with composites of nontransgenic flax plants. The aim of the current study was to both histologically and histomorphometrically, evaluate the effect of polymer-flax composites on the osteogenesis process, using a model of unperforated bone defects at the skull top of rats.

## 2. Material and Methods

**2.1. Surgical Procedure and Experimental Design.** For the study, flax composites were used which have already been described [35–37]. The osteogenic potential of flax composites was investigated in 42 adult Lewis 1A rats (2 months old, body weight between 250 g and 350 g, and of both sexes). The animals were randomly divided into the following 7 groups:

- (i) Group 1, controls ( $n = 6$ ): untreated bone defects.
- (ii) Group 2, PLA ( $n = 6$ ): bone defects treated with pure PLA-composites.
- (iii) Group 3, PLA-transgen ( $n = 6$ ): bone defects treated with composites of PLA and transgenic PHB-producing flax.
- (iv) Group 4, PLA-wt ( $n = 6$ ): bone defects treated with composites of PLA and fibers from wildtype flax.
- (v) Group 5, PCL ( $n = 6$ ): bone defects treated with pure PCL composites.
- (vi) Group 6, PCL-transgen ( $n = 6$ ): bone defects treated with composites of PCL and transgenic PHB-producing flax.
- (vii) Group 7, PCL-wt ( $n = 6$ ): bone defects treated with composites of PLA and fibers from wildtype flax.

The approval for all surgical and experimental procedures was issued by the Animal Welfare Committee on the State Government (LALLF M-V/TSD/7221.3-1.1-094/11). All surgical procedures were performed according to standard protocol. This protocol has been published several times [27, 36, 38–40].

In order to compare the data obtained with the molecular-biological findings [35] the skulls were dissected four weeks after composite insertion and fixed in 4% PBS-buffered formalin, dehydrated in a graded series of alcohol, and separately embedded in methylmethacrylate (Technovit 9100 neu, Kulzer, Germany) as previously described [41–44] or in paraffin after decalcification as previously described [40, 45].

**2.2. Histology.** Serial longitudinal sections of about 5  $\mu\text{m}$  were stained with hematoxylin/eosin (HE) for recognizing various tissue types and Masson's trichrome for differentiation between collagen and bone tissue. With Masson's trichrome histological structures were stained as follows: collagen and nonmineralized bone in blue or green, mineralized bone in orange or red, and cell nuclei in dark brown or black [46].

The slices were observed and photographed under a light microscope (BX61, Olympus, Hamburg, Germany) equipped with a calibrated digital camera (Color View II; Soft Imaging System, Olympus Optical GmbH, Hamburg, Germany).

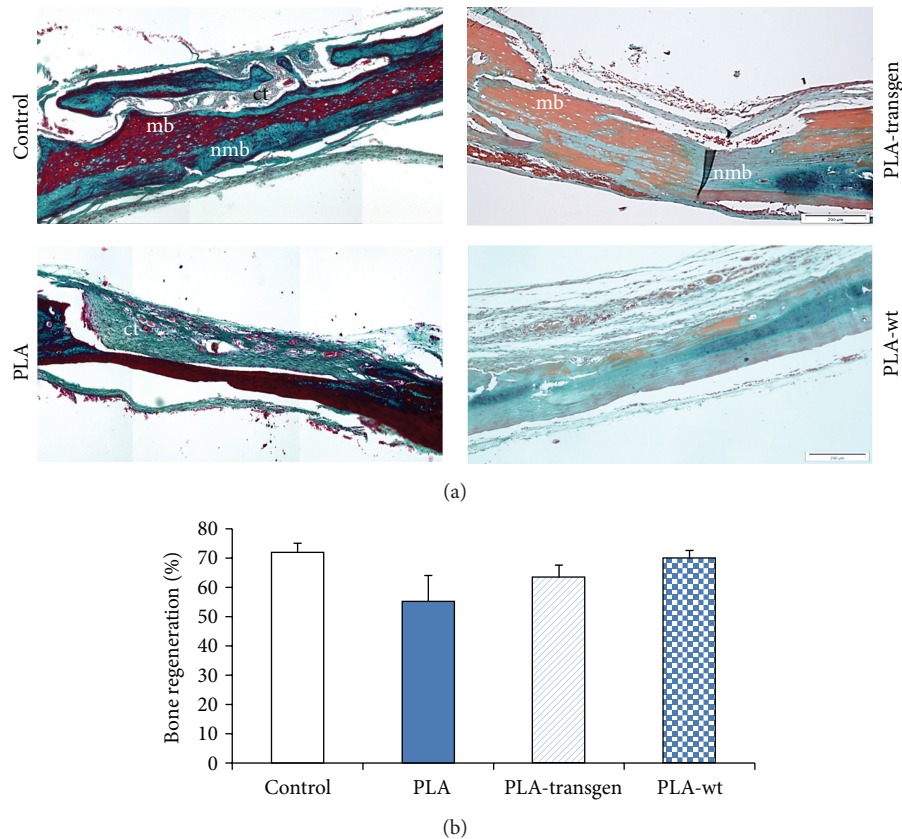


FIGURE 1: (a) Cranial cross-section embedded in paraffin (control and PLA) or methylmethacrylate (PLA-transgen and PLA-wt) stained with Masson-Goldner four weeks after PLA-composite insertion; collagen and nonmineralized bone in blue or green, mineralized bone in orange or red, and cell nuclei in dark brown or black; (b) histomorphometric analysis of bone regeneration. Stated is mean  $\pm$  standard error. Bars represent 200  $\mu$ m. ct = connective tissue; mb = mineralized bone; nmb = nonmineralized bone.

Image analysis was performed on composed pictures showing the complete cavity with a magnification of  $\times 100$  as previously described [40, 47] using the software cell<sup>^</sup>F (analysis Image Processing Olympus, Münster, Germany). From each skull a minimum of 10 sections were histomorphometrically analysed. With this approach we are able to perform an overall conclusion about the bone regeneration in the cavity.

**2.3. Statistical Analysis.** The statistical analyses of variance between groups were made using Mann-Whitney *U* Rank sum test (SigmaStat 3.5 Software, Systat Software, Inc., 1735, Technology Drive, San Jose, CA 95110, USA). Data were given as means  $\pm$  SEM.  $P < 0.05$  was considered statistically significant.

### 3. Results

Wound healing proceeded in all operated animals without any complications and relatively fast. During sampling of bone treated part of calvaria, no signs of inflammation reactions in that tissue could be macroscopically detected.

The histological sections showed nearly finished bone healing in untreated bone defects. The surgically created lesions at the beginning of this study were filled after four

weeks with nonmineralized bone as well as bone marrow. In addition, a so-called bridging between origin bone and newly formed bone could also be observed (Figures 1(a) and 2(a)).

When using pure PLA, solely connective tissue was detected in the bone defects. In contrast, both flax composites, PLA-transgen and PLA-wt, caused bone regeneration, which was comparable to that of control animals (Figure 1(a)).

In case of bone defects covered with different PCL composites, there was nearly completed bone regeneration with evidence of bone marrow and nonmineralized bone, respectively (Figure 2(a)). Osteolysis and bone resorption did not occur. In addition, it should be noted that all composites are completely embedded in connective tissue in the form of a capsule. When using flax composites, this capsule became thicker (exemplary for PCL and PCL-wt; Figure 2(a)).

Histomorphometric analysis, as shown in Figures 1(b) and 2(b), revealed a regenerated bone mean value of 72.0%  $\pm$  3.1% in untreated control animals. After treatment with PLA composites, the level of bone regeneration was achieved between 55.3 and 70.0%. These results have not shown any statistically significant differences in comparison with bone healing processes in controls. Similar results were obtained after usage of PCL and PCL-transgen, though significantly reduced bone regeneration in bone lesions was found after

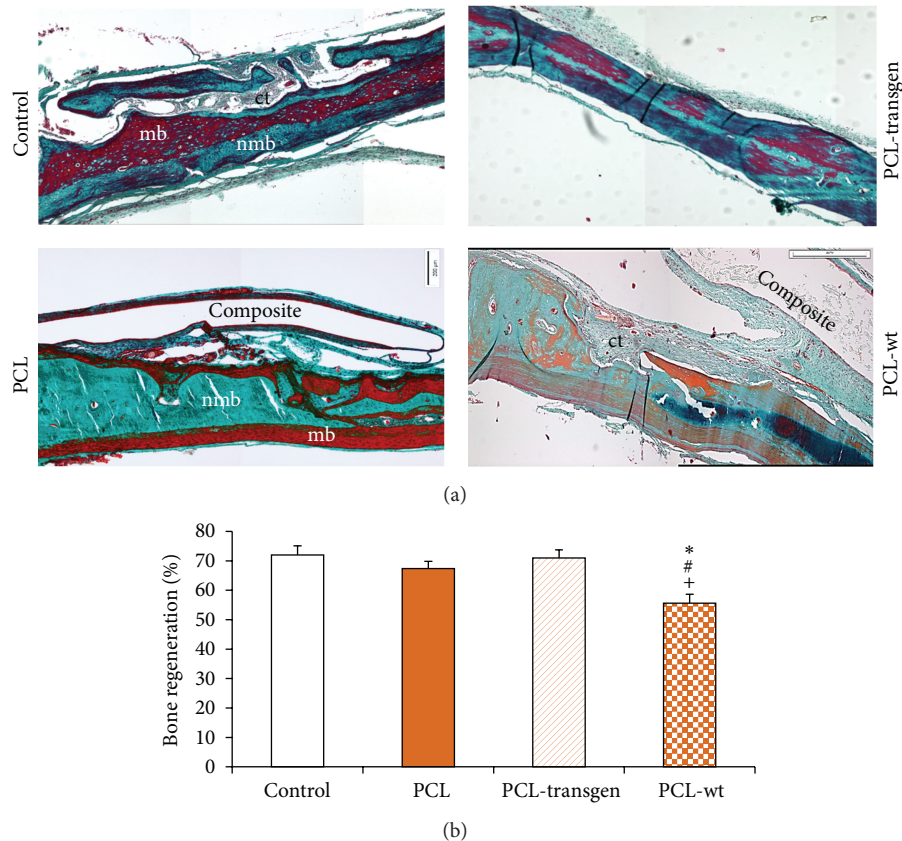


FIGURE 2: (a) Cranial cross-section embedded in methylmethacrylate (PCL and PCL-wt) or paraffin stained with Masson-Goldner four weeks after PCL-composite insertion; collagen and nonmineralized bone in blue or green, mineralized bone in orange or red, and cell nuclei in dark brown or black; (b) histomorphometric analysis of bone regeneration. Stated is mean  $\pm$  standard error. Bars represent 200  $\mu$ m. \* $P < 0.05$  PCL-wt versus control; # $P < 0.05$  PCL-wt versus PCL; + $P < 0.05$  PCL-wt versus PCL-transgen. ct = connective tissue; mb = mineralized bone; nmb = nonmineralized bone.

treatment with PCL-wt (control versus PCL-wt:  $72.0 \pm 3.1\%$  versus  $55.6 \pm 3.0$ ,  $P = 0.002$ , power: 0.931; PCL versus PCL-wt:  $67.4 \pm 2.4\%$  versus  $55.6 \pm 3.0$ ,  $P = 0.011$ , power: 0.737; PCL-transgen versus PCL-wt:  $71.0 \pm 2.7\%$  versus  $55.6 \pm 3.0$ ,  $P = 0.003$ , power: 0.924; Figure 2(b)).

#### 4. Discussion

In the current study, we evaluated the osteogenic potential of new polymer/flax composites in an animal model. Bone histological examination of cavities after treatment with PLA, PCL, or their composites as well as of the empty reference cavities showed spontaneous regeneration of the bony bed, though after four weeks their areas were not completely filled with new bone and they exhibited a large amount of connective tissue, especially after using of pure PLA. The nonsignificant stronger percentage increase of bone regeneration was noticed after using of pure PCL rather than after treatment with PLA. If only the histological preparations were considered, the hypothesis could be proposed that PCL and its composites have contributed to a higher quantity of the regenerated bone, compared to pure PLA.

Biodegradable polymers have already been used for various bone surgical procedures, and in general, they are considered as safe for clinical use [48]. With regard to bone regeneration, many studies have shown that PLA is applicable with satisfactory results as plates, membranes, suture anchors, interference screws, and pins [49, 50]. The adhesive and proliferative behaviors of bone forming cells on various surfaces have been well studied. *In vitro* tests for bone regeneration have demonstrated that rat osteoblasts cultured on PLA retained their phenotype by high expression of alkaline phosphatase activity and collagen synthesis [51]. It was found that additional coating of PLA scaffolds with apatite or apatite/collagen was more efficient for osteoblast-like cells adhesion and proliferation [52]. Further biocompatibility tests of subcutaneously implanted PLA in rat have not detected any acute inflammatory reactions [53, 54]. However, the long-lasting degradation time of PLA can induce late foreign body reactions due to crystalline remnants or a decrease of the pH value during the decomposition [55–57]. Moreover, bone resorption could be observed following degradation of the polymer due to release of nondegraded PLA microparticles [58] or change in the tissue surrounding the degrading PLA implants associated with the leaching of

residual monomer or lactic acid [59, 60]. A close contact between the amorphous polymer poly(D,L-lactic acid) and the surrounding tissue without trace of inflammatory tissue, signs of infection, bony necrosis, or any interference of the bone healing process could be recently demonstrated [61]. Our results showed that PLA devices are highly tolerated by host tissues after 4 weeks, which was in agreement with Annunziata et al. [61]. We could affirm a good biocompatibility *in vitro* as well as *in vivo* of PLA and their composites in previous studies [35–37]. The biocompatibility of composites from transgenic flax plants producing PHB did not differ from composites of nontransgenic flax plants and the covering materials composed of flax fibers and PLA or PCL had no influence of the attachment, growth, and survival of the fibroblast cells [37].

PCL degrades much slower than other known biodegradable polymers [62, 63]. It has already been used for bone and cartilage repairs [64] because of its good biocompatibility and high bone inductive potential [65]. A better bone regeneration was achieved using more permeable PCL scaffolds with regular architecture [66]. PCL membranes supported attachment, growth, and osteogenic differentiation of human primary osteoblast-like cells [67]. Previously, it was shown that PCL and PCL-based scaffolds were able to deliver recombinant human bone morphogenetic protein-2 as well as provide sufficient structural support to promote bone healing [68]. A good compatibility of 3D PCL scaffolds was showed, *inter alia*, in an animal study after insertion of PCL implants into the rat skull with direct contact to the brain. According to the investigations of neurogenic potential and neurons, it was demonstrated that PCL did not evoke an undesirable inflammatory response [69]. Moreover, PCL-based scaffolds did not cause further changes to the vascular supply in and around the defect region [70]. In our study, we could also observe a high tolerance of PCL devices by host tissues. Bone healing proceeded without any complications and signs of inflammation. Similar observations were described in other studies [59, 69, 71]. Furthermore, it was found that all composites were completely embedded in connective tissue in the form of a capsule. The encapsulation, as a natural reaction to foreign materials in the body, has also been described previously [59, 72].

In our study, good bone regeneration was observed under the covering materials made of pure polymers and their composites. In all cases, a new bone formation was verified by histological examination. In addition, there were no sufficient differences between the controls and treated bone cavities. Recently it was shown that biodegradable PLA membranes, as bone defect coverage, were tested in a sheep model. Enhanced remodeling of the spongiosa into native bony under the membranes could be detected in cranial defects but also without an osteopromoting effect. In contrast to our study, a foreign body reaction around the tested membranes was observed in sheep [73].

Our histological results were partially reflected in the previously published molecular-biological analyses [36]. The significant decrease of expression of 3 genes, which play an important role in bone formation, osteocalcin (Bglap), osteopontin (Opn), and transcription factor Runx2, might

be linked to the reduced amount of new bone formation under cover material of PCL-wt. Furthermore, an unchanged gene expression of Runx2 and Phex was detected after treatment with PLA and its flax composites. Osteocalcin, also called “bone gamma-carboxyglutamate protein,” is a hydroxyapatite-binding protein, which is almost exclusively formed by osteoblasts in large quantities at the beginning of the bone mineralization [74–76]. The differentiation of preosteoblasts is triggered in the progenitor cells involving Runx2 and other transcription factors. It has been shown that a lack of Runx2 can lead to disturbances in the bone formation and mineralization [77]. In knock-out mice with deficiency of Runx2, any ossification processes of the bone tissue were not demonstrated [78]. Phex, a marker for osteocytes, has a significant impact on the transformation of osteoblasts into osteocytes and thus affects the bone mineralization [79, 80].

Based on the presented data, it could be concluded that neither the transgenic nor the native flax fibers can accelerate bone regeneration; however, they did not show any negative influence on new bone formation. This might be attributed, on the one hand, to very low content of flax fibers in the composite (only 20%) and thereby a small proportion of PHB and, on the other hand, to shielding of fibers by embedding in a polymer matrix and to the very slow degradation of used polymers. A further exacerbating factor is that cellulose, main component of flax, is not metabolized and degraded in the body [81, 82]. Therefore, these flax covering materials in presented form are not clinically applicable. Further modifications, for example, the oxidation of cellulose fibers to produce oxycellulose which is absorbable *in vivo* within a short time [83] could have a positive impact on properties of the materials and their osteogenic potential.

## Competing Interests

The authors declare that they have no competing interests regarding the publication of this paper.

## Acknowledgments

The flax composites used were kindly provided by Professor Szopa (Faculty of Biotechnology, University of Wrocław). The authors would like to thank Diana Jünger and Michaela Krause for the excellent technical assistance.

## References

- [1] G. F. Rogers and A. K. Greene, “Autogenous bone graft: basic science and clinical implications,” *Journal of Craniofacial Surgery*, vol. 23, no. 1, pp. 323–327, 2012.
- [2] A. Albert, T. Leemrijse, V. Druetz, C. Delloye, and O. Cornu, “Are bone autografts still necessary in 2006? A three-year retrospective study of bone grafting,” *Acta Orthopaedica Belgica*, vol. 72, no. 6, pp. 734–740, 2006.
- [3] C. Delloye, P. de Nayer, N. Allington, E. Munting, L. Coutelier, and A. Vincent, “Massive bone allografts in large skeletal defects after tumor surgery: a clinical and microradiographic

- evaluation," *Archives of Orthopaedic and Traumatic Surgery*, vol. 107, no. 1, pp. 31–41, 1987.
- [4] D. L. Wheeler and W. F. Enneking, "Allograft bone decreases in strength in vivo over time," *Clinical Orthopaedics and Related Research*, vol. 435, pp. 36–42, 2005.
  - [5] B. H. Berrey Jr., C. F. Lord, M. C. Gebhardt, and H. J. Mankin, "Fractures of allografts. Frequency, treatment, and end-results," *The Journal of Bone & Joint Surgery—American Volume*, vol. 72, no. 6, pp. 825–833, 1990.
  - [6] A. Abalo, A. Dossim, A. F. Ouro Bangna, K. Tomta, A. Assiobo, and A. Walla, "Dynamic hip screw and compression plate fixation of ipsilateral femoral neck and shaft fractures," *Journal of Orthopaedic Surgery*, vol. 16, no. 1, pp. 35–38, 2008.
  - [7] W. C. Ardary, "Plate and screw fixation in the management of mandible fractures," *Clinics in Plastic Surgery*, vol. 16, no. 1, pp. 61–67, 1989.
  - [8] J. D. Boerckel, Y. M. Kolambkar, H. Y. Stevens, A. S. P. Lin, K. M. Dupont, and R. E. Guldborg, "Effects of in vivo mechanical loading on large bone defect regeneration," *Journal of Orthopaedic Research*, vol. 30, no. 7, pp. 1067–1075, 2012.
  - [9] S. Radzi, G. Cowin, M. Robinson et al., "Metal artifacts from titanium and steel screws in CT, 1.5T and 3T MR images of the tibial Pilon: a quantitative assessment in 3D," *Quantitative Imaging in Medicine and Surgery*, vol. 4, no. 3, pp. 163–172, 2014.
  - [10] T. Terjesen, A. Nordby, and V. Arnulf, "Bone atrophy after plate fixation: computed tomography of femoral shaft fractures," *Acta Orthopaedica Scandinavica*, vol. 56, no. 5, pp. 416–418, 1985.
  - [11] Y. H. An, S. K. Woolf, and R. J. Friedman, "Pre-clinical in vivo evaluation of orthopaedic bioabsorbable devices," *Biomaterials*, vol. 21, no. 24, pp. 2635–2652, 2000.
  - [12] Z. S. Bagheri, E. Giles, I. El Sawi et al., "Osteogenesis and cytotoxicity of a new Carbon Fiber/Flax/Epoxy composite material for bone fracture plate applications," *Materials Science and Engineering C*, vol. 46, pp. 435–442, 2015.
  - [13] L. Eschbach, "Nonresorbable polymers in bone surgery," *Injury*, vol. 31, supplement 4, pp. D22–D27, 2000.
  - [14] J. F. Mano, R. A. Sousa, L. F. Boesel, N. M. Neves, and R. L. Reis, "Bioinert, biodegradable and injectable polymeric matrix composites for hard tissue replacement: state of the art and recent developments," *Composites Science and Technology*, vol. 64, no. 6, pp. 789–817, 2004.
  - [15] B. Gasser, "About composite materials and their use in bone surgery," *Injury*, vol. 31, supplement 4, pp. D48–D53, 2000.
  - [16] B. L. Seal, T. C. Otero, and A. Panitch, "Polymeric biomaterials for tissue and organ regeneration," *Materials Science and Engineering R: Reports*, vol. 34, no. 4-5, pp. 147–230, 2001.
  - [17] K. A. Athanasiou, G. G. Niederauer, and C. M. Agrawal, "Sterilization, toxicity, biocompatibility and clinical applications of polylactic acid/polyglycolic acid copolymers," *Biomaterials*, vol. 17, no. 2, pp. 93–102, 1996.
  - [18] K. A. Athanasiou, C. M. Agrawal, F. A. Barber, and S. S. Burkhart, "Orthopaedic applications for PLA-PGA biodegradable polymers," *Arthroscopy*, vol. 14, no. 7, pp. 726–737, 1998.
  - [19] Z. Zhang, S. H. Lee, C. W. Gan, and S.-S. Feng, "In vitro and in vivo investigation on PLA-TPGS nanoparticles for controlled and sustained small molecule chemotherapy," *Pharmaceutical Research*, vol. 25, no. 8, pp. 1925–1935, 2008.
  - [20] G. G. Pitt, M. M. Gratzl, G. L. Kimmel, J. Surlis, and A. Sohndler, "Aliphatic polyesters II. The degradation of poly (DL-lactide), poly ( $\epsilon$ -caprolactone), and their copolymers in vivo," *Biomaterials*, vol. 2, no. 4, pp. 215–220, 1981.
  - [21] D. W. Hutmacher, "Scaffolds in tissue engineering bone and cartilage," *Biomaterials*, vol. 21, no. 24, pp. 2529–2543, 2000.
  - [22] R. Dell'Erba, G. Groeninckx, G. Maglio, M. Malinconico, and A. Migliozi, "Immiscible polymer blends of semicrystalline biocompatible components: thermal properties and phase morphology analysis of PLLA/PCL blends," *Polymer*, vol. 42, no. 18, pp. 7831–7840, 2001.
  - [23] M. P. Hiljanen-Vainio, T. Karjalainen, and J. Seppälä, "Biodegradable lactone copolymers. I. Characterization and mechanical behavior of  $\epsilon$ -caprolactone and lactide copolymers," *Journal of Applied Polymer Science*, vol. 59, no. 8, pp. 1281–1288, 1996.
  - [24] T. Gredes, A. Spassov, R. Mai et al., "Changes in insulin like growth factors, myostatin and vascular endothelial growth factor in rat musculus latissimus dorsi by poly-3-hydroxybutyrate implants," *Journal of Physiology and Pharmacology*, vol. 60, supplement 3, pp. 77–81, 2009.
  - [25] V. Hasrc, K. Lewandrowski, J. D. Gresser, D. L. Wise, and D. J. Trantolo, "Versatility of biodegradable biopolymers: degradability and an in vivo application," *Journal of Biotechnology*, vol. 86, no. 2, pp. 135–150, 2001.
  - [26] R. Mai, M. G. Hagedorn, M. Gelinsky et al., "Ectopic bone formation in nude rats using human osteoblasts seeded poly(3)hydroxybutyrate embroidery and hydroxyapatite-collagen tapes constructs," *Journal of Cranio-Maxillofacial Surgery*, vol. 34, supplement 2, pp. 101–109, 2006.
  - [27] T. Gredes, T. Gedrange, C. Hinüber, M. Gelinsky, and C. Kunert-Keil, "Histological and molecular-biological analyses of poly(3-hydroxybutyrate) (PHB) patches for enhancement of bone regeneration," *Annals of Anatomy*, vol. 199, pp. 36–42, 2015.
  - [28] A. M. Ballo, E. A. Akca, T. Ozen, L. Lassila, P. K. Vallittu, and T. O. Närhi, "Bone tissue responses to glass fiber-reinforced composite implants—a histomorphometric study," *Clinical Oral Implants Research*, vol. 20, no. 6, pp. 608–615, 2009.
  - [29] S. M.-R. Tuusa, M. J. Peltola, T. Tirri et al., "Reconstruction of critical size calvarial bone defects in rabbits with glass-fiber-reinforced composite with bioactive glass granule coating," *Journal of Biomedical Materials Research Part B: Applied Biomaterials*, vol. 84, no. 2, pp. 510–519, 2008.
  - [30] A. K. Mohanty, M. Misra, and G. Hinrichsen, "Biofibres, biodegradable polymers and biocomposites: an overview," *Macromolecular Materials and Engineering*, vol. 276–277, pp. 1–24, 2000.
  - [31] K. Skórkowska-Telichowska, A. Kulma, M. Zk, T. Czuj, and J. Szopa, "The effects of newly developed linen dressings on decubitus ulcers," *Journal of Palliative Medicine*, vol. 15, no. 2, pp. 146–148, 2012.
  - [32] M. Wróbel, J. Zebrowski, and J. Szopa, "Polyhydroxybutyrate synthesis in transgenic flax," *Journal of Biotechnology*, vol. 107, no. 1, pp. 41–54, 2004.
  - [33] M. Wróbel-Kwiatkowska, M. Czemplik, A. Kulma et al., "New biocomposites based on bioplastic flax fibers and biodegradable polymers," *Biotechnology Progress*, vol. 28, no. 5, pp. 1336–1346, 2012.
  - [34] M. Wróbel-Kwiatkowska, K. Skórkowska-Telichowska, L. Dymińska, M. Mączka, J. Hanuza, and J. Szopa, "Biochemical, mechanical, and spectroscopic analyses of genetically engineered flax fibers producing bioplastic (poly- $\beta$ -hydroxybutyrate)," *Biotechnology Progress*, vol. 25, no. 5, pp. 1489–1498, 2009.
  - [35] T. Gredes, C. Kunert-Keil, M. Dominiak, T. Gedrange, M. Wróbel-Kwiatkowska, and J. Szopa, "The influence of biocomposites containing genetically modified flax fibers on gene

- expression in rat skeletal muscle,” *Biomedizinische Technik*, vol. 55, no. 6, pp. 323–329, 2010.
- [36] T. Gredes, M. Wróbel-Kwiatkowska, M. Dominiak, T. Gedrange, and C. Kunert-Keil, “Osteogenic capacity of transgenic flax scaffolds,” *Biomedizinische Technik*, vol. 57, no. 1, pp. 53–58, 2012.
- [37] C. Kunert-Keil, T. Gredes, A. Meyer, M. Wróbel-Kwiatkowska, M. Dominiak, and T. Gedrange, “The survival and proliferation of fibroblasts on biocomposites containing genetically modified flax fibers: an in vitro study,” *Annals of Anatomy*, vol. 194, no. 6, pp. 513–517, 2012.
- [38] T. Gredes, F. Heinemann, M. Dominiak et al., “Bone substitution materials on the basis of BONITmatrix® up-regulate mRNA expression of IGF1 and Collal,” *Annals of Anatomy*, vol. 194, no. 2, pp. 179–184, 2012.
- [39] T. Gredes, T. Kracht, T. Gedrange, and C. Kunert-Keil, “Influence of BONITmatrix® and OSSA NOVA on the expression of bone specific genes,” *Annals of Anatomy*, vol. 194, no. 6, pp. 524–528, 2012.
- [40] C. Kunert-Keil, F. Scholz, T. Gedrange, and T. Gredes, “Comparative study of biphasic calcium phosphate with beta-tricalcium phosphate in rat cranial defects—a molecular-biological and histological study,” *Annals of Anatomy*, vol. 199, pp. 79–84, 2015.
- [41] S. Allegrini Jr., M. R. F. Allegrini, M. Yoshimoto et al., “Soft tissue integration in the neck area of titanium implants—an animal trial,” *Journal of Physiology and Pharmacology*, vol. 59, supplement 5, pp. 117–132, 2008.
- [42] T. Gedrange, R. Mai, F. Mack et al., “Evaluation of shape and size changes of bone and remodelled bone substitute after different fixation methods,” *Journal of Physiology and Pharmacology*, vol. 59, supplement 5, pp. 87–94, 2008.
- [43] C. Kunert-Keil, T. Gedrange, R. Mai et al., “Morphological evaluation of bone defect regeneration after treatment with two different forms of bone substitution materials on the basis of BONITmatrix,” *Journal of Physiology and Pharmacology*, vol. 60, supplement 8, pp. 57–60, 2009.
- [44] R. Mai, T. Gedrange, H. Leonhardt, N. Sievers, and G. Lauer, “Immunohistochemical comparison of markers for wound healing on plastic-embedded and frozen mucosal tissue,” *Cells Tissues Organs*, vol. 190, no. 1, pp. 34–41, 2009.
- [45] L. Canullo, F. Heinemann, T. Gedrange, R. Biffar, and C. Kunert-Keil, “Histological evaluation at different times after augmentation of extraction sites grafted with a magnesium-enriched hydroxyapatite: double-blinded randomized controlled trial,” *Clinical Oral Implants Research*, vol. 24, no. 4, pp. 398–406, 2013.
- [46] M. Mulisch and U. Welsch, *Romeis—Mikroskopische Technik*, Spektrum Akademischer, Heidelberg, Germany, 2010.
- [47] R. Mai, C. Kunert-Keil, A. Grafe et al., “Histological behaviour of zirconia implants: an experiment in rats,” *Annals of Anatomy*, vol. 194, no. 6, pp. 561–566, 2012.
- [48] R. Suuronen, I. Kallela, and C. Lindqvist, “Bioabsorbable plates and screws: current state of the art in facial fracture repair,” *Journal of Cranio-Maxillofacial Trauma*, vol. 6, no. 1, pp. 19–27, 2000.
- [49] E. Pilling, R. Mai, F. Theissig, B. Stadlinger, R. Loukota, and U. Eckelt, “An experimental in vivo analysis of the resorption to ultrasound activated pins (Sonic weld®) and standard biodegradable screws (ResorbX®) in sheep,” *British Journal of Oral and Maxillofacial Surgery*, vol. 45, no. 6, pp. 447–450, 2007.
- [50] T. Suzuki, H. Kawamura, T. Kasahara, and H. Nagasaka, “Resorbable poly-L-lactide plates and screws for the treatment of mandibular condylar process fractures: a clinical and radiologic follow-up study,” *Journal of Oral and Maxillofacial Surgery*, vol. 62, no. 8, pp. 919–924, 2004.
- [51] S. L. Ishaug, M. J. Yaszemski, R. Bizios, and A. G. Mikos, “Osteoblast function on synthetic biodegradable polymers,” *Journal of Biomedical Materials Research*, vol. 28, no. 12, pp. 1445–1453, 1994.
- [52] Y. Chen, A. F. T. Mak, M. Wang, and J. Li, “Composite coating of bonelike apatite particles and collagen fibers on poly L-lactic acid formed through an accelerated biomimetic coprecipitation process,” *Journal of Biomedical Materials Research Part B: Applied Biomaterials*, vol. 77, no. 2, pp. 315–322, 2006.
- [53] R. R. M. Bos, F. B. Rozema, G. Boering et al., “Degradation of and tissue reaction to biodegradable poly(L-lactide) for use as internal fixation of fractures: a study in rats,” *Biomaterials*, vol. 12, no. 1, pp. 32–36, 1991.
- [54] W. Heidemann, J. H. Fischer, J. Koebke, C. Bussmann, and K. L. Gerlach, “In vivo study of degradation of poly-(D,L-) lactide and poly-(L-lactide-co-glycolide) osteosynthesis material,” *Mund-, Kiefer- und Gesichtschirurgie*, vol. 7, no. 5, pp. 283–288, 2003.
- [55] J. E. Bergsma, W. C. de Bruijn, F. R. Rozema, R. R. M. Bos, and G. Boering, “Late degradation tissue response to poly(l-lactide) bone plates and screws,” *Biomaterials*, vol. 16, no. 1, pp. 25–31, 1995.
- [56] H. Pistner, R. Gutwald, R. Ordnung, J. Reuther, and J. Mühling, “Poly(l-lactide): a long-term degradation study in vivo. I. Biological results,” *Biomaterials*, vol. 14, no. 9, pp. 671–677, 1993.
- [57] C. C. P. M. Verheyen, J. R. de Wijn, C. A. Van Blitterswijk, P. M. Rozing, and K. de Groot, “Examination of efferent lymph nodes after 2 years of transcortical implantation of poly(L-lactide) containing plugs: a case report,” *Journal of Biomedical Materials Research*, vol. 27, no. 8, pp. 1115–1118, 1993.
- [58] J. Sukanuma and H. Alexander, “Biological response of intramedullary bone to poly-L-lactic acid,” *Journal of Applied Biomaterials*, vol. 4, no. 1, pp. 13–27, 1993.
- [59] X.-H. Qu, Q. Wu, K.-Y. Zhang, and G. Q. Chen, “In vivo studies of poly(3-hydroxybutyrate-co-3-hydroxyhexanoate) based polymers: biodegradation and tissue reactions,” *Biomaterials*, vol. 27, no. 19, pp. 3540–3548, 2006.
- [60] A. van Sliedregt, J. A. van Loon, J. van der Brink, K. de Groot, and C. A. van Blitterswijk, “Evaluation of polylactide monomers in an in vitro biocompatibility assay,” *Biomaterials*, vol. 15, no. 4, pp. 251–256, 1994.
- [61] M. Annunziata, L. Natri, A. Borgonovo, M. Benigni, and P. P. Poli, “Poly-D-L-lactic acid membranes for bone regeneration,” *Journal of Craniofacial Surgery*, vol. 26, no. 5, pp. 1691–1696, 2015.
- [62] C. L. Salgado, E. M. S. Sanchez, C. A. C. Zavaglia, and P. L. Granja, “Biocompatibility and biodegradation of polycaprolactone-sebacic acid blended gels,” *Journal of Biomedical Materials Research Part A*, vol. 100, no. 1, pp. 243–251, 2012.
- [63] H. Sun, L. Mei, C. Song, X. Cui, and P. Wang, “The in vivo degradation, absorption and excretion of PCL-based implant,” *Biomaterials*, vol. 27, no. 9, pp. 1735–1740, 2006.
- [64] J. M. Williams, A. Adewunmi, R. M. Schek et al., “Bone tissue engineering using polycaprolactone scaffolds fabricated via selective laser sintering,” *Biomaterials*, vol. 26, no. 23, pp. 4817–4827, 2005.
- [65] Y. Aahmat, T. Chen, Z. Chen, D. Liu, and Z. Wang, “An experimental study on repairing bone defect with the biodegradable

- polycaprolactone material," *Zhongguo Xiu Fu Chong Jian Wai Ke Za Zhi*, vol. 19, no. 6, pp. 439–442, 2005.
- [66] A. G. Mitsak, J. M. Kempainen, M. T. Harris, and S. J. Hollister, "Effect of polycaprolactone scaffold permeability on bone regeneration in vivo," *Tissue Engineering Part A*, vol. 17, no. 13-14, pp. 1831–1839, 2011.
- [67] J.-T. Schantz, D. W. Hutmacher, K. W. Ng, H. L. Khor, T. C. Lim, and S. H. Teoh, "Evaluation of a tissue-engineered membrane-cell construct for guided bone regeneration," *International Journal of Oral and Maxillofacial Implants*, vol. 17, no. 2, pp. 161–174, 2002.
- [68] B. Rai, S. H. Teoh, D. W. Hutmacher, T. Cao, and K. H. Ho, "Novel PCL-based honeycomb scaffolds as drug delivery systems for rhBMP-2," *Biomaterials*, vol. 26, no. 17, pp. 3739–3748, 2005.
- [69] D. K. S. Choy, V. D. W. Nga, J. Lim et al., "Brain tissue interaction with three-dimensional, honeycomb polycaprolactone-based scaffolds designed for cranial reconstruction following traumatic brain injury," *Tissue Engineering Part A*, vol. 19, no. 21-22, pp. 2382–2389, 2013.
- [70] V. D. W. Nga, J. Lim, D. K. S. Choy et al., "Effects of polycaprolactone-based scaffolds on the blood-brain barrier and cerebral inflammation," *Tissue Engineering Part A*, vol. 21, no. 3-4, pp. 647–653, 2015.
- [71] C. X. F. Lam, M. M. Savalani, S.-H. Teoh, and D. W. Hutmacher, "Dynamics of in vitro polymer degradation of polycaprolactone-based scaffolds: accelerated versus simulated physiological conditions," *Biomedical Materials*, vol. 3, no. 3, Article ID 034108, 2008.
- [72] P. Galgut, R. Pitrola, I. Waite, C. Doyle, and R. Smith, "Histological evaluation of biodegradable and non-degradable membranes placed transcutaneously in rats," *Journal of Clinical Periodontology*, vol. 18, no. 8, pp. 581–586, 1991.
- [73] G. Schmidmaier, K. Baehr, S. Mohr, M. Kretschmar, S. Beck, and B. Wildemann, "Biodegradable polylactide membranes for bone defect coverage: biocompatibility testing, radiological and histological evaluation in a sheep model," *Clinical Oral Implants Research*, vol. 17, no. 4, pp. 439–444, 2006.
- [74] C. M. Gundberg, P. V. Hauschka, J. B. Lian, and P. M. Gallop, "Osteocalcin: isolation, characterization, and detection," *Methods in Enzymology*, vol. 107, pp. 516–544, 1984.
- [75] P. V. Hauschka, J. B. Lian, D. E. Cole, and C. M. Gundberg, "Osteocalcin and matrix Gla protein: vitamin K-dependent proteins in bone," *Physiological Reviews*, vol. 69, no. 3, pp. 990–1047, 1989.
- [76] T. Nakase, K. Takaoka, K. Hirakawa et al., "Alterations in the expression of osteonectin, osteopontin and osteocalcin mRNAs during the development of skeletal tissues in vivo," *Bone and Mineral*, vol. 26, no. 2, pp. 109–122, 1994.
- [77] G. Karsenty, "Transcriptional control of skeletogenesis," *Annual Review of Genomics and Human Genetics*, vol. 9, pp. 183–196, 2008.
- [78] T. Komori, H. Yagi, S. Nomura et al., "Targeted disruption of Cbfa1 results in a complete lack of bone formation owing to maturational arrest of osteoblasts," *Cell*, vol. 89, no. 5, pp. 755–764, 1997.
- [79] R. Sapir-Koren and G. Livshits, "Osteocyte control of bone remodeling: is sclerostin a key molecular coordinator of the balanced bone resorption-formation cycles?" *Osteoporosis International*, vol. 25, no. 12, pp. 2685–2700, 2014.
- [80] I. Westbroek, K. E. De Rooij, and P. J. Nijweide, "Osteocyte-specific monoclonal antibody MAb OB73 is directed against Phex protein," *Journal of Bone and Mineral Research*, vol. 17, no. 5, pp. 845–853, 2002.
- [81] P. Maijala, M. Mäkinen, S. Galkin, K. Fagerstedt, T. Härkäsalmi, and L. Viikari, "Enzymatic modification of flaxseed fibers," *Journal of Agricultural and Food Chemistry*, vol. 60, no. 44, pp. 10903–10909, 2012.
- [82] E. Zini and M. Scandola, "Green composites: an overview," *Polymer Composites*, vol. 32, no. 12, pp. 1905–1915, 2011.
- [83] B. Martina, K. Kateřina, R. Miloslava, G. Jan, and M. Ruta, "Oxycellulose: significant characteristics in relation to its pharmaceutical and medical applications," *Advances in Polymer Technology*, vol. 28, no. 3, pp. 199–208, 2009.

## Research Article

# Influence of Botulinumtoxin A on the Expression of Adult MyHC Isoforms in the Masticatory Muscles in Dystrophin-Deficient Mice (Mdx-Mice)

**Ute Ulrike Botzenhart, Constantin Wegenstein, Teodor Todorov, and Christiane Kunert-Keil**

*Department of Orthodontics, Carl Gustav Carus Campus, TU Dresden, Fetscherstrasse 74, 01307 Dresden, Germany*

Correspondence should be addressed to Ute Ulrike Botzenhart; [ute.botzenhart@uniklinikum-dresden.de](mailto:ute.botzenhart@uniklinikum-dresden.de)

Received 29 April 2016; Revised 27 June 2016; Accepted 10 July 2016

Academic Editor: Patrizia Rovere-Querini

Copyright © 2016 Ute Ulrike Botzenhart et al. This is an open access article distributed under the Creative Commons Attribution License, which permits unrestricted use, distribution, and reproduction in any medium, provided the original work is properly cited.

The most widespread animal model to investigate Duchenne muscular dystrophy is the mdx-mouse. In contrast to humans, phases of muscle degeneration are replaced by regeneration processes; hence there is only a restricted time slot for research. The aim of the study was to investigate if an intramuscular injection of BTX-A is able to break down muscle regeneration and has direct implications on the gene expression of myosin heavy chains in the corresponding treated and untreated muscles. Therefore, paralysis of the right masseter muscle was induced in adult healthy and dystrophic mice by a specific intramuscular injection of BTX-A. After 21 days the mRNA expression and protein content of MyHC isoforms of the right and left masseter, temporal, and the tongue muscle were determined using quantitative RT-PCR and Western blot technique. MyHC-IIa and MyHC-I-mRNA expression significantly increased in the paralyzed masseter muscle of control-mice, whereas MyHC-IIb and MyHC-IIx/d-mRNA were decreased. In dystrophic muscles no effect of BTX-A could be detected at the level of MyHC. This study suggests that BTX-A injection is a suitable method to simulate DMD-pathogenesis in healthy mice but further investigations are necessary to fully analyse the BTX-A effect and to generate sustained muscular atrophy in mdx-mice.

## 1. Introduction

The stomatognathic system is based on a close mutual and functional network of different hard and soft tissues from those the masticatory muscles illustrate as an essential component. They are one of the strongest muscles of the body [1].

In mammals, muscle contraction is possible due to highly organized motor units consisting of a motor neurone located in the brain stem [2], its axons, and a colony of corresponding fibres [2, 3]. Motor units show a large variability in morphological and physiological characteristics [2] and can be distinguished on the basis of the differences in contraction time, twitch tension, susceptibility to fatigue, and histochemical staining [3]. Three classes of motor units called slow fatigue resistant, fast fatigable, and fast fatigue resistant were initially identified in mammalian skeletal

muscles composed by slow oxidative type I and fast glycolytic type IIa and IIb fibres, respectively [3–5]. A fourth motor unit type with fast contractile characteristics and intermediate fatigability composed by type IIx fibres was subsequently detected in rat skeletal muscles [6, 7]. Due to that fact, the most informative methods to delineate muscle fibre types are based on specific myosin profiles, especially the myosin heavy chain isoform complement [8] possibly being more related to functional behaviour of jaw muscle motor units than past histochemical classifications [6].

Myosin heavy chains exist in multiple isoforms that are differentially distributed in the various fibre types [9]. At least, four different isoforms of myosin heavy chains are expressed in adult skeletal muscle: slow isoform type I coded by Myh7 gene [10] and fast isoforms type IIa, IIx/d, and IIb [8, 11–14] coded by Myh2, Myh1, and Myh4, respectively [10]. The distribution of different MHCs and fibre types varies in

a muscle-specific as well as a species-specific manner [3, 15] and depending on the function, the anatomical location, and structure of the muscle [3, 12, 14]. For example, limb muscles predominantly contain type I fibres [3]. In the orofacial muscles, especially the masseter muscle, a different fibre distribution has been reported showing a wide variation in fibre type composition as demonstrated in biopsy studies [16]. Presumably depending on functional partitioning of activity of this muscle [6], a predominance of type I fibres in the anterior part and a general presence of hybrid fibres have been described as a normal feature of this muscle in humans [17, 18]. For temporal muscle a predominance of type I fibres in the anterior part (46%) [19] and lower portion of type I fibres (24%) in the posterior part may be also due to functional compartmenting.

Muscle fibres are versatile and dynamic entities capable of adjusting their phenotypic properties under various conditions and in response to altered functional demands and display a great adaptive potential [8, 20]. The dynamic nature of skeletal muscle fibres is achieved by the adaptation of its MyHCs composition [1, 21], and changes in its expression result in fibre type transitions [8]. This process can be regarded as a significant contribution to improve survival [8]. In developing muscles, fibre composition of individual muscle groups varies dramatically [12], fibre transitions is usually seen, and MHCs expression is regulated by neural, hormonal, mechanical, and other factors [9, 22, 23], but transitions of fibre types can also be found in adult muscle fibres due to biological ageing [2, 8, 24], activation intensity [2], neuromuscular activity [8, 25] or electrical stimulation [26, 27], hormone levels [2, 8, 28], exercises [29–32], training, during muscle atrophy induced by denervation [33], physical damage, and also muscle disease [34].

Duchenne muscular dystrophy (DMD), a X-linked recessive disease [35, 36], is one the most common and most serious myopathies which affects approximately 1:3500 life born males [36, 37]. Its onset is between 2 and 5 years of age [35] with clinical symptoms of muscle weakness in the limbs and pseudohypertrophy of calf muscles [38, 39]. At the age of 10–12 years, due to the loss of ambulation, the patients are wheelchair bound [40, 41] and usually the onset of masticatory involvement comes along with that time span. Interestingly the orofacial muscles are affected approximately 2 years later [42], which results in muscle imbalance and severe craniofacial and dental abnormalities [42–44].

The disease is caused by mutations in the dystrophin gene [35], encoding for the sarcolemmal protein product dystrophin, which is part of the DGC (dystrophin glycoprotein complex) and links the motor protein actin to the cytoskeleton [45]. It thus provides mechanical stability to striated muscles [46]. Absence of dystrophin leads to disintegration of the DGC, instability of muscle cell membrane, uncontrolled calcium influx [47], sterile inflammation, and progressive muscle degeneration [35, 48].

Currently the best-characterized and most widely used [49] animal model for DMD is the naturally occurring dystrophin-deficient mdx-mouse [50, 51], which carries a null mutation in exon 23 of the dystrophin gene [35, 47, 49]. Mdx-mice are a genetically biochemical homologue of the

disease [37] but show a relative mild pathology [47], and severity of the phenotype is less than that in the human condition [36, 52]. Mdx-mice display hallmark symptoms of the diseases, changes in skeletal muscle histology, respiratory insufficiency, cardiomyopathy, and muscle weakness [36].

Botulinumtoxin A (BTX-A), a neurotoxin that blocks the release of acetylcholine at the neuromuscular junction and thus muscle contraction [53, 54] may lead to loss of muscle function caused by muscle atrophy [55, 56]. The therapeutic effects of BTX-A first appear in 1 to 3 days, peak in 1 to 4 weeks, and decline after 3 to 4 months [57].

Due to the fact that the mdx-mouse shows a higher regenerative capacity that ensures a more benign phenotype and essentially normal function [58], there is only a restricted time slot for research. To extend the time frame for evaluation of muscle influence on craniofacial growth and deformities, the purpose of this study was to determine the effects of BTX-A injection in the right masseter muscle of healthy and mdx-mice on the MyHC expression and protein content, to draw conclusions concerning remodelling and adaptation of the injected muscle as well as the adjacent noninjected masseter, temporal, and tongue muscles.

## 2. Materials and Methods

In this study the experimental protocol and all procedures were approved by the Laboratory Animal Research Committee of Saxony with the number 24-9168.11-1/2013-46.

**2.1. Animals.** As subjects mice of the line C57Bl/10ScSn (control group,  $n = 10$ ) and C57/Bl10ScSn-Dmdy (mdx) (test group,  $n = 10$ ) of both genders, aged 100 days at baseline of the trial and a body weight of approximately 30 g, were used in this study. The mice originally obtained from Jackson Laboratory (Bar Harbor, USA) were borne in the laboratory animal experimental centre of Dresden and up to the beginning of the experiments housed in standard cages in groups of 2–6 animals under standardised conditions in a temperature-controlled room of 21–23°C maintained on a 12:12 h light-dark cycle with standard mice chow and water available ad libitum.

**2.2. Chemodenervation Using Botulinumtoxin A (BTX-A).** For chemodenervation the mice were temporally anesthetized by an intraperitoneal injection consisting of a mixture of 10% ketamine (Ceva, Tiergesundheits GmbH, Düsseldorf, Germany) and 2% Rompun (Bayer, HealthCare AG, Leverkusen, Germany) in a relation to 3:2 at a dose of 0.1 mL per 100 g biomass.

To induce muscle paralysis, one single specific intramuscular injection of 0.025 mL BTX-A (Botox®, Allergan®, Irvine, California, USA; 1.25 IU/0.1 mL in physiologic NaCl-solution) was administered in the superficial and deep venter of the right masseter muscle. Both, healthy and mdx-mice were injected.

Postinjection care included a three-time daily control of the health state of the mice after they had awoken from anaesthesia and the verification of paralysis. The effects

of chemodenervation after BTX-A injection usually start delayed. Paralysis in the BTX-A injection masseter is typically evident by the refusal of solid food and tooth chattering 3 days after injection. Due to that fact, the mice were kept under standard conditions described above with the possibility to choose between soft or solid food for the first 7 days. After that time, only solid food was offered. Until the terminal experiments the weight of the mice was controlled regularly.

**2.3. Muscle Sample Preparation and Processing.** 21 days after intramuscular BTX-A injection, the animals were painlessly killed accordingly of the international guidelines for animal protection by means of an overdose of Isoflurane. The head was immediately separated from the body and the following muscles were carefully dissected and harvested by the same trained operator: masseter muscle (superficial venter) and temporal muscle from the injection side and contralateral side, respectively, as well as the tongue muscle.

According to Baverstock et al. [59], the dissected masseter muscle tissue corresponded to the superficial and (in parts) the deep masseter, accounting for 19% and 33% of overall masticatory muscle mass, respectively. The dissected temporal muscle, usually described as consisting of two parts and in the mouse distinguished as lateral and medial part, corresponded to the medial temporal muscle, which accounts for 77% of overall temporal muscle mass and is the larger portion of both parts [59].

For each of the examined muscles mRNA expression and protein content of myosin heavy chain (MyHC) isoforms were assessed. In addition, directly after dissection the right and left masseter muscles were weighted with a precision balance for direct comparison of muscle wet mass of the injected as well as the untreated contralateral side. The muscles were then flash-frozen in liquid nitrogen at  $-173^{\circ}\text{C}$  and up to subsequent analysis stored in a deep fridge at  $-80^{\circ}\text{C}$ .

**2.4. RNA-Extraction and Reverse Transcription Reaction.** Total RNA isolation from the muscle tissues was performed using Trizol (QIAzol Lysis Reagent QIAGEN, Hilden, Germany) and the RNeasy<sup>®</sup> Mini Kit (QIAGEN, Hilden, Germany) according to manufacturer's instructions. RNA concentrations and purity of the eluate were determined photometrically by ultraviolet absorbance measurements in the Eppendorf BioPhotometer<sup>®</sup> (Eppendorf Vertrieb Deutschland GmbH, Wesseling-Berzdorf, Germany) at a wavelength of 260 nm, a background compensation for the absorbance at 280 nm, and distilled water for calibration. Reverse transcription for synthesis of cDNA was performed in the Thermocycler TOptical (Analytik Jena AG, Jena, Germany) using an amount of 200 ng RNA and the innuSCRIPT Reverse Transcriptase in Nucleotide Mix and Random primer (Analytik Jena AG) following manufacturer's protocol.

**2.5. qRT-PCR (Quantitative Real-Time Polymerase Chain Reaction).** The mRNA quantification of four different myosin heavy chain isoforms (Myh1, Myh2, Myh4, and Myh7) in the concerning muscle tissues was performed by qRT-PCR (Taq-Man<sup>®</sup> Assays; PE Applied Biosystems<sup>®</sup>,

Weierstadt, Germany) in comparison to 18S rRNA (Eucaryotic 18S rRNA Endogenous control: 4310893E; PE Applied Biosystems<sup>®</sup>, Weierstadt, Germany) using gene-specific TaqMan PCR probes and primers which have been previously described elsewhere [60]. The master mix contained innuMix qPCR Master Mix Probe (Analytik Jena AG), 10x specific probes and primers, and RNase free water. For quantification of gene expression of the different MyHCs, 8 ng cDNA was used in a final volume of 20  $\mu\text{L}$ . Gene amplification was performed with the TOptical cyclor (Analytik Jena AG) at  $95^{\circ}\text{C}$  for 10 minutes for initial denaturation followed by 40 cycles, in each case 10 seconds at  $95^{\circ}\text{C}$  and 45 seconds at  $60^{\circ}\text{C}$ . Absolute copy numbers of the studied genes and 18S cDNA were determined using calibration curves generated with cloned PCR fragment standards [60]. Copy numbers of individual transcripts were given in relation to those of 18S cDNA. Each probe was performed twice and a "nontemplate control" was carried out parallel in all experiments to validate results.

**2.6. Western Blot.** To extract muscle protein, the interphase and phenophase from the RNA isolation protocol were used. Protein isolation was performed following the manufacturer's protocol (isolation of DNA and protein from QIAzol Reagent-lysed samples (RY16 May-04) (QIAGEN, Hilden, Germany)). To identify the MyHC isoforms, 15  $\mu\text{g}$  of proteins from each muscle was loaded onto Citerion<sup>™</sup> TGX Stain-free<sup>™</sup> Precast Gels (Bio-RAD Laboratories GmbH, Munich, Germany) and separated by 100 V (constant Voltage) for 60 minutes. Following the electrophoresis, the proteins were transferred to the Western blot membrane, using the Trans-Blot<sup>®</sup> Semi-Dry transfer system (Trans-Blot<sup>®</sup> Turbo<sup>™</sup> Midi PVDF Transfer Packs; Bio-RAD Laboratories GmbH) and the Trans-Blot Turbo blotting apparatus (Bio-RAD Laboratories GmbH). After protein transfer to the PVDF membrane, membranes were blocked over night at  $4^{\circ}\text{C}$  with 5% dry milk in phosphate-buffered saline (PBS) buffer with Tween.

Blots were incubated with monoclonal antibodies against MyHC proteins (anti-fast skeletal myosin antibody [My-32] (1:1000; Abcam, Cambridge, UK) and monoclonal Anti-Myosin (Skeletal, Slow) antibody produced in mouse (clone NOQ 7.5.4D; 1:1000; Sigma-Aldrich GmbH, Munich, Germany) diluted in PBS containing 5% dry milk and 0.025%  $\text{NaN}_3$  for 2-3 h at room temperature. Horseradish peroxidase- (HRP-) conjugate goat anti-mouse immunoglobulins (1:5000; Dako, Hamburg, Germany) were used afterwards. Bound antibodies were detected and visualized using an enhanced chemiluminescence system (WesternBright Chemilumineszenz Substrat Quantum, Advansta Inc., Menlo Park, USA). On each gel monoclonal anti-glyceraldehyde-phosphate dehydrogenase (GAPDH) antibody (clone 6C5; 1:1000; Millipore, Billerica, Massachusetts, USA) served as loading control of the gels to finally calculate the protein content (incubation at room temperature for 2 h). Quantitative analyses of protein bands from MyHC isoforms and GAPDH in the examined masticatory muscle of the 100-day-old healthy and mdx-mice were undertaken using GelScan 5.2 software (Serva, Heidelberg, Germany). Mean optical

density  $\pm$  SEM are given in all cases for  $n = 4$  muscle samples of different animals and three-independent Western blot analysis.

**2.7. Statistics.** To evaluate differences in the mRNA expression and protein content of the different fibre types in the analysed masticatory muscles of healthy and mdx-mice, statistical analysis was performed using the Software SigmaStat® Version 3.5 (Systat Software Inc., San Jose, California, USA) and Mann Whitney  $U$  test. In case of a normal distribution, the  $t$ -test was applied. Results  $p \leq 0.05$  were regarded as statistically significant.

### 3. Results

**3.1. Body Weight and Muscle Dimensions.** An initial decrease in body weight in the very early postinjection days, which might be attributed to the beginning paralysis and reduced food ingestion, was followed by a steady increase during the experimental protocol up to its closure. A statistical difference in body weight between the control and mdx group was not obvious at any time. During the entire experimental setup the body weight was similar in both groups.

To verify BTX-A induced atrophy, muscle mass of the injected masseter muscle and the corresponding contralateral noninjected muscle was measured. A comparison of the muscle tissue mass revealed a statistically significant difference between the weight and size of the injected (right) and untreated (left) masseter muscles for both control and mdx-mice (Figure 1). Compared to the untreated left masseter muscles, injected right masseter muscles were 56% and 45% smaller in the control and mdx group, respectively.

**3.2. mRNA Expression of MyHC Isoforms.** At first, the already known expression difference between dystrophic and healthy mice was also detectable, such as a decrease of Myh2 mRNA and an increase of Myh4 mRNA in dystrophic masseter muscle as well as an increase of Myh7 mRNA expression levels (encoding for fibre type I) in dystrophic temporal muscle compared to control.

21 days after BTX-A injection in the right masseter muscle, mRNA expression of MyHCs in the extracted muscle tissues of injected atrophic masseter muscle of control-mice differed significantly from the untreated noninjection side. A significant decrease of Myh4 mRNA and Myh1 mRNA encoding for the fast fibre types IIb and IIx/d, respectively, could be detected, whereas Myh2 and Myh7 mRNA expression, corresponding to the fibre types IIa and I, were significantly increased. In control temporal muscle tissue of healthy mice no differences between the right and left side were found. In tongue muscle a high expression level of Myh4 mRNA in the control as well as mdx group, with no statistically significant differences between both groups, could be detected.

The mRNA expression of all tested MyHC isoforms remained unchanged in mdx muscle tissue from both sides. No differences between BTX-A treated and untreated masseter muscle as well as right and left side could be observed in this mice strain (Table 1).

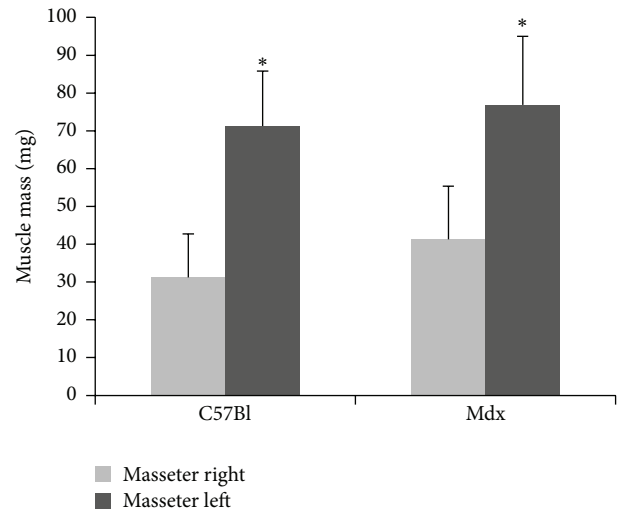


FIGURE 1: Muscle weight of treated (right) and untreated (left) masseter in control (C57Bl;  $n = 10$ ) and mdx-mice ( $n = 10$ ) 21 days after BTX-A injection. Mean values  $\pm$  standard deviations; Student's  $t$ -test ( $* p \leq 0.05$ ).

**3.3. Protein Content.** Semiquantitative analysis of fast and slow skeletal myosin proteins were performed with Western blot analysis. Single immune-reactive bands of approximately 220 kDa were detected. These bands correspond to the expected molecular weights of slow as well as fast myosin, respectively (Figure 2(a)). The quantitative evaluation of Western blots only showed significant increased protein levels of MyHC-II in BTX-A treated control masseter muscle compared to contralateral untreated masseter muscle tissue of control-mice ( $p = 0.006$ ; Figure 2(c)). In neither other muscle samples from control-mice nor all muscle samples from dystrophic mice differences in the expression levels of fast and slow myosin heavy chains could be detected (Figure 2).

### 4. Discussion

In the present study the effects of different masticatory muscles after BTX-A injection in the right masseter of healthy and mdx-mice muscles were evaluated concerning mRNA and protein expression of MyHC isoforms. BTX-A was used to reduce masticatory function and to prolong dystrophic features of muscle fibres in the masseter muscle of mdx-mice. Usually muscle pathology of mdx-mice is most pronounced and peaks at the age of 3-4 weeks [35, 61] and goes to cycles of de- and regeneration by 9-12 weeks of age, where regeneration overcomes degeneration of muscle fibres [62, 63]. In our study 100-day-old control and dystrophic mice were used. It has previously been shown that muscle fibres of mdx-mice of this age have centralized nuclei in 75% of all muscle fibres, a typical sign of muscle fibre regeneration [64].

BTX-A injection and inactivation of the right masseter muscle clearly resulted in a reduction of muscle weight 21 days after injection. It is well known that BTX-A treatment indirectly induces masticatory hypofunction and muscle

TABLE 1: mRNA expression of MyHC isoforms (Myh1, Myh2, Myh4, and Myh7) in BTX-A treated and untreated muscle tissue, 21 days after injection into the right masseter muscle of 100-day-old mice (control/mdx; n = 10 each). Means ± standard deviations; Student's *t*-test \* *p* ≤ 0.05 treated versus untreated masseter muscle; # *p* ≤ 0.05 control versus mdx. Significant values are indicated by bold lettering.

Gene name	Fibre type	Masseter right		Masseter left		Temporal right		Temporal left		Tongue	
		Control	Mdx	Control	Mdx	Control	Mdx	Control	Mdx	Control	Mdx
Myh 1	IIs/d	<b>1.06 ± 0.71</b> * <i>p</i> = 0.041	1.37 ± 0.64	<b>1.65 ± 0.87</b>	1.19 ± 0.56	1.27 ± 0.88	1.14 ± 0.67	1.68 ± 1.35	1.82 ± 1.2	0.25 ± 0.16	0.63 ± 0.67
Myh 2	Ila	<b>2.29 ± 0.79</b> * <i>p</i> < 0.001	<b>1.23 ± 0.61</b> # <i>p</i> = 0.014	<b>0.77 ± 0.59</b>	0.75 ± 0.45	4.41 ± 2.97	3.41 ± 0.54	3.67 ± 1.85	4.37 ± 3.05	0.02 ± 0.02	0.07 ± 0.09
Myh 4	I Ib	<b>1.18 ± 0.90</b> * <i>p</i> = 0.023	<b>2.63 ± 1.57</b> # <i>p</i> = 0.019	<b>2.99 ± 2.43</b>	2.60 ± 1.85	9.36 ± 6.66	9.80 ± 8.79	19.47 ± 17.15	10.12 ± 12.48	25.8 ± 17.1	33.02 ± 17.29
Myh 7	I	<b>0.000133 ± 3.15E5</b> * <i>p</i> = 0.012	0.000084 ± 3.53E5	<b>0.000053 ± 8.98E6</b>	0.000041 ± 8.59E6	0.000151 ± 2.93E5	0.000215 ± 3.77E5	<b>0.000113 ± 1.8E5</b> # <i>p</i> = 0.019	<b>0.000261 ± 7.27E5</b>	0.000005 ± 2.36E6	0.00001 ± 6.07E6

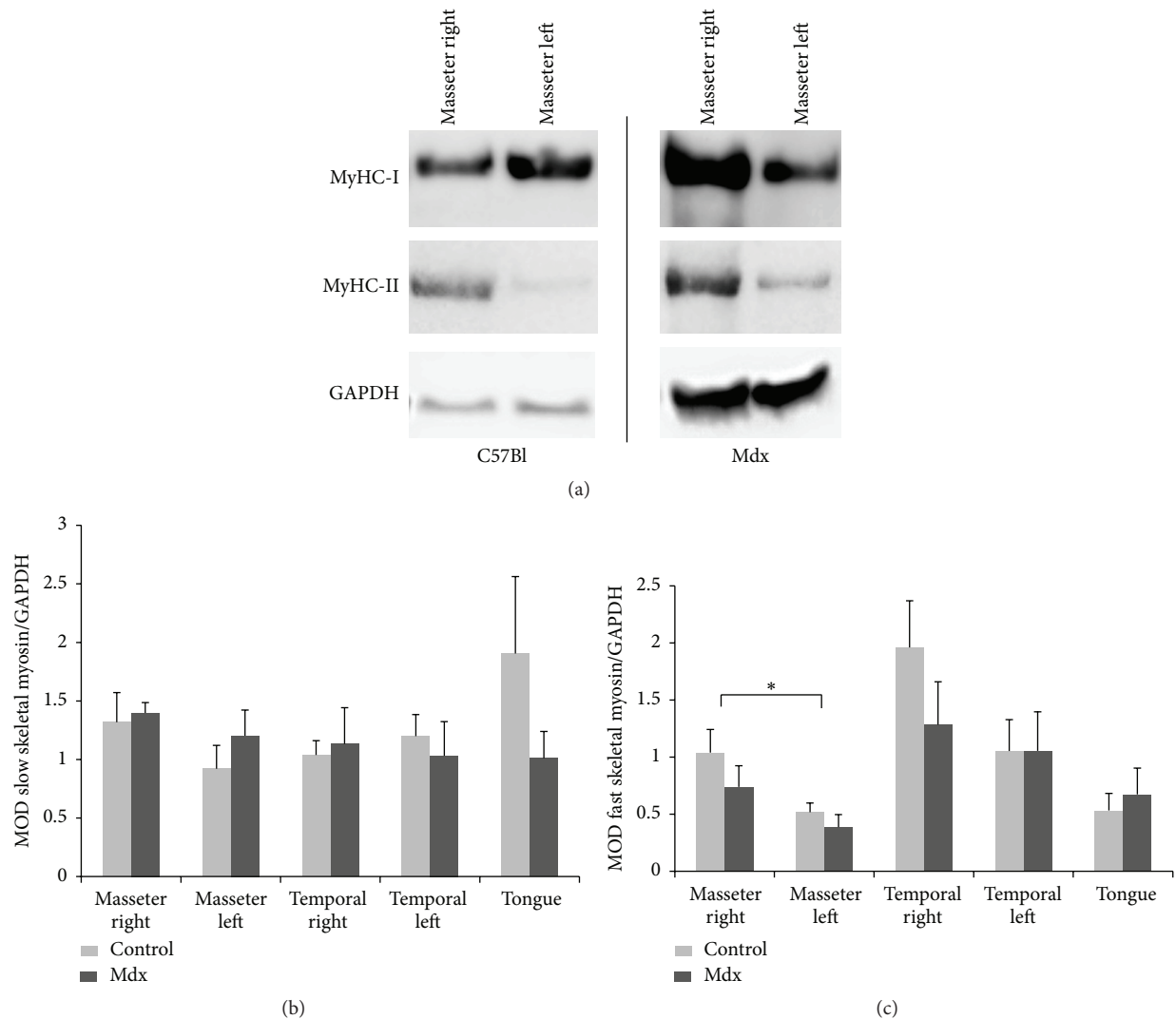


FIGURE 2: Western blot analysis of fast and slow skeletal muscle myosin extracted from 100-day-old mice (control/mdx) 21 days after BTX-A injection into the right masseter muscle. (a) Representative blots, (b) quantitative analyses of slow myosin (MyHC-I), and (c) fast myosin (MyHC-II) compared to GAPDH in masticatory muscle of BTX-A treated control- (C57Bl) and mdx-mice. Mean optical density (MOD)  $\pm$  SEM are given in all cases for  $n = 4$  muscle samples of different animals and three-independent Western blot analysis (Student's  $t$ -test; \* $p \leq 0.05$  treated versus untreated masseter muscle).

atrophy due to chemoinactivation [53]. Changes in muscle weight after BTX-A injection could also previously be found [65] and marked atrophy of paralyzed muscle fibres [5, 55] is a common feature also seen under clinical conditions taking advantage of BTX-A treatment for masseter hypertrophy [66, 67] and bruxism [68, 69]. In animal experiments, the muscle fibres begin to show atrophy histologically within 10–14 days after injection and this atrophy continues to develop over 4–6 weeks [70]. As shown previously, BTX-A influences the expression of MyHC isoforms. After BTX-A injection into the right masseter muscle of pigs a fibre shift towards faster isoforms in the injected as well as to slower isoforms in the noninjected masseter muscle could be demonstrated [71]. Slow-to-fast fibre shift is also well known from other denervation studies where no nerve stimulation exists [5]. In our study at protein level similar effects could be

seen in injected control masseter muscle with a statistically significant increase of type II myofibres compared to the contralateral noninjection side, whereas treated dystrophic masseter muscle does not show any statistically significant differences compared to untreated masseter muscle of mdx-mice.

By contrast, at mRNA level some other effects have been demonstrated in wild-type mice. In the right masseter muscle of control-mice a decrease in MyHC-IIb and -IIx mRNA expression as well as an increase in MyHC-IIa encoding for the slowest form of type II myofibres and an increase of MyHC-I encoding for slow muscle fibres could be identified. It is well known that healthy mouse masseter muscle (superficial part) predominantly consists of fast type IIb myofibres [72, 73]. A reduction of fast muscle fibres is typically seen in dystrophic muscles. Petrof et al. have proved preferential

degeneration of type II fibres in mdx limb and trunk muscles [74] and in dystrophic masticatory muscles reduced MyHC-IIb mRNA expression was also detected [60]. Furthermore, it was reported that the IIb fibres degenerate first in DMD patients [75]. Analyses of MHC isoforms in the affected diaphragm of canine X-linked muscular dystrophy (CXMDJ) also indicated a marked increase of type I and decrease of type IIa myosin isoforms [76]. In histological studies a fibre shift with more pronounced portion of slow type I fibres has been described for the superficial masseter muscle as a hallmark of disease progression obvious in 14-week-old mdx-mice [77]. Lee et al. by their study indicated that after degeneration the regenerated muscle acquires muscle fibre characteristics entirely different from those in its normal counterpart, with a very strong expression of MyHC-I in mdx-mouse masseter at 9 weeks of age [63]. The MyHC-IIx isoform has already been reported to represent the transition from fast type II to slow type I myofibres [22] and subsequently this transition results in a decrease of type II fibres. Based on these findings, it is to be assumed that chemical denervation, induced by BTX-A, simulates dystrophic appearance in healthy mice masticatory muscles with regard to fibre composition.

Muscles can also induce a fibre shift towards slower isoforms to adapt to varying functional load and endurance training [78]. In 10-week-old pigs, after chronic sagittal advancement of the mandible, a significant increase in the cross-sectional area of type I fibres and type I MyHC expression in the anterior part of the masseter, distal part of the temporal and the medial pterygoid muscle could be shown, which was simultaneously accompanied by a comparable decrease in type II MyHCs in these muscles [21]. Step-by-step transition of muscle fibres from type IIb via type IIa to type I under activity was also found by Goldspink [79] and Pette and Staront [80] and they stated that under higher muscle stress the increase in cross-sectional area of type I fibres is more efficient for long-term energy accumulation. In our study, in healthy mice after BTX-A injection a decrease in fast muscle fibres was observed in the untreated masseter muscle, which was statistically significantly different from the injection side showing at once an increase in type II fibres. It is well known that stretch overload influences fibre type transition towards slower MyHC isoform expression [8], and the same transition takes place in case of functional overload on skeletal muscles [81]. In the right temporal muscle of control-mice an increase of MyHC-II protein expression could also be observed, but these results were not statistically significantly different from the contralateral side. However this tendency of type II fibre increase seen could possibly be traced back to a compensatory effect of functional loss of the right masseter muscle and the rapid force increase and high stress, which is known to induce a fibre shift towards faster isoforms [78]. Harzer et al. emphasized that short-time and long-term strain on muscles due to endurance and fast-force training lead to different reactions, respectively. Though endurance training promotes a fibre shift from fast type II muscle fibres to slow type I with a more efficient energy supply during constant load [82], whereas fast-force training promotes a fibre shift in the opposite direction [78]. It can be assumed that due to the BTX-A induced inactivation

of the right masseter muscle, by simultaneous preservation of the chewing function, other muscle groups might have experienced more stress and might have adapted by changing their fibre type composition. Nevertheless this effect was only significant for the left masseter muscle in control-mice. On the other hand the effect seen at protein level in healthy mice could also be explained by BTX-A induced fibre shift towards faster isoforms in the injected muscle tissue whereas fibre type composition of left masseter muscle might not have been changed. This explanation seems to be more suitable because at protein level a statistically significant increase of type I fibres in left masseter muscle tissue was missing.

In contrast to healthy control-mice, muscles of mdx-mice showed no remarkable changes induced by BTX-A injection. It had been expected that the dystrophic injected masseter muscle had been reacted in the same way the healthy muscle did, but at protein level a statistically significant shift towards faster isoforms could not be seen in this muscle although such a tendency could be found. One explanation could be that the regeneration potential of this muscle was already exhausted due to the disease, and a shift towards faster isoforms could not be realized. Another possible explanation is due the role of dystrophin, which attributes particular importance in the expression of type IIb fibres. Webster et al. already emphasized that fast fibres are preferentially affected in DMD, and it has been suggested that dystrophin gene product plays a specific and essential role in IIb fibre function, a subpopulation of muscle fibres specialized to respond to the highest frequency of neuronal stimulation with maximal rates of contraction [75]. Possibly dystrophin is essential for accepting the high-frequency activity of fast motor neurons to carry out the high-frequency contraction demanded for type IIb muscle fibres [75]. In this case, the defect in the muscle fibre would be manifested only under neural influence [83]. Hence, with innervation being absent no degeneration of IIb fibres should occur. Vice versa, even though with innervation and strong IIb mRNA expression being present, which could be seen on mRNA level in our study, on account of dystrophin deficiency, no translation for MyHC-IIb exists. So that the last mentioned explanation is more appropriate to explain our results. Perhaps by this reason the reaction to BTX-A injection occurs temporally delayed in this mouse strain. Usually mRNA expression goes ahead to protein expression which occurs as time-delayed. In this context the fact that only one time point was investigated needs to be considered critically. On the other hand, it was of special interest to investigate both protein and mRNA expression in the same muscle tissues after BTX-A injection to estimate changes occurring at exactly one time point during the process of muscle fibre adaption. The mRNA response to stress is very rapid; thus mRNA content represents a steady state of muscle adaption, but with the additional analysis of protein content more distinctive effects of BTX-A injection could be demonstrated.

Effects on mRNA expression encoding for MyHC isoforms found in injected muscles in our study, especially in healthy mice, could also be attributed to reinnervation process which is known to occur 3-4 weeks after denervation [84]. Nayyar et al. stated that after that time, at the

cellular level, upregulation of the muscle nicotinic receptors and accordingly reappearance of muscle innervation, due to sprouting could be found in mice after a single BTX-A injection [84]. Hence, the results presented here may reflect the sum of fibre shifts in specific masticatory muscles evoked by BTX-A induced immobilisation and subsequent recovery of muscle function, reflected by fibre type diversity in different muscles and accumulation of specific types during fibre shift to one end of the fibre spectrum.

In conclusion, our study confirmed that a fibre shift due to BTX-A injection is possible in healthy mice muscle tissue, inducing different fibre type transformations. Likewise, the mRNA MyHC expression demonstrated similar changes to those observed in the untreated dystrophic muscles. However, in dystrophic mice BTX-A injection did elicit neither detectable direct or indirect compensatory fibre shifts, nor a prolongation of the dystrophic phenotype. Further research at different time points is necessary to fully elucidate the impact of BTX-A injection on masticatory muscles and to better estimate whether this medication or treatment method is likely to be able to selectively switch off the active regeneration processes of the musculature in the mdx-mouse and therefore to be able to use this effect for research concerning craniofacial changes induced by functional adaptations.

## Competing Interests

The authors declare that they have no competing interests regarding the publication of this paper.

## Acknowledgments

The authors like to thank Mrs. Krause for excellent technical assistance.

## References

- [1] T. Gedrange and W. Harzer, "Muscle influence on postnatal craniofacial development and diagnostics," *Fortschritte der Kieferorthopädie*, vol. 65, no. 6, pp. 451–466, 2004.
- [2] T. M. G. J. van Eijden and S. J. J. Turkawski, "Morphology and physiology of masticatory muscle motor units," *Critical Reviews in Oral Biology and Medicine*, vol. 12, no. 1, pp. 76–91, 2001.
- [3] A. J. McComas, "Oro-facial muscles: internal structure, function and ageing," *Gerodontology*, vol. 15, no. 1, pp. 3–14, 1998.
- [4] R. E. Burke, D. N. Levine, P. Tsairis, and F. E. Zajac III, "Physiological types and histochemical profiles in motor units of the cat gastrocnemius," *The Journal of Physiology*, vol. 234, no. 3, pp. 723–748, 1973.
- [5] S. Ciciliot, A. C. Rossi, K. A. Dyar, B. Blaauw, and S. Schiaffino, "Muscle type and fiber type specificity in muscle wasting," *The International Journal of Biochemistry & Cell Biology*, vol. 45, no. 10, pp. 2191–2199, 2013.
- [6] A. G. Hannam and A. S. McMillan, "Internal organization in the human jaw muscles," *Critical Reviews in Oral Biology and Medicine*, vol. 5, no. 1, pp. 55–89, 1994.
- [7] L. Larsson, L. Edstrom, B. Lindgren, L. Gorza, and S. Schiaffino, "MHC composition and enzyme-histochemical and physiological properties of a novel fast-twitch motor unit type," *The American Journal of Physiology—Cell Physiology*, vol. 261, no. 1, pp. C93–C101, 1991.
- [8] D. Pette and R. S. Staron, "Myosin isoforms, muscle fiber types, and transitions," *Microscopy Research and Technique*, vol. 50, no. 6, pp. 500–509, 2000.
- [9] S. Schiaffino and C. Reggiani, "Myosin isoforms in mammalian skeletal muscle," *Journal of Applied Physiology*, vol. 77, no. 2, pp. 493–501, 1994.
- [10] S. Schiaffino and C. Reggiani, "Fiber types in mammalian skeletal muscles," *Physiological Reviews*, vol. 91, no. 4, pp. 1447–1531, 2011.
- [11] J. J. Sciote and T. J. Morris, "Skeletal muscle function and fiber types: the relationship between occlusal function and the phenotype of jaw-closing muscles in human," *Journal of Orthodontics*, vol. 27, no. 1, pp. 15–30, 2000.
- [12] A. Weiss and L. A. Leinwand, "The mammalian myosin heavy chain gene family," *Annual Review of Cell and Developmental Biology*, vol. 12, pp. 417–439, 1996.
- [13] M. Maejima, S. Abe, K. Sakiyama et al., "Changes in the properties of mouse tongue muscle fibres before and after weaning," *Archives of Oral Biology*, vol. 50, no. 12, pp. 988–993, 2005.
- [14] K. Gojo, S. Abe, and Y. Ide, "Characteristics of myofibres in the masseter muscle of mice during postnatal growth period," *Anatomia, Histologia, Embryologia*, vol. 31, no. 2, pp. 105–112, 2002.
- [15] N. Hamalainen and D. Pette, "Patterns of myosin isoforms in mammalian skeletal muscle fibres," *Microscopy Research and Technique*, vol. 30, no. 5, pp. 381–389, 1995.
- [16] J. J. Sciote, A. M. Rowleron, C. Hopper, and N. P. Hunt, "Fibre type classification and myosin isoforms in the human masseter muscle," *Journal of the Neurological Sciences*, vol. 126, no. 1, pp. 15–24, 1994.
- [17] M. Ringqvist, "Fiber types in human masticatory muscles. Relation to function," *Scandinavian Journal of Dental Research*, vol. 82, no. 4, pp. 333–355, 1974.
- [18] F. Yu, P. Stål, L.-E. Thornell, and L. Larsson, "Human single masseter muscle fibers contain unique combinations of myosin and myosin binding protein C isoforms," *Journal of Muscle Research and Cell Motility*, vol. 23, no. 4, pp. 317–326, 2002.
- [19] J. A. M. Korfage and T. M. G. J. Van Eijden, "Regional differences in fibre type composition in the human temporalis muscle," *Journal of Anatomy*, vol. 194, part 3, pp. 355–362, 1999.
- [20] W. A. Weijs, "Masticatory muscles. Part II. Functional properties of the masticatory muscle fibers," *Nederlands tijdschrift voor tandheelkunde*, vol. 104, no. 6, pp. 210–213, 1997.
- [21] T. Gedrange, A. Lupp, C. Kirsch, W. Harzer, and R. Klinger, "Influence of the sagittal advancement of mandibulae on myofibrillar ATPase activity and myosin heavy chain content in the masticatory muscles of pigs," *Folia Histochemica et Cytobiologica*, vol. 40, no. 3, pp. 277–284, 2002.
- [22] S. Schiaffino and C. Reggiani, "Molecular diversity of myofibrillar proteins: gene regulation and functional significance," *Physiological Reviews*, vol. 76, no. 2, pp. 371–423, 1996.
- [23] P. Gunning and E. Hardeman, "Multiple mechanisms regulate muscle fiber diversity," *The FASEB Journal*, vol. 5, no. 15, pp. 3064–3070, 1991.
- [24] L. Larsson, T. Ansved, L. Edstrom, L. Gorza, and S. Schiaffino, "Effects of age on physiological, immunohistochemical and biochemical properties of fast-twitch single motor units in the rat," *The Journal of Physiology*, vol. 443, pp. 257–275, 1991.

- [25] D. Pette and G. Vrbova, "Invited review: neural control of phenotypic expression in mammalian muscle fibers," *Muscle and Nerve*, vol. 8, no. 8, pp. 676–689, 1985.
- [26] D. Pette and G. Vrbová, "Adaptation of mammalian skeletal muscle fibers to chronic electrical stimulation," *Reviews of Physiology Biochemistry and Pharmacology*, vol. 120, pp. 115–202, 1992.
- [27] A. Maier, L. Gorza, S. Schiaffino, and D. Pette, "A combined histochemical and immunohistochemical study on the dynamics of fast-to-slow fiber transformation in chronically stimulated rabbit muscle," *Cell and Tissue Research*, vol. 254, no. 1, pp. 59–68, 1988.
- [28] T. Soukup and I. Jirmanová, "Regulation of myosin expression in developing and regenerating extrafusal and intrafusal muscle fibers with special emphasis on the role of thyroid hormones," *Physiological Research*, vol. 49, no. 6, pp. 617–633, 2000.
- [29] R. R. Roy, K. M. Baldwin, and V. R. Edgerton, "The plasticity of skeletal muscle: effects of neuromuscular activity," *Exercise and Sport Sciences Reviews*, vol. 19, no. 1, pp. 269–312, 1991.
- [30] P. Stål, P.-O. Eriksson, S. Schiaffino, G. S. Butler-Browne, and L.-E. Thornell, "Differences in myosin composition between human oro-facial, masticatory and limb muscles: enzyme-, immunohisto- and biochemical studies," *Journal of Muscle Research and Cell Motility*, vol. 15, no. 5, pp. 517–534, 1994.
- [31] S. Schiaffino and G. Salviati, "Molecular diversity of myofibrillar proteins: isoforms analysis at the protein and mRNA level," *Methods in Cell Biology*, vol. 52, pp. 349–369, 1997.
- [32] H. Klitgaard, O. Bergman, R. Betto et al., "Co-existence of myosin heavy chain I and IIa isoforms in human skeletal muscle fibres with endurance training," *Pflügers Archiv: European Journal of Physiology*, vol. 416, no. 4, pp. 470–472, 1990.
- [33] M. F. Patterson, G. M. M. Stephenson, and D. G. Stephenson, "Denervation produces different single fiber phenotypes in fast- and slow-twitch hindlimb muscles of the rat," *American Journal of Physiology—Cell Physiology*, vol. 291, no. 3, pp. C518–C528, 2006.
- [34] D. F. Goldspink, "The influence of activity on muscle size and protein turnover," *The Journal of Physiology*, vol. 264, no. 1, pp. 283–296, 1977.
- [35] A. Nakamura and S. Takeda, "Mammalian models of duchenne muscular dystrophy: pathological characteristics and therapeutic applications," *Journal of Biomedicine and Biotechnology*, vol. 2011, Article ID 184393, 8 pages, 2011.
- [36] J. Manning and D. O'Malley, "What has the mdx mouse model of duchenne muscular dystrophy contributed to our understanding of this disease?" *Journal of Muscle Research and Cell Motility*, vol. 36, no. 2, pp. 155–167, 2015.
- [37] C. A. Collins and J. E. Morgan, "Duchenne's muscular dystrophy: animal models used to investigate pathogenesis and develop therapeutic strategies," *International Journal of Experimental Pathology*, vol. 84, no. 4, pp. 165–172, 2003.
- [38] V. Jay and J. Vajsar, "The dystrophy of Duchenne," *The Lancet*, vol. 357, no. 9255, pp. 550–552, 2001.
- [39] A. E. H. Emery, "The muscular dystrophies," *The Lancet*, vol. 359, no. 9307, pp. 687–695, 2002.
- [40] K. R. Wagner, "Approaching a new age in duchenne muscular dystrophy treatment," *Neurotherapeutics*, vol. 5, no. 4, pp. 583–591, 2008.
- [41] D. J. Wells and K. E. Wells, "Gene transfer studies in animals: what do they really tell us about the prospects for gene therapy in DMD?" *Neuromuscular Disorders*, vol. 12, supplement 1, pp. S11–S22, 2002.
- [42] L. Eckardt and W. Harzer, "Facial structure and functional findings in patients with progressive muscular dystrophy (Duchenne)," *American Journal of Orthodontics and Dentofacial Orthopedics*, vol. 110, no. 2, pp. 185–190, 1996.
- [43] S. Kiliaridis and C. Katsaros, "The effects of myotonic dystrophy and Duchenne muscular dystrophy on the orofacial muscles and dentofacial morphology," *Acta Odontologica Scandinavica*, vol. 56, no. 6, pp. 369–374, 1998.
- [44] C. Morel-Verdebout, S. Botteron, and S. Kiliaridis, "Dentofacial characteristics of growing patients with Duchenne muscular dystrophy: a morphological study," *European Journal of Orthodontics*, vol. 29, no. 5, pp. 500–507, 2007.
- [45] E. Le Rumeur, "Dystrophin and the two related genetic diseases, Duchenne and Becker muscular dystrophies," *Bosnian Journal of Basic Medical Sciences*, vol. 15, pp. 14–20, 2015.
- [46] J. Shin, M. M. Tajrishi, Y. Ogura, and A. Kumar, "Wasting mechanisms in muscular dystrophy," *The International Journal of Biochemistry & Cell Biology*, vol. 45, no. 10, pp. 2266–2279, 2013.
- [47] R. Willmann, S. Possekel, J. Dubach-Powell, T. Meier, and M. A. Ruegg, "Mammalian animal models for Duchenne muscular dystrophy," *Neuromuscular Disorders*, vol. 19, no. 4, pp. 241–249, 2009.
- [48] D. C. Górecki, "Dystrophin: the dead calm of a dogma," *Rare Diseases*, vol. 4, no. 1, article e1153777, 2016.
- [49] T. A. Partridge, "The mdx mouse model as a surrogate for Duchenne muscular dystrophy," *The FEBS Journal*, vol. 280, no. 17, pp. 4177–4186, 2013.
- [50] G. R. Coulton, N. A. Curtin, J. E. Morgan, and T. A. Partridge, "The mdx mouse skeletal muscle myopathy: II. Contractile properties," *Neuropathology and Applied Neurobiology*, vol. 14, no. 4, pp. 299–314, 1988.
- [51] G. Bulfield, W. G. Siller, P. A. L. Wight, and K. J. Moore, "X chromosome-linked muscular dystrophy (mdx) in the mouse," *Proceedings of the National Academy of Sciences of the United States of America*, vol. 81, no. 4 I, pp. 1189–1192, 1984.
- [52] P. Huang, X. S. Zhao, M. Fields, R. M. Ransohoff, and L. Zhou, "Imatinib attenuates skeletal muscle dystrophy in mdx mice," *The FASEB Journal*, vol. 23, no. 8, pp. 2539–2548, 2009.
- [53] C. Y. Tsai, Y. C. Lin, B. Su, L. Y. Yang, and W. C. Chiu, "Masseter muscle fibre changes following reduction of masticatory function," *International Journal of Oral and Maxillofacial Surgery*, vol. 41, no. 3, pp. 394–399, 2012.
- [54] P. E. Setler, "Therapeutic use of botulinum toxins: background and history," *The Clinical Journal of Pain*, vol. 18, no. 6, pp. S119–S124, 2002.
- [55] S. L. Dodd, J. Selsby, A. Payne, A. Judge, and C. Dott, "Botulinum neurotoxin type A causes shifts in myosin heavy chain composition in muscle," *Toxicon*, vol. 46, no. 2, pp. 196–203, 2005.
- [56] K. Legerlotz, K. G. Matthews, M. D. Christopher, and H. K. Smith, "Botulinum toxin-induced paralysis leads to slower myosin heavy chain isoform composition and reduced titin content in juvenile rat gastrocnemius muscle," *Muscle and Nerve*, vol. 39, no. 4, pp. 472–479, 2009.
- [57] G. T. Clark, A. Stiles, L. Z. Lockerman, and S. G. Gross, "A critical review of the use of botulinum toxin in orofacial pain disorders," *Dental Clinics of North America*, vol. 51, no. 1, pp. 245–261, 2007.
- [58] V. Nigro and G. Piluso, "Spectrum of muscular dystrophies associated with sarcolemmal-protein genetic defects," *Biochimica et Biophysica Acta*, vol. 1852, no. 4, pp. 585–593, 2015.

- [59] H. Baverstock, N. S. Jeffery, and S. N. Cobb, "The morphology of the mouse masticatory musculature," *Journal of Anatomy*, vol. 223, no. 1, pp. 46–60, 2013.
- [60] A. Spassov, T. Gredes, T. Gedrange et al., "Differential expression of myosin heavy chain isoforms in the masticatory muscles of dystrophin-deficient mice," *European Journal of Orthodontics*, vol. 33, no. 6, pp. 613–619, 2011.
- [61] J. K. McGeachie, M. D. Grounds, T. A. Partridge, and J. E. Morgan, "Age-related changes in replication of myogenic cells in mdx mice: quantitative autoradiographic studies," *Journal of the Neurological Sciences*, vol. 119, no. 2, pp. 169–179, 1993.
- [62] J. X. DiMario, A. Uzman, and R. C. Strohman, "Fiber regeneration is not persistent in dystrophic (mdx) mouse skeletal muscle," *Developmental Biology*, vol. 148, no. 1, pp. 314–321, 1991.
- [63] W.-H. Lee, S. Abe, H.-J. Kim et al., "Characteristics of muscle fibers reconstituted in the regeneration process of masseter muscle in an mdx mouse model of muscular dystrophy," *Journal of Muscle Research and Cell Motility*, vol. 27, no. 3-4, pp. 235–240, 2006.
- [64] A. Spassov, T. Gredes, T. Gedrange, S. Lucke, D. Pavlovic, and C. Kunert-Keil, "Histological changes in masticatory muscles of mdx mice," *Archives of Oral Biology*, vol. 55, no. 4, pp. 318–324, 2010.
- [65] J. D. Porter, S. Strebeck, and N. F. Capra, "Botulinum-induced changes in monkey eyelid muscle. Comparison with changes seen in extraocular muscle," *Archives of Ophthalmology*, vol. 109, no. 3, pp. 396–404, 1991.
- [66] O. K. Arikan, F. U. Tan, T. Kendi, and C. Koc, "Use of botulinum toxin type A for the treatment of masseteric muscle hypertrophy," *Journal of Otolaryngology*, vol. 35, no. 1, pp. 40–43, 2006.
- [67] H. J. Kim, K.-W. Yum, S.-S. Lee, M.-S. Heo, and K. Seo, "Effects of botulinum toxin type A on bilateral masseteric hypertrophy evaluated with computed tomographic measurement," *Dermatologic Surgery*, vol. 29, no. 5, pp. 484–489, 2003.
- [68] S. J. Lee, W. D. McCall, Y. K. Kim, S. C. Chung, and J. W. Chung, "Effect of botulinum toxin injection on nocturnal bruxism: a randomized controlled trial," *American Journal of Physical Medicine and Rehabilitation*, vol. 89, no. 1, pp. 16–23, 2010.
- [69] E.-K. Tan and J. Jankovic, "Treating severe bruxism with botulinum toxin," *Journal of the American Dental Association*, vol. 131, no. 2, pp. 211–216, 2000.
- [70] G. E. Borodic, R. J. Ferrante, and L. B. Pearce, "Pharmacology and histology of the therapeutic application of botulinum toxin," in *Therapy with Botulinum Toxin*, J. Jankovic and M. Hallett, Eds., p. 119, Marcel Dekker, New York, NY, USA, 1994.
- [71] T. Gedrange, T. Gredes, A. Spassov et al., "Histological changes and changes in the myosin mRNA content of the porcine masticatory muscles after masseter treatment with botulinum toxin A," *Clinical Oral Investigations*, vol. 17, no. 3, pp. 887–896, 2013.
- [72] J. M. Eason, G. A. Schwartz, G. K. Pavlath, and A. W. English, "Sexually dimorphic expression of myosin heavy chains in the adult mouse masseter," *Journal of Applied Physiology*, vol. 89, no. 1, pp. 251–258, 2000.
- [73] A. Tuxen and S. Kirkeby, "An animal model for human masseter muscle: histochemical characterization of mouse, rat, rabbit, cat, dog, pig, and cow masseter muscle," *Journal of Oral and Maxillofacial Surgery*, vol. 48, no. 10, pp. 1063–1067, 1990.
- [74] B. J. Petrof, H. H. Stedman, J. B. Shrager, J. Eby, H. L. Sweeney, and A. M. Kelly, "Adaptations in myosin heavy chain expression and contractile function in dystrophic mouse diaphragm," *The American Journal of Physiology*, vol. 265, no. 3, pp. C834–C841, 1993.
- [75] C. Webster, L. Silberstein, A. P. Hays, and H. M. Blau, "Fast muscle fibers are preferentially affected in Duchenne muscular dystrophy," *Cell*, vol. 52, no. 4, pp. 503–513, 1988.
- [76] K. Yuasa, A. Nakamura, T. Hijikata, and S. Takeda, "Dystrophin deficiency in canine X-linked muscular dystrophy in Japan (CXMDJ) alters myosin heavy chain expression profiles in the diaphragm more markedly than in the tibialis cranialis muscle," *BMC Musculoskeletal Disorders*, vol. 9, article 1, 2008.
- [77] M. Ukai, N. Maeda, and K. Osawa, "Postnatal changes in the extrafusal muscle fiber and muscle spindle in the masseter muscle of the dystrophic mouse," *Biomedical Research*, vol. 14, no. 6, pp. 419–425, 1993.
- [78] W. Harzer, M. Worm, T. Gedrange, M. Schneider, and P. Wolf, "Myosin heavy chain mRNA isoforms in masseter muscle before and after orthognathic surgery," *Oral Surgery, Oral Medicine, Oral Pathology, Oral Radiology and Endodontology*, vol. 104, no. 4, pp. 486–490, 2007.
- [79] G. Goldspink, "Gene expression in muscle in response to exercise," *Journal of Muscle Research and Cell Motility*, vol. 24, no. 2-3, pp. 121–126, 2003.
- [80] D. Pette and R. S. Staront, "Mammalian skeletal muscle fiber type transitions," *International Review of Cytology*, vol. 170, pp. 143–223, 1997.
- [81] S. Banzet, N. Koulmann, H. Sanchez, B. Serrurier, A. Peinnequin, and A. X. Bigard, "Musclin gene expression is strongly related to fast-glycolytic phenotype," *Biochemical and Biophysical Research Communications*, vol. 353, no. 3, pp. 713–718, 2007.
- [82] R. Thayer, J. Collins, E. G. Noble, and A. W. Taylor, "A decade of aerobic endurance training: histological evidence for fibre type transformation," *The Journal of Sports Medicine and Physical Fitness*, vol. 40, no. 4, pp. 284–289, 2000.
- [83] G. Vrbova, "Duchenne dystrophy viewed as a disturbance of nerve-muscle interactions," *Muscle & Nerve*, vol. 6, no. 9, pp. 671–675, 1983.
- [84] P. Nayyar, P. Kumar, P. V. Nayyar, and A. Singh, "Botox: broadening the horizon of dentistry," *Journal of Clinical and Diagnostic Research*, vol. 8, no. 12, pp. ZE25–ZE29, 2014.

## Research Article

# Long-Term Fatigue and Its Probability of Failure Applied to Dental Implants

**María Prados-Privado,<sup>1,2</sup> Juan Carlos Prados-Frutos,<sup>1</sup> Sérgio Alexandre Gehrke,<sup>3,4</sup> Mariano Sánchez Siles,<sup>5</sup> José Luis Calvo Guirado,<sup>6</sup> and José Antonio Bea<sup>2</sup>**

<sup>1</sup>Department of Medicine and Surgery (Stomatology Area), Rey Juan Carlos University, C/ Tulipán s/n, Móstoles, 28933 Madrid, Spain

<sup>2</sup>Applied Modelling and Instrumentation Group, Aragón Institute of Engineering Research, University of Zaragoza, C/ Mariano Esquillor s/n, 50018 Zaragoza, Spain

<sup>3</sup>Biotecnos Research Center, Rua Dr. Bozano 571, 97015-001 Santa Maria, RS, Brazil

<sup>4</sup>University Catholic San Antonio de Murcia (UCAM), Guadalupe, 30107 Murcia, Spain

<sup>5</sup>Oral Medicine, University of Murcia, 30001 Murcia, Spain

<sup>6</sup>International Dental Research Cathedra, Faculty of Medicine and Dentistry, University Catholic San Antonio de Murcia (UCAM), Guadalupe, 30107 Murcia, Spain

Correspondence should be addressed to María Prados-Privado; [mariapradosprivado@gmail.com](mailto:mariapradosprivado@gmail.com)

Received 13 April 2016; Revised 16 June 2016; Accepted 22 June 2016

Academic Editor: Christiane Kunert-Keil

Copyright © 2016 María Prados-Privado et al. This is an open access article distributed under the Creative Commons Attribution License, which permits unrestricted use, distribution, and reproduction in any medium, provided the original work is properly cited.

It is well known that dental implants have a high success rate but even so, there are a lot of factors that can cause dental implants failure. Fatigue is very sensitive to many variables involved in this phenomenon. This paper takes a close look at fatigue analysis and explains a new method to study fatigue from a probabilistic point of view, based on a cumulative damage model and probabilistic finite elements, with the goal of obtaining the expected life and the probability of failure. Two different dental implants were analysed. The model simulated a load of 178 N applied with an angle of 0°, 15°, and 20° and a force of 489 N with the same angles. Von Mises stress distribution was evaluated and once the methodology proposed here was used, the statistic of the fatigue life and the probability cumulative function were obtained. This function allows us to relate each cycle life with its probability of failure. Cylindrical implant has a worst behaviour under the same loading force compared to the conical implant analysed here. Methodology employed in the present study provides very accuracy results because all possible uncertainties have been taken in mind from the beginning.

## 1. Introduction

Implants are widely used, as Misch discussed in [1], “to restore the patient to normal contour, function comfort, esthetics, speech, and health, whether restoring a single tooth with caries or replacing several teeth. What makes implant dentistry unique is the ability to achieve this goal regardless of the atrophy, disease, or injury of the stomatognathic system.”

The use of dental implants to replace missing teeth has become a routine in dental practice. Despite dental implants have a high success rate [2], there are a lot of factors that can involve complications and failure. On occasion, prosthetic implants fail because of mechanical and biological causes [3].

The primary causes of implant failure in clinical observations include incomplete osseointegration [4], infection, and impaired healing [5]. In addition to this, the failure of dental implants can be attributed to poor planning or the use of an improper implant for a given region of the maxilla or mandible [6, 7]. Occlusal conditions such as parafunctional habits have been identified as other important and potential causes of fracture.

Overload is, as it was said previously, an important factor in dental implant failure and one of the reason is bruxism. Misch explains in [1] that forces involved in bruxist person are significantly more important than normal physiologic masticatory loads. This situation affects above everything the

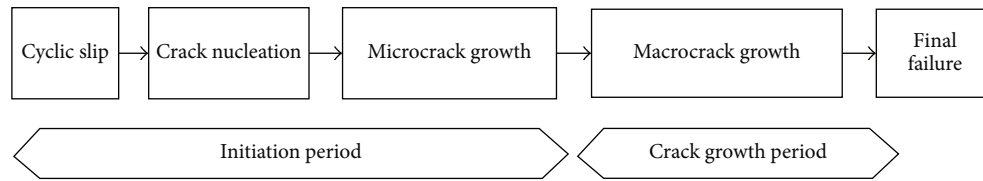


FIGURE 1: Different phases of fatigue life [18].

teeth, bone, implants, and prostheses although its consequences depend on the bruxism type (diurnal or nocturnal). Although this parafunction increases the risk of failure in dental implants, bruxism does not necessarily represent a contraindication for implants, but it does dramatically influence treatment planning [1].

Nowadays, most of dental implants are made of titanium, both pure or alloy, which is a highly biocompatible biomaterial (both *in vitro* and *in vivo*) and show excellent performance balance between biofunctional, mechanical, and physicochemical properties [3, 8]. However, its rigidity as compared with alveolar bone is an important disadvantage of titanium. Due to the fact that it reduces the stresses in the bone, a loss of bone mass appears. An important implication of this bone loss is the risk of implant fracture [9].

Given that failure is an important occurrence in dental implants, several papers have been published where this problem has been treated from different points of view such as clinical studies and finite element analysis [10–14]. However, most of these studies have been done from a deterministic point of view. Due to the fact that fatigue in dental implants is very sensitive to many different parameters, a probabilistic fatigue analysis is crucial in order to have a more accurate prediction on probability of failure and mean life. The randomness of material properties and loads have been considered in this study, as well as its influence on the life of the structural components [15].

Fatigue phenomenon is known as the change that appears on materials when cyclic loads are applied. The International Organization for Standardization published in 1964 a report entitled General Principles for Fatigue Testing of Metals where fatigue was defined as “a term which applies to changes in properties which can occur in a metallic material due to the repeated application of stresses or strains, although usually this term applies specially to those changes with lead to cracking or failure” [16].

The fatigue life is the number of stress cycles required to cause failure. This number relies on several variables, such as stress level, stress state, cyclic wave form, fatigue environment, and metallurgical condition of the material [17]. Prediction of fatigue life can be difficult because small changes in the specimen or test conditions can significantly affect fatigue behaviour. Boyer detailed in [17] that fatigue cracking is normally the outcome of cyclic stresses. These stresses are sufficiently below the static yield strength of the material. Fatigue cracks initiate and propagate in regions where the strain is most severe. This area of high deformation becomes the initiation for a fatigue crack, which propagates under the applied stress through the material until the complete fracture.

Fatigue process can be divided into two periods: the crack initiation period and the crack growth period, as Figure 1 shows. As Schijve detailed in [18] in the crack initiation period, fatigue is a material surface phenomenon and it finishes when microcrack growth is no longer depending on the material surface conditions [18].

In crack initiation testing, the specimen is exposed to the number of cycles required for a fatigue crack to initiate and to grow large enough to produce failure. In crack propagation testing, to determine the crack growth rates, fracture mechanics methods are used [17].

It is also known that fatigue life is more sensitive to this influence in the initiation period. In any case, laboratories try to eliminate these sources of variability in order to obtain more confident results, so fatigue tests are carried out under closely controlled conditions [18].

This paper shows a new method of studying long-term life in dental implants and its components both with normal conditions and functional overload. Authors propose here a new way of studying fatigue based on cumulative damage model and probabilistic finite elements. This method allows us to know what is the probability of failure in each cycle without doing any mechanical test as previously explained, or, what it is the same, the methodology employed here allows us to obtain the failure probability without breaking any implant.

## 2. Materials and Methods

The aim of the method explained in this section is to obtain the mean life and the probability of failure associated with each cycle without doing any fatigue test as previously explained. Novelty of this method is based, mainly, in the perspective from the study involved. Most of fatigue studies are addressed from a deterministic point of view, while we here consider the randomness of some variables, as load magnitude and direction or material properties (i.e., Young modulus). Once stress distribution under a particular condition is known, long-term life and probability of failure can be determined by employing a probabilistic model developed by Bogdanoff and Kozin and by the Stochastic Finite Elements Method [19–21]. To develop this method, the use of ANSYS® (version 14.5, Canonsburg, Pennsylvania, United States) and Mathematica® (version 10, Oxfordshire, United Kingdom) is only required.

Geometry in IGES format has been used to generate the finite element mesh employing the commercial software ANSYS® and once geometry was meshed, boundary conditions can be applied and stress analysis can be done. Use of finite element software makes the efforts to obtain

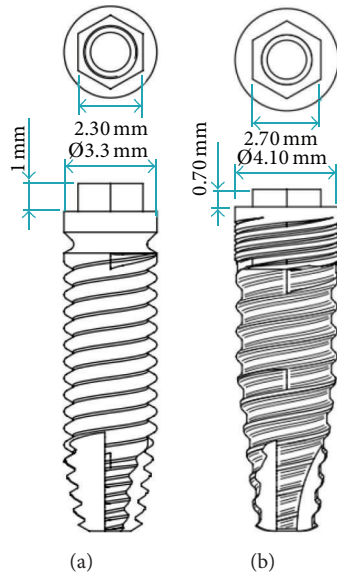


FIGURE 2: Dental implants characteristics: (a) IP861 and (b) IP804.

TABLE 1: Characteristics of each implant.

Implant name	Connection	Diameter
IP861	External hexagon	4.1
IP804		3.3

stress distribution on dental implants under different load situations easier.

*2.1. Dental Implants Characteristics.* Dental implants employed in the present study are manufactured by Avenir S.L. (Rimini, Italy) and sold by Proclinic S.A. (Madrid, Spain), with the characteristics as described in Table 1. The implant name employed here is the same as the catalogue.

These two implants were used in this study: cylindrical external Ø3.30 mm (IP804) and conical external Ø4.10 mm (IP861). Figure 2 illustrates the dimensions and appearance of the implants (14.5 mm in length).

*2.2. Material Properties.* Implants were modelled with linear, elastic, isotropic, and homogeneous properties. Both implants are made from Titanium Grade IV (Young modulus = 114 GPa, provided by the manufacturer).

*2.3. Boundary Conditions and Loading Configuration.* All degrees-of-freedom (DOFs) were restrained in all directions at the nodes on the apical part of the implants and ideal osseointegration was simulated in the rest of the implant. Boundary conditions applied are shown in Figure 3.

Tables 2 and 3 detail bite force values in molar and anterior region found in the literature, where N represents the International System units for load. In the view of the literature, we have decided to employ in this study forces and angle detailed in Table 4.

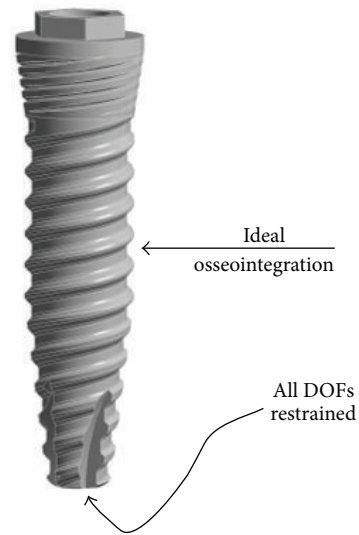


FIGURE 3: Boundary conditions applied in all situations.

TABLE 2: Bite forces on molar region in the literature.

According to	Maximum bite force [N]	Range age [year]
[22]	300–600	10–70
[23]	387.79–392.34 (mean) 836–884 (maximum)	20–50 (mean = 24.89; SD = 5.658)
[24]	497.3–629.65	15–18
[25]	583,49	—

Thus, the literature suggests maximum bite forces in the region area in the range of 300–629 and 65 N for adults

TABLE 3: Bite forces on anterior region in the literature.

According to	Maximum bite force [N]
[26]	150
[27]	146
[28]	178

and maximum forces in the anterior region between 146 and 178 N. In the current study, forces in two different regions with different angles were simulated: a static load of 489 N in the molar region and a load of 178 N in the anterior region.

**2.4. Methodology Proposed.** The hypothesis employed for the development of the current study was the following:

- (1) Literature available about fatigue is experimental in most cases. Therefore, equations that describe material behaviour under cyclic loads cannot be too much realistic.
- (2) Fatigue studies in dental implants available in the literature are addressed from a deterministic point of view. Stochastic variations of the geometry and dimensions, material properties, and load history have a decisive influence on the fatigue phenomenon in dental implants, inducing important deviations from the mean or characteristic values of the fatigue life when considered as deterministic [29].
- (3) Fatigue is therefore recognised as a random process, which only recently has started to be analysed with the tools of the probability theory.

Steps to obtain the results with the methodology employed in the present study are the following:

- (i) Obtain the mesh of the geometry by the used of ANSYS.
- (ii) Apply boundary conditions and loading configuration with ANSYS.
- (iii) Apply the probabilistic finite element method with the aim of obtaining the statistics of the stress.
- (iv) Apply the cumulative damage model to obtain the mean life, the variance, and the probability of failure.

The reader is referred to Prados-Privado et al. [19] for further details.

### 3. Results and Discussion

Probabilistic finite element method proposed in the current study has been applied on Proclinic® dental implants. Two different situations have been studied: fatigue behaviour in molar and fatigue behaviour in anterior region. Magnitude forces employed are shown in Table 4 and these loads were applied with three different angles. All results shown here have been measured in the neck (point A), body (point B), and apical region (point C).

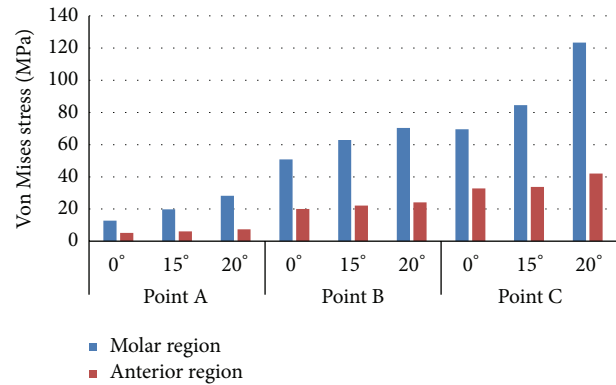


FIGURE 4: Von Mises stress in implant IP861.

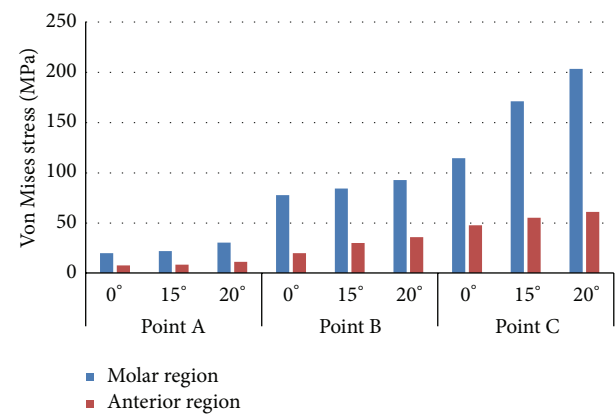


FIGURE 5: Von Mises stress in implant IP804.

**3.1. Stress Distribution.** Von Mises stresses on implants were used to assess the stress distribution in each situation. The Von Mises stress values in each point of study are shown Figures 4 and 5. When the stress distribution in both implants was compared, it was found that all investigated stress values in molar region were higher than the values in anterior region. Maximum Von Mises stress values were found in both dental implants and in each point when the static load is applied with the maximum angle.

**3.2. Mean Fatigue Life and Variance.** Applying the model proposed here, which was explained in detail in [19], the mean fatigue life and its variance have been obtained in all situations described. Figures 6 and 7 depict the mean fatigue life for dental implants employed. The most breakable part of the implant, independently of the configuration load, is the apical part. However, under the same loading conditions, the minimum mean life is relatively similar under the same situation in both dental implants.

With the aim of having a good accuracy on the results, fatigue life must be correctly defined by statistic parameters. Therefore, the variance was also obtained and represented in Figures 8 and 9. Cylindrical implant (IP804) has more variability in terms of fatigue than the conical implants

TABLE 4: Bite force magnitude and angle employed in this study.

	Magnitude force [N]	Angle [°]
Molar region	489 [25]	0, 15, 20
Anterior region	178 (maximum value in the literature) [28]	0, 15, 20

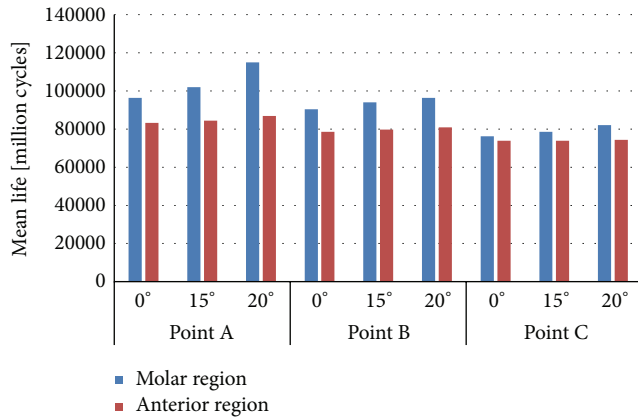


FIGURE 6: Mean fatigue life in implant IP861.

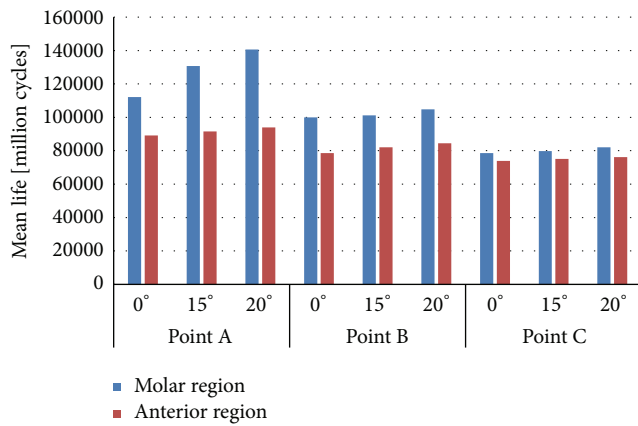


FIGURE 7: Mean fatigue life in implant IP804.

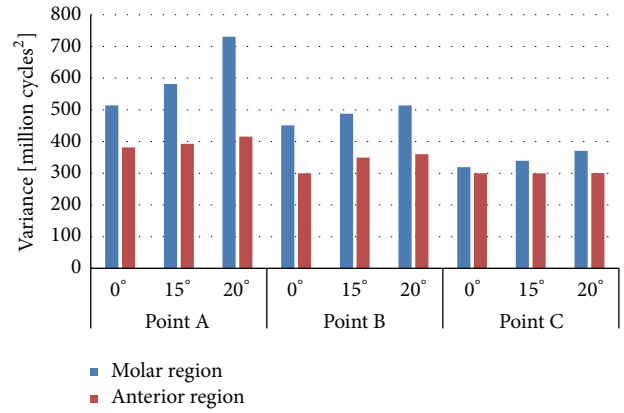


FIGURE 8: Variance of the mean fatigue life in implant IP861.

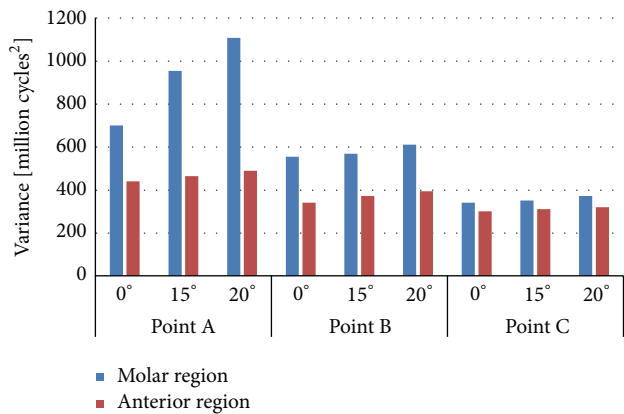


FIGURE 9: Variance of the mean fatigue life in implant IP804.

under the same situation of boundary conditions and loading configuration.

3.3. *Probability of Failure.* Once the statistic parameters of the long-term life are defined, the probability cumulative function can be drawn. Two examples, which correspond to axial load situation, are shown in Figures 10 and 11.

In view of Figures 10 and 11, implant IP861 has a better behaviour in terms of failure because this implant has more cycles with a probability of failure equal to zero.

#### 4. Discussion

The present study focused on the problem of the fatigue behaviour in different areas of the jaw. This paper presents the application of a probabilistic methodology to dental implants

with the aim of knowing the fatigue behaviour and the probability of failure under two different loads with three different angles of application. The methodology employed offers a technique to define the influence of the variability and uncertainty of the most important factor in the efficacy of dental implants performance.

Different from most of studies available on the literature about fatigue in dental implants, this study has been proposed from a probabilistic point of view. As forces act on a repeated way, fatigue failure is introduced in dental implant [30]. Mastication habits are also different depending on the patient [22–28, 31]. Therefore, this decision is justified because dental implants have stochastic characteristics and, also, because they are very sensitive to many factors such as load and material. As opposed to the conventional way of studying fatigue, our results provided the mean fatigue life, its variance, and the probability of failure associated with each cycle.

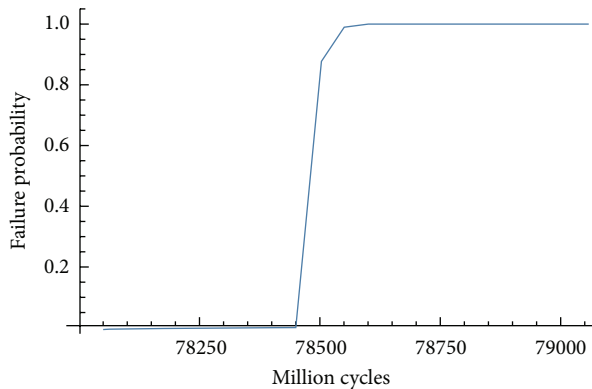


FIGURE 10: Cumulative probability function for implant IP861 and axial molar load.

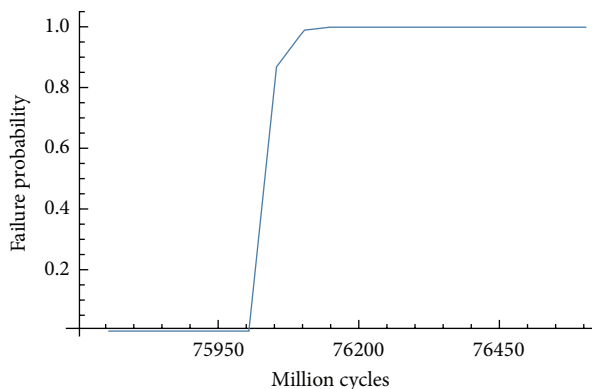


FIGURE 11: Cumulative probability function for implant IP804 and axial molar load.

Probabilistic models on dental applications are relatively new; thus, most of finite element and fatigue studies on dental implants available on the literature are deterministic [26, 32–34].

A realistic finite element model has been applied in the present work with the goal of obtaining the mean fatigue life, its variance, and the probability of failure. The influence of the material properties and the loading conditions on probability of failure has been demonstrated.

Several assumptions have been made with regard to the material properties and model generation. Implant material properties were assumed to be homogenous, linear, and isotropic and were assumed to be 100% osseointegrated.

Our results showed that the stress was mainly concentrated at the apical part of the implant when the highest angle was applied. The mathematical model proposed in the current work provided a relative similar mean life in all implants analysed under the same situation. However, the variance of the long-term fatigue life suggests that cylindrical implants have more variability because their variance is bigger than the values obtained in conical implants. According to the clinical experience, the conical implant employed here has a better behaviour than the cylindrical.

Finally, the cumulative probability functions were obtained. These functions provide the failure probability associated with each cycle in a determined condition. The model proposed in this study is focused on the study of fatigue with a probabilistic point of view obtaining accuracy results.

## 5. Conclusions

Variables involved in implant behaviour introduce randomness in the process due to the fact that masticatory forces are not constant and material properties can be different along the implant. Method to study fatigue employed here reduces the unrestrained elements.

To be able to quantify the randomness in this process, a cumulative damage model based on Markoff chains and the probabilistic finite element have been applied. This is the novelty of this paper because most finite element studies on dental implants are static analyses [34–38].

Proclinic® dental implant has been studied under two different load magnitudes, one bruxism and one a common masticatory load. As it was expected, stresses in all benchmark are bigger under bruxism condition. In light of the results of this study, the cylindrical implants have a greater uncertainty in the fatigue process, which is reflected in greater probability of failure.

## Competing Interests

The authors declare that there are no competing interests regarding the publication of this paper.

## Authors' Contributions

María Prados-Privado and Juan Carlos Prados-Frutos contributed equally.

## Acknowledgments

Proclinic-URJC Grant A-285 financially supported the research for this paper.

## References

- [1] C. E. Misch, *Dental Implant Prosthetics*, Elsevier-Mosby, St. Louis, Mo, USA, 2014.
- [2] Z. Ormianer, D. Piek, S. Livne et al., "Retrospective clinical evaluation of tapered implants: 10-year follow-up of delayed and immediate placement of maxillary implants," *Implant Dentistry*, vol. 21, no. 4, pp. 350–356, 2012.
- [3] M. G. Manda, P. P. Psyllaki, D. N. Tsipas, and P. T. Koidis, "Observations on an *in-vivo* failure of a titanium dental implant/abutment screw system: a case report," *Journal of Biomedical Materials Research Part B: Applied Biomaterials*, vol. 89, no. 1, pp. 264–273, 2009.
- [4] S. A. Gehrke, M. S. dos Santos Vianna, and B. A. Dedavid, "Influence of bone insertion level of the implant on the fracture strength of different connection designs: an *in vitro* study," *Clinical Oral Investigations*, vol. 18, no. 3, pp. 715–720, 2014.

- [5] S. Sakka and P. Coulthard, "Implant failure: etiology and complications," *Medicina Oral, Patología Oral y Cirugía Bucal*, vol. 16, no. 1, Article ID 16870, pp. e42–e44, 2011.
- [6] A. A. Siddiqui, M. Sosovicka, and M. Goetz, "Use of mini implants for replacement and immediate loading of 2 single-tooth restorations: a clinical case report," *Journal of Oral Implantology*, vol. 32, no. 2, pp. 82–86, 2006.
- [7] N. T. Green, E. E. Machtei, J. Horwitz, and M. Peled, "Fracture of dental implants: literature review and report of a case," *Implant Dentistry*, vol. 11, no. 2, pp. 137–143, 2002.
- [8] T. Albrektsson, P.-I. Brånemark, H.-A. Hansson, and J. Lindström, "Osseointegrated titanium implants: requirements for ensuring a long-lasting, direct bone-to-implant anchorage in man," *Acta Orthopaedica*, vol. 52, no. 2, pp. 155–170, 1981.
- [9] C. D. Koller, T. Pereira-Cenci, and N. Boscatto, "Parameters associated with marginal bone loss around implant after prosthetic loading," *Brazilian Dental Journal*, vol. 27, no. 3, pp. 292–297, 2016.
- [10] C. Maiorana, P. P. Poli, A. E. Borgonovo et al., "Long-term retrospective evaluation of dental implants placed in resorbed jaws reconstructed with appositional fresh-frozen bone allografts," *Implant Dentistry*, vol. 25, no. 3, pp. 400–408, 2016.
- [11] A. Veitz-Keenan, "Marginal bone loss and dental implant failure may be increased in smokers," *Evidence-Based Dentistry*, vol. 17, no. 1, pp. 6–7, 2016.
- [12] A. Y. Wu, J. T. Hsu, W. Chee, Y. T. Lin, L. J. Fuh, and H. L. Huang, "Biomechanical evaluation of one-piece and two-piece small-diameter dental implants: in-vitro experimental and three-dimensional finite element analyses," *Journal of the Formosan Medical Association*, 2016.
- [13] S.-H. Chang, S.-R. Huang, S.-F. Huang, and C.-L. Lin, "Mechanical response comparison in an implant overdenture retained by ball attachments on conventional regular and mini dental implants: a finite element analysis," *Computer Methods in Biomechanics and Biomedical Engineering*, vol. 19, no. 8, pp. 911–921, 2016.
- [14] P. de Kok, C. J. Kleverlaan, N. de Jager, R. Kuijs, and A. J. Feilzer, "Mechanical performance of implant-supported posterior crowns," *Journal of Prosthetic Dentistry*, vol. 114, no. 1, pp. 59–66, 2015.
- [15] H. O. Madsen, S. Krenk, and N. C. Lind, *Methods of Structural Safety*, Prentice-Hall, Englewood Cliffs, NJ, USA, 1986.
- [16] S. Suresh, *Fatigue of Materials*, Cambridge University Press, New York, NY, USA, 2006.
- [17] H. E. Boyer, *Atlas of Fatigue Curves*, ASM International, Materials Park, Ohio, USA, 1986.
- [18] J. Schijve, *Fatigue of Structures and Materials*, Springer, Amsterdam, The Netherlands, 2009.
- [19] M. Prados-Privado, J. C. Prados-Frutos, J. L. Calvo-Guirado, and J. A. Bea, "A random fatigue of mechanize titanium abutment studied with Markoff chain and stochastic finite element formulation," *Computer Methods in Biomechanics and Biomedical Engineering*, vol. 13, pp. 1–9, 2016.
- [20] J. L. Bogdanoff and F. Kozin, *Probabilistic Models of Cumulative Damage*, Wiley-Interscience, New York, NY, USA, 1985.
- [21] T. Hisada and S. Nakagiri, "Stochastic finite element method developed for structural safety and reliability," in *Proceedings of the 3rd International Conference on Structural Safety and Reliability (ICOSSAR '81)*, pp. 395–408, Elsevier, Trondheim, Norway, December 1981.
- [22] M. Bakke, "Bite force and occlusion," *Seminars in Orthodontics*, vol. 12, no. 2, pp. 120–126, 2006.
- [23] J. Živko-Babić, J. Pandurić, V. Jerolimov, M. Mioč, I. Pižeta, and M. Jakovac, "Bite force in subjects with complete dentition," *Collegium Antropologicum*, vol. 26, no. 1, pp. 293–302, 2002.
- [24] S. Varga, S. Spalj, M. Lapter Varga, S. Anic Milosevic, S. Mestrovic, and M. Slaj, "Maximum voluntary molar bite force in subjects with normal occlusion," *European Journal of Orthodontics*, vol. 33, no. 4, pp. 427–433, 2011.
- [25] G. T. Clark and M. C. Carter, "Electromyographic study of human jaw-closing muscle endurance, fatigue and recovery at various isometric force levels," *Archives of Oral Biology*, vol. 30, no. 7, pp. 563–569, 1985.
- [26] I. Hasan, C. Bourauel, L. Keilig, S. Reimann, and F. Heinemann, "The influence of implant number and abutment design on the biomechanical behaviour of bone for an implant-supported fixed prosthesis: a finite element study in the upper anterior region," *Computer Methods in Biomechanics and Biomedical Engineering*, vol. 14, no. 12, pp. 1113–1116, 2011.
- [27] R. Sadrimanesh, H. Siadat, P. Sadr-Eshkevari, A. Monzavi, P. Maurer, and A. Rashad, "Alveolar bone stress around implants with different abutment angulation: an FE-analysis of anterior maxilla," *Implant Dentistry*, vol. 21, no. 3, pp. 196–201, 2012.
- [28] C. C. Montes, F. A. Pereira, G. Thomé et al., "Failing factors associated with osseointegrated dental implant loss," *Implant Dentistry*, vol. 16, no. 4, pp. 404–412, 2007.
- [29] J. A. Bea and M. Doblaré, "Enhanced B-PFEM model for fatigue life prediction of metals during crack propagation," *Computational Materials Science*, vol. 25, no. 1–2, pp. 14–33, 2002.
- [30] M. G. Manda, P. P. Psyllaki, D. N. Tsipas, and P. T. Koidis, "Observations on an in-vivo failure of a titanium dental implant/abutment screw system: a case report," *Journal of Biomedical Materials Research Part B: Applied Biomaterials*, vol. 89, no. 1, pp. 264–273, 2009.
- [31] C. H. Gibbs, K. J. Anusavice, H. M. Young, J. S. Jones, and J. F. Esquivel-Upshaw, "Maximum clenching force of patients with moderate loss of posterior tooth support: a pilot study," *Journal of Prosthetic Dentistry*, vol. 88, no. 5, pp. 498–502, 2002.
- [32] H.-J. Han, S. Kim, and D.-H. Han, "Multifactorial evaluation of implant failure: a 19-year retrospective study," *The International Journal of Oral & Maxillofacial Implants*, vol. 29, no. 2, pp. 303–310, 2014.
- [33] L. Baggi, I. Cappelloni, F. Maceri, and G. Vairo, "Stress-based performance evaluation of osseointegrated dental implants by finite-element simulation," *Simulation Modelling Practice and Theory*, vol. 16, no. 8, pp. 971–987, 2008.
- [34] C. S. Petrie and J. L. Williams, "Comparative evaluation of implant designs: influence of diameter, length, and taper on strains in the alveolar crest—a three-dimensional finite-element analysis," *Clinical Oral Implants Research*, vol. 16, no. 4, pp. 486–494, 2005.
- [35] M.-L. Hsu, F.-C. Chen, H.-C. Kao, and C.-K. Cheng, "Influence of off-axis loading of an anterior maxillary implant: a 3-dimensional finite element analysis," *The International Journal of Oral & Maxillofacial Implants*, vol. 22, no. 2, pp. 301–309, 2007.
- [36] W. K. Liu, T. B. Belytschko, and G. H. Besterfield, "Probabilistic finite element method," in *Computational Mechanics of Probabilistic and Reliability Analysis*, pp. 70–105, Elmepress International, Lausanne, Switzerland, 1989.

- [37] T. J. R. Hughes, *Linear Static and Dynamic Finite Element Analysis*, Prentice Hall, New York, NY, USA, 1987.
- [38] H. Van Oosterwyck, J. Duyck, J. V. Sloten et al., "The influence of bone mechanical properties and implant fixation upon bone loading around oral implants," *Clinical Oral Implants Research*, vol. 9, no. 6, pp. 407–418, 1998.